Levulinic acid as a renewable source for novel polymers

Chalid, Mochamad

Levulinic Acid as a Renewable Source for Novel Polymers

Mochamad Chalid

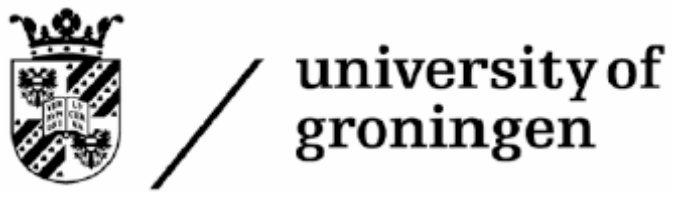

The author thanks the University of Groningen for the financial support through an Ubbo Emmius Scholarship.

RIJKSUNIVERSITEIT GRONINGEN

Levulinic Acid
as a Renewable Source for Novel Polymers

Proefschrift

ter verkrijging van het doctoraat in de
Wiskunde en Natuurwetenschappen
aan de Rijksuniversiteit Groningen
op gezag van de
Rector Magnificus, dr. E. Sterken,
in het openbaar te verdedigen op
maandag 18 juni 2012
om 14.30 uur

door

Mochamad Chalid

geboren op 17 april 1971

te Jakarta, Indonesië

Promotores	:	Prof. dr. A.A. Broekhuis Prof. dr. ir. H.J. Heeres
Beoordelingscommissie	:	Prof. dr. J.G. de Vries Prof. dr. F. Picchioni Prof. dr. K.U. Loos

ISBN: 978-90-367-5555-9
ISBN: 978-90-367-5540-5 (electronic version)

Aan: Mijn Schaatje Nona & Mijn Jongen Farhan

Table of contents

Chapter 1
Introduction

Abstract

In this introduction, routes to synthesize levulinic acid from ligno-cellulosic biomass and its subsequent use as a renewable source for biobased polymers will be discussed. Next, an outline of this thesis will be provided.

1.1. Synthesis and properties of levulinic acid (LA)

Ligno-cellulosic biomass has been identified as a potentially attractive source for chemical products and is considered to become a promising raw material to (partly) substitute fossil carbon resources.[1,2] It is available in enormous quantities from agricultural resources, forestry, aquatic plants, and industrial waste streams (e.g. paper manufacture). Large research efforts are currently undertaken to develop and commercialize processes to convert this biomass to bulk chemicals and derivatives (e.g. novel bio-based polymers), see Figure 1 for details.[3,4]

A well-known example of a very attractive chemical from biomass is levulinic acid. An important conversion route involves the treatment of the ligno-cellulosic biomass source by treatment with mineral acids.[5-11]

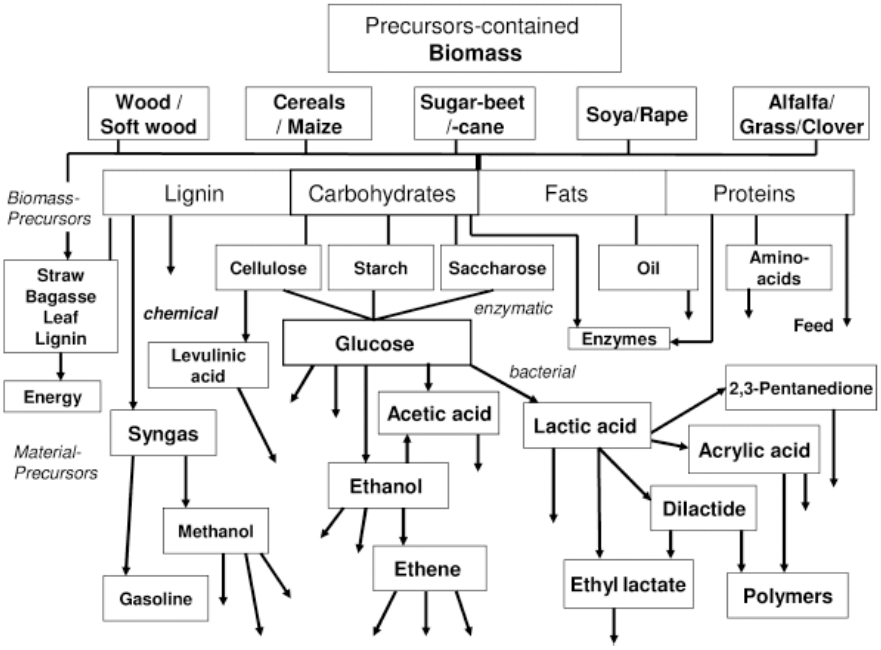

Figure 1. Attractive product trees for ligno-cellulosic biomass (adapted from [11]. Reprinted by permission of Wiley-VCH Verlag GmbH & Co. KGaA)

The first reports on the synthesis of LA, also known as γ-ketovaleric acid and 4-ketopentanoic acid, are from Mulder in 1840.[4,11,12] Sucrose was used as the feedstock and a mineral acid (HCl) was used as the catalyst. As shown in Scheme 1, the reaction involves sucrose cleavage and dehydration to give LA and formic acid in a one-to-one molar ratio.[12]

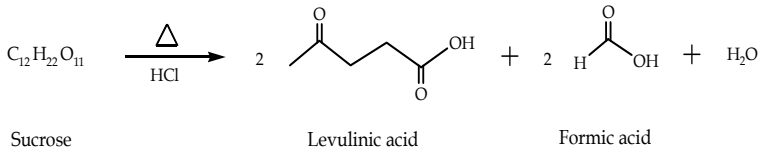

Scheme 1. Synthesis of levulinic acid from sucrose

LA is readily soluble in water and various organic solvents like ethanol, diethyl ether, and acetone.[13,14] Some relevant physical properties of levulinic acid are given in Table 1.

Table 1. Relevant physical properties of levulinic acid[15]

Property	Value
Melting point, ˚C	37
Boiling point, ˚C	246
Density at 25 ˚C, gram cm^{-3}	1.14
Heat of vaporization at 150 ˚C, kJ mol^{-1}	0.58
Heat of fusion, kJ mol^{-1}	79.8
pKa	4.59

In 1951, Frost and Kurth[16] showed that LA may also be obtained from low-cost cellulosic feedstocks. Controlled degradation of hexoses still is the most widely used method to obtain LA from ligno-cellulosic biomass. Although the theoretical yield of levulinic acid is 67.8 wt %, the remainder being formic acid,[16] levulinic acid yields from C6-sugars are commonly less than the theoretical value due to the formation of humins as by-product.[17] An overview of various feeds used for the synthesis of levulinic acid and the corresponding yields is given in Table 2.

Table 2 Overview of acid catalyzed LA synthesis from various feeds[18-23]

Feedstock	C_0 (wt %) [a]	Acid	C_{acid} (wt %)	T (°C)	t (h)	Y_{LA} (wt %) [b]
Cane sugar	28	HCl	18	100	24	15
Glucose	32	HCl	20	R.T. [c]	24	15
Corn starch	29	HCl	6.5	162	1	26
Sucrose	29	HCl	6.5	162	1	29
Glucose	29	HCl	6.5	162	1	24
Fructose	29	HCl	6.5	162	1	25
Hydrol [d]	42	HCl	7.4	R.T. [c]	22	25
Corn starch	33	HCl	1.8	200	0.5	35
Starch	26.5	HCl	5.2	R.T. [c]	24	19
Rice hulls	14	HCl	1	160	3	10.3
Rice straw	14	HCl	1	160	3	5.5
Corn stalks	14	HCl	1	160	3	7.5
Cotton linters	14	HCl	1	160	3	7.4
Sucrose	6	H_2SO_4	9	125	16	30
Sucrose	6	HCl	9.7	125	16	43
Sucrose	6	HBr	9	125	16	50
Sucrose	27	Amberlite IR-120	19	R.T.	41	15.6
Fructose	27	Amberlite IR-120	19	R.T.	27	23.5
Glucose	27	Amberlite IR-120	19	R.T.	124	5.8
Glucose	5-20	H_2SO_4	0.1−4	160−240	$f(T)$ [e]	35.4
Pulp slurry	10	HCl	6	160	1	40.5
Glucose	10	HCl	6	160	0.25	41.4
Cotton stems	n.a. [f]	H_2SO_4	5	180−190	2	6.13
Wood sawdust	20	HCl	1.5	190	0.5	9
Oakwood	n.a.	H_2SO_4	3	180	3	17.5
Bagasse	9	H_2SO_4	1.3	25−195	2	17.5
Fructose	4.5-18	HCl	2−7.5	100	24	52
Sucrose	20	Resin-Dowex	6.25	100	24	17
Sawdust	n.a.	HCl	8	n.a.	n.a.	6.9

Shredded paper	n.a.	HCl	8	n.a.	n.a.	17.2
Fructose	50	LZY-zeolite	50	140	15	43.2
Glucose	12	Clay-catalyst [g]	3	150	24	12
Glucose	12	HY-zeolite	3	150	24	6
Cellulose	10	H_2SO_4	3	250	2	25.2
Various woods [h]	10-20	H_2SO_4	5	200−240	2−4	13−18
Cellulose	10	H_2SO_4	1–5	150−250	2−7	≤ 25.2
Cellulose	10	HCl	1–5	150−250	2−7	≤ 28.8
Cellulose	10	HBr	1–5	150−250	2−7	≤ 26.9
Aspen wood	10	H_2SO_4	1–5	150−250	2−7	≤ 15.5
Aspen wood	10	HCl	1–5	150−250	2−7	≤ 12.4
Aspen wood	10	HBr	1–5	150−250	2−7	≤ 13.0
Newspaper	30	H_2SO_4	10	150	8	12.8
Sorghum grain	10	H_2SO_4	8	200	0.67	32.6
Extruded starch	25	H_2SO_4	4	200	0.67	47.5
Wheat straw	6.4	H_2SO_4	3.5	209.3	0.63	19.8
Glucose	4.8	H_2SO_4	5	170	1	7.7
Wheat Straw	43	HCl	4.5	220	0.75	23
Water Hyacinth	1	H_2SO_4	10	175	0.5	35
Cellulose	6	Nafion SAC-13	3	190	24	2 – 5
Steam exploded rice straw	6	S_2O_2 [-8]/ZrO_2 - SiO_2 - Sm_2O_3	13.3	200	0.6	49.7

[a] C_0 is the initial concentration of feedstock and defined as the ratio between the mass of feedstock and the total mass; [b] Y_{LA} is defined as the ratio between the mass of LA and the mass of feedstock; [c] R.T. = Refluxed Temperature; [d] Mother liquor of crystalline corn starch; [e] Time is a function of temperature; [f] n.a. = data is not available; [g] Fe-pillared montmorillonite; [h] Types of wood are beech, aspen, pine and spruce.

Scheme 2 shows alternative methods for the LA synthesis, viz. the hydrolysis of furfurylalcohol obtained from the hydrogenation of furfural[24, 25,14], the oxidation of a dihydrofuran obtained from reaction of the α–silylated γ-butyrolactone with a Grignard reagent,[26] ozonolysis of an alicyclic α,β- unsaturated ketone in an aqueous alcohol medium,[27] carbonylation of a ketone such as 4-hydroxy-2-butanon,[14] and oxidation of a nitro-alkanal.[28] However, these methods are less attractive than the conventional acid catalyzed hydrolysis pathways due to the high feedstock costs, the number of processing steps, and the cost and availability of the reagents.

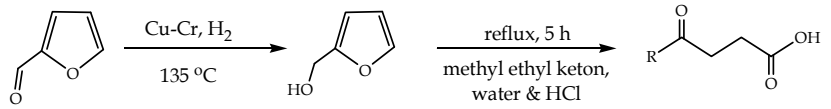

(i)

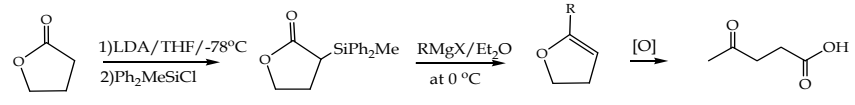

(ii)

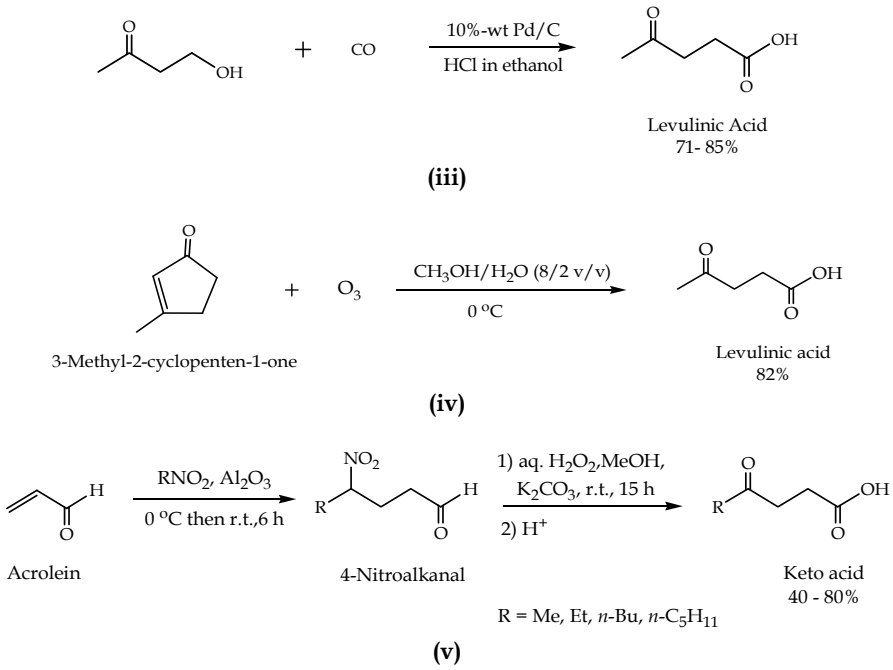

Scheme 2. Alternative methods to obtain levulinic acid. (i) ref. [24,25,14,] (ii) ref.[26], (iii) ref.[27], (iv) ref.[14], (v) ref.[28]

Thus, it appears that the most attractive synthetic pathway to levulinic acid is the acid hydrolysis of the C6 sugars obtained from ligno-cellulosic feedstock, in particular, cellulose-containing waste materials.[29]

Till today, however, commercial large scale processes for LA are not on stream due to the relatively low LA yields, issues related with recycling of the mineral acid catalysts and excessive equipment costs. However, pilot scale trials have been successful and on the basis of these findings a cost price for levulinic acid below 0.2 $/kg is estimated for large scale production.[9,30] At present levulinic acid is a specialty with a price of 6 – 9 €/kg and an annual production level of 450 tons.[31]

One of the technologies to produce levulinic acid is the Biofine process, which received the Presidential Green Chemistry Award in 1999.[4] This process involves a two-step reaction in a two reactor design scheme. Detailed descriptions of the technology are available in the literature.[32]

1.2. LA derivatives

Due to the presence of two reactive functional groups, i.e. a ketone and a carboxylic group, levulinic acid has been identified as a valuable bio-based multi-purpose building block.[3,5,16,33] Figure 3 depicts some selected levulinic acid derivatives.

γ-Valerolactone (GVL) is considered an interesting levulinic acid derivative. It may be obtained by (catalytic) hydrogenation and subsequent ring-closure of the intermediate 4-hydroxypentanoic acid (Scheme 3). To reduce the number of processing steps, studies have been performed to obtain the GVL from a C6-sugar in a one-pot-approach through the combined action of an acid and a hydrogenation catalyst without isolating the intermediate levulinic acid.[34-37]

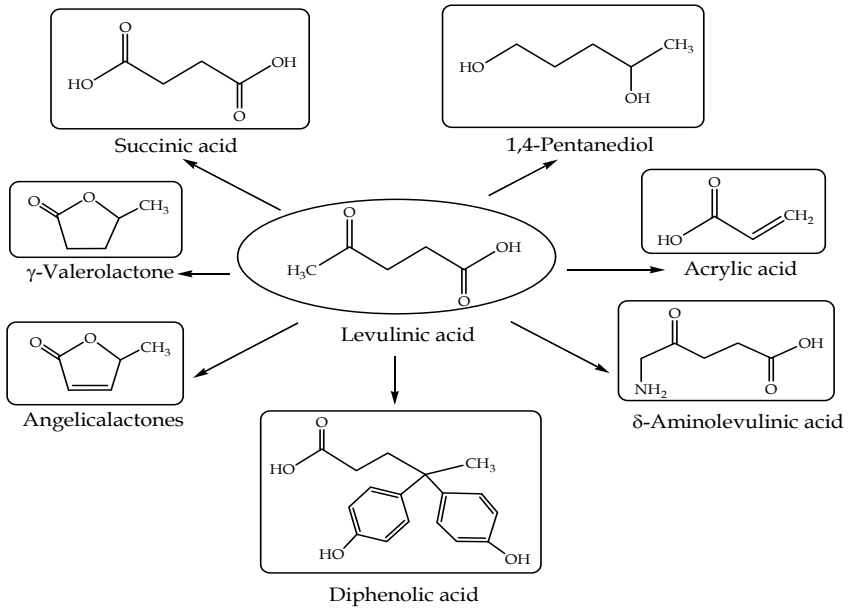

Figure 3. Selected derivatives of levulinic acid[3]

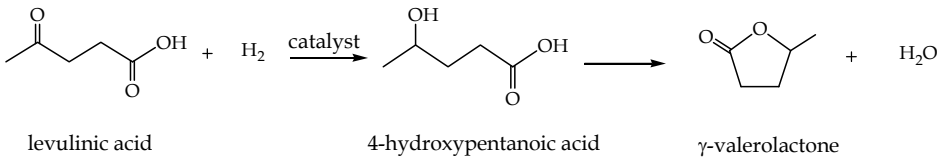

Scheme 3. Synthesis of GVL from levulinic acid

GVL may be used as ingredient in a drug delivery system,[6] as renewable component in a transportation fuel[38] and as a substitute for ethanol in gasoline-ethanol blends.[39]

The conversion of LA or its derivatives to novel bio-based polymers is a very popular topic.[40-52] It is stimulated by the increase in crude oil prices and environmental concerns regarding the use of fossil derived products.[53-54] This movement to 'green' renewable resource-based polymers is ongoing since the 1971's.[55-58]

GVL appears to be an attractive green polymer precursor for bio-based polymers. A limited number of studies on the ring-opening of GVL has been performed.[59-62] Solaro *et al.*[44] reported that homopolymerization of GVL in toluene in the presence of a bis(diethyl)aluminum sulphate (DEAS) catalyst is not possible. However, successful co-polymerization studies have been reported. For example, Lee *et al.*[45] reported the co-polymerization of GVL with β-butyrolactone (BBL) using $BF_3.OEt_2$ as the catalyst, as shown in Scheme 4. The 4-hydroxyvaleric (4-HV) content in the co-polymer was relatively low (12-34%), though significant. $BF_3.OEt_2$ was more active than typical anionic catalysts, and coordinating systems like $AlEt_3$ and $ZnEt_2$ were more active than strong acid catalysts such as CF_3SO_3H.

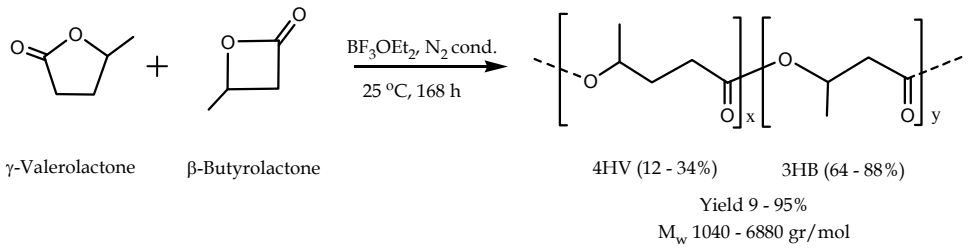

Scheme 4. Copolymerization of GVL and BBL[45]

Solaro *et al.*[44] reported the copolymerization of GVL and methyl methacrylate (MMA) in toluene with bis(diethyl)aluminum sulphate (DEAS) as the catalyst (Scheme 5). Analyses of the copolymer showed that γ-valerolactone has a low reactivity compared to MMA.

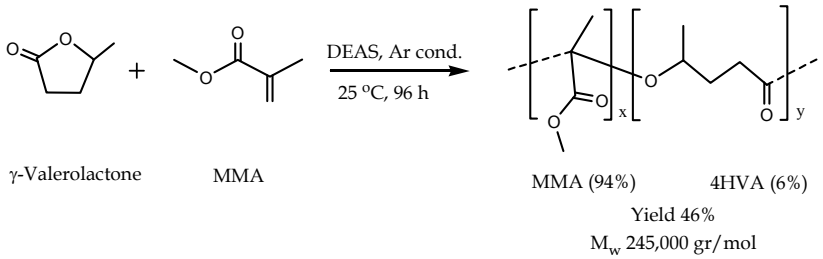

Scheme 5. Copolymerization of γ-valerolactone and methyl methacrylate[44]

Valentin *et al.*[43,63] reported a terpolyester consisting of γ-valerolactone, β-butyrolactone and β-propiolactone. The polymerization, as shown in Scheme 6, may be performed by aerobic bacteria such as the *Alcaligenes* species and several *Pseudomonas* species.

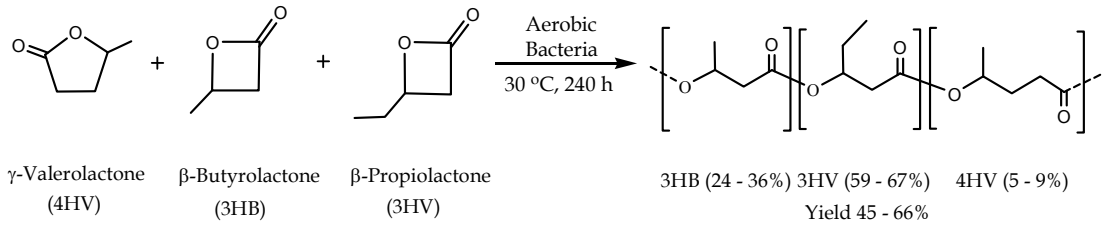

Scheme 6. Poly(3HB-*co*-3HV-*co*-4HV) terpolyester[43]

Thus, it may be concluded that GVL is a poorly polymerizable monomer. This is likely caused by the low ringstrain compared to other lactones like butyrolactone.[64-66] Various routes have been proposed to convert GVL to more reactive monomers and these will be discussed in the following section.

1.3. γ-Valerolactone(GVL)-based polymer precursors

Bio-based polymer precursors from GVL are accessible by two distinct synthetic strategies viz., the introduction of (reactive) substituents on the 5-membered ring of GVL and ring opening reactions with reactive compounds.

1.3.1. Introduction of reactive substituents on the 5-membered ring of GVL

An important reaction to introduce reactive substituents on the 5-membered ring of GVL involves the Na-induced addition of ethylformate in diethylether (Scheme 7). The reaction, first reported by McGraw[67], resulted in the formation of α-methylene-γ-valerolactone (MGVL). Details on reaction conditions and MGVL yields were not reported.

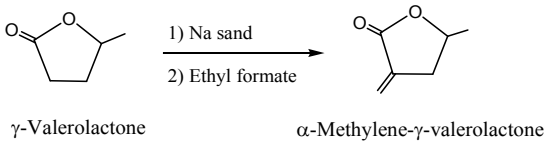

Scheme 7. Synthesis of MGVL[67]

Aiming at large scale MGVL production, a low-cost continuous, catalytic, single step process was reported by Manzer *et al.* (Scheme 8).[68-69] The reaction involves the addition of formaldehyde to GVL in a gas phase reaction, catalyzed by supported metals (such as Ba, Rb, K, Cs, Sr, and Ca) on SiO_2 at 340 °C.[69] Typical residence times were 1-6 s. The highest conversion of GVL after 15 min on stream was 60 mole %. Longer times on stream resulted in lower conversions due to catalyst deactivation.

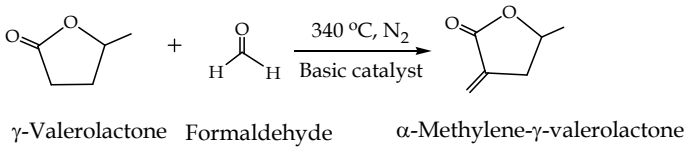

Scheme 8. MGVL synthesis proposed by Manzer *et al.*[69]

Polymerization studies with MGVL have been reported. For instance, (poly-α-methylene-γ-valerolactone, Scheme 9) was obtained by a free radical polymerization in chloroform with azo-bis-isobutyronitrile (AIBN) as the initiator. The resulting polymer has a glass transition temperature higher than 200 °C.[70]

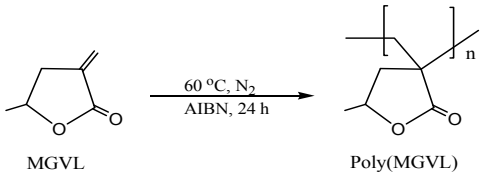

Scheme 9. Radical polymerization of MGVL[70]

Arasa *et al.*[71-72] reported the synthesis of γ-valerolactone-derived pre-polymer by reactions of GVL with the diglycidylether of bisphenol A (DGBA) using $BF_3.OEt_2$ as the Lewis acid catalyst. Subsequent curing at high temperature resulted in a higher molecular weight thermoset (Scheme 10). The reactions may also be carried out with other Lewis acid catalysts such as triflates of scandium, ytterbium and lanthanum.

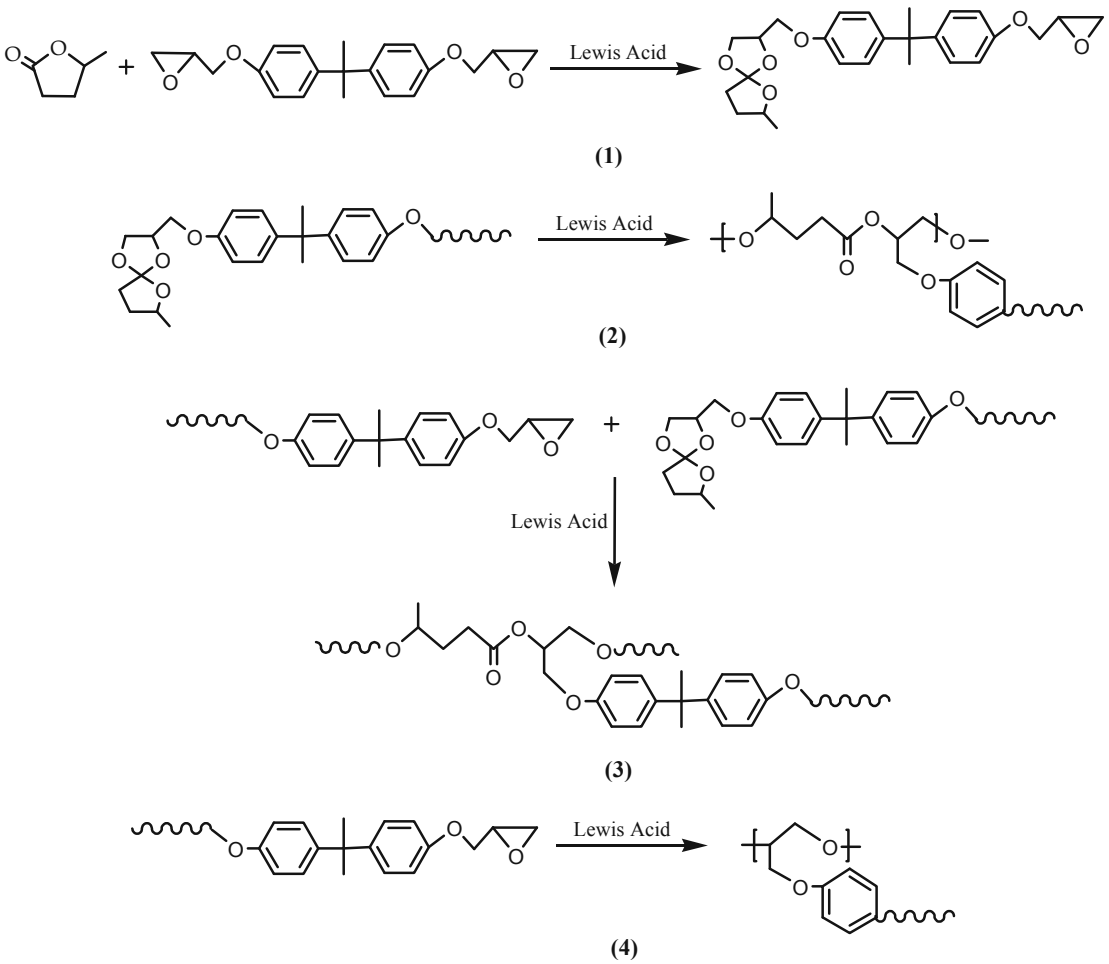

Scheme 10. Synthetic route for γ–valerolactone-derived thermoset[71-72]

1.3.2. Ring-opening reactions of GVL

GVL can also be modified by a ring-opening reaction of the lactone, leading to either polymer precursors or functionalized non-polymerizable compounds.

1. Ring opening reactions to polymer precursors

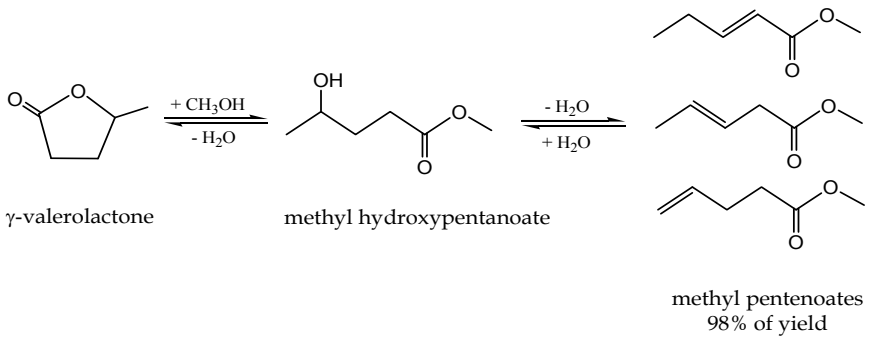

Scheme 11. Ring opening of GVL into methyl pentenoates[62]

Lange *et al*. have performed studies on the ring-opening of GVL to nylon precursors[62] (*see* Scheme 11) and particularly to methylpentenoates. The reaction was performed in a fed-batch mode at 200 °C and 1 atm, with methanol being slowly and continuously fed to a distillation flask containing the lactone and an

acid catalyst, viz. *para*-toluene sulfonic acid (pTSA). The distillate consists of unconverted methanol, methyl-pentenoates and water. The yield of methyl pentenoates was typically 98% at 200 °C. The methylesters consisted of a mixture of various isomers, namely pent-4-enoate (25-35%), the *cis/trans* pent-3-enoates (65-75%, mainly the *trans*-isomer) and the *cis/trans* pent-2-enoates (1-5%).

Methylpentenoates have been proposed as interesting intermediates[62] for valuable monomers such as caprolactone *via* hydroformylation, caprolactam *via* hydrocyanation and adipic acid *via* hydrocarbonylation.

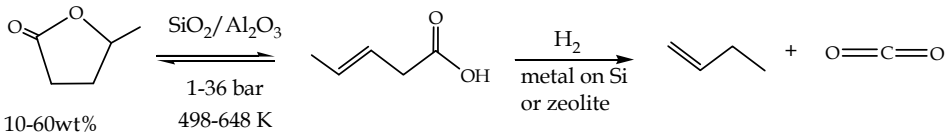

Scheme 12. Ring opening of GVL into 1-butene[73]

Bond *et al.* have carried out the reversible ring-opening of GVL to pentenoic acid (PEA) followed by decarboxylation to form 1-butene and CO_2 (Scheme 12). The reaction is catalyzed by a SiO_2/Al_2O_3 catalyst at pressures from atmospheric to 36 bar and temperatures from 225 to 375 °C.[73]

2. Ring-opening pathways to obtain functional non-polymerizable compounds

A synthetic methodology for the ring-opening of GVL was introduced by Brauman *et al.*[59] and involves a Friedel-Crafts alkylation with benzene to give γ-phenylvaleric acid as the main product and two by-products (Scheme 13).

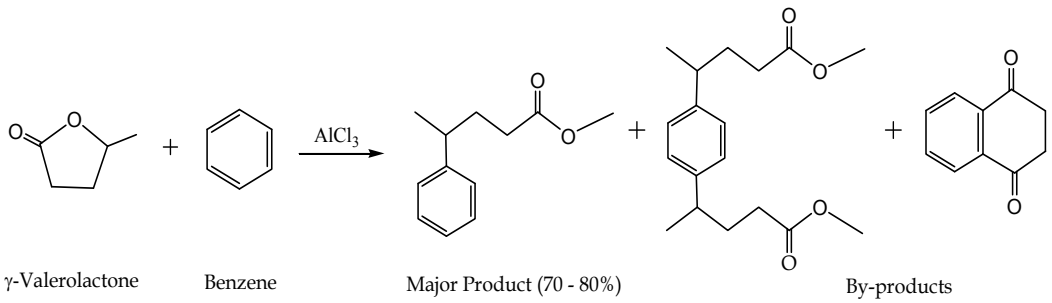

Scheme 13. Ring opening of GVL with benzene[59]

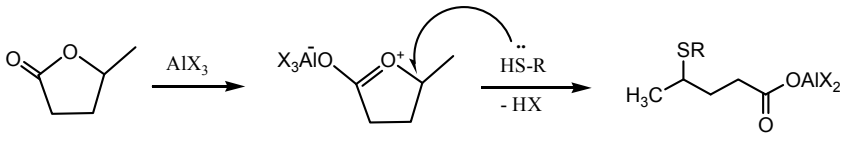

Scheme 14. Ring opening of GVL with a thiol compound[60]

Node *et al*. have modified the GVL ring opening reaction to γ-alkylthio or γ-arylthio carboxylic acids by using an aluminum halide catalyst and a thiol.[60] The reaction was conducted in ethanethiol at room temperature for 23 h to obtain the product in 80.5 – 84.6 % yield (Scheme 14).

Van den Brink *et al.*[61] performed the hydrogenation of γ-valerolactone into pentanoic acid using acidic heterogeneous catalysts comprising of a metal such as Pt and Ni on silica or a zeolite, as shown in Scheme 15. The reaction was performed in batch (4 h) at a temperature of 250 °C and 80 bar hydrogen pressure in the presence or absence of ethanol. In the absence of ethanol, the PA selectivity was 68% at a GVL conversion of 68%. In the presence of ethanol, the ethylester of PA is formed in selectivities up to 75% at 95% GVL conversion.

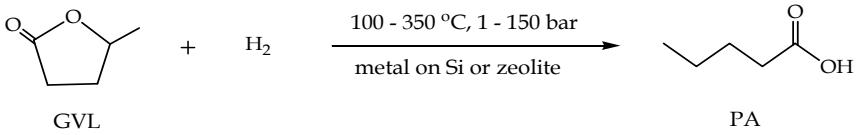

GVL PA

Scheme 15. Ring opening of GVL by catalytic hydrogenation[61]

Dumesic *et al.*[74] have carried out the reaction of GVL to pentanoic acid (PA) in a continuous set up at elevated temperatures in the presence of hydrogen and a bifunctional acidic niobia catalyst (Scheme 16). At 573 K, 35 bar and a WHSV of 3.1 h^{-1}, the initial GVL conversions were higher than 95% with a selectivity to PA exceeding 80%.

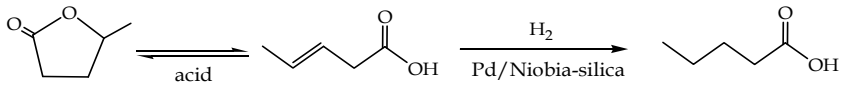

GVL PA

Scheme 16. Reaction scheme for the conversion of GVL to PA[74]

Based on these findings, it can be concluded that only a limited amount of research has been performed on the ring opening reaction of GVL. Particularly mild synthetic routes for ring-opening reactions of GVL to generate novel green polymer building blocks are highly desirable.

1.4. Thesis outline

The primary objective of the research described in this thesis is the development of novel synthetic pathways for bio-based polymers derived from levulinic acid. A two step approach has been applied and involves the conversion of LA to novel monomeric building blocks and the subsequent polymerization to higher molecular weight products. The monomeric building blocks were derived from GVL, which is accessible in high yields from LA. These were subsequently used as one of the components in a polymerization system, with an emphasis on polyurethanes (Scheme 17)

In Chapter 2, the hydrogenation of LA to GVL, using a heterogeneous catalyst, (Ru/C) in a batch autoclave is reported. Various solvents were screened and important process variables were studied to determine optimum conditions with respect to product yield. Catalyst recycling at optimum conditions was investigated to gain insight in the stability of the catalyst.

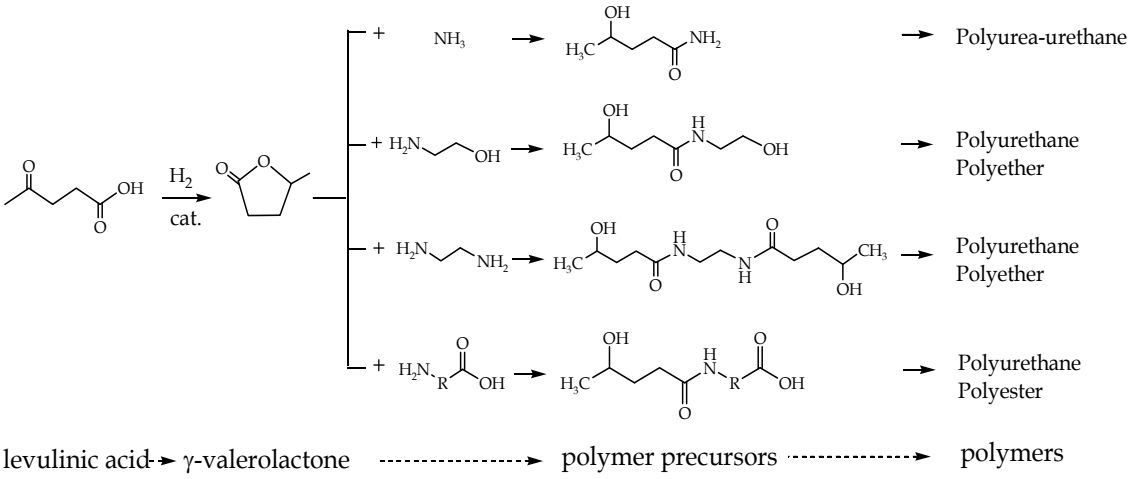

Scheme 17. Synthetic routes for bio-based polymers derived from LA

Chapter 3 describes the biphasic hydrogenation of LA to GVL using a homogeneous water-soluble Ru(TPPTS) catalyst. Important process variables were studied to determine optimum reaction conditions. Catalyst recycling at optimum conditions was investigated to study the stability of the catalyst. The kinetics of the hydrogenation reaction was determined and a kinetic model was developed.

The ring opening of GVL under mild conditions by reactions with mono- and di-amines is provided in Chapter 4. Important process variables for the di-addition of ethylenediamine to GVL were determined.

In Chapter 5, some of the GVL-based diols, such as N,N'-1,2-ethanediylbis-(4-hydroxy-pentanamide) and 4-hydroxy-N-(2-hydroxyethyl)-pentanamide, were reacted with di-isocyanates to obtain polyurethanes. The effect of process variables was studied in detail to determine optimum reaction conditions. Product properties and particularly the mechanical properties of the GVL-derived polyurethanes are reported in Chapter 6.

1.5. References

[1] A. Corma, S. Iborra and A. Velty, *Chem. Rev.*, 107, 2411-2502 (2007)

[2] A. Effendi, H. Gerhauser and A.V. Bridgwater, *Renew. Sust. Energ. Rev.*, 12, 2092-2116 (2007)

[3] T. Werpy and G. Petersen, *the National Renewable Energy Laboratory and the Pacific Northwest National Laboratory - US*, August 2004

[4] R.W. Pike, D. Sengupta and T.A. Hertwig, *Integrating Biomass Feedstocks into Chemical Production Complecex using New and Exixting Processes*, November 3 (2008)

[5] V. Ghorpade and M.A. Hanna, *US Patent*, US 5859563 (1999)

[6] W.A. Farone and J.E.Cuzens, *US Patent*, US 6054611 (2000)

[7] J.Y. Cha and M.A. Hanna, *Ind. Crop. Prod.*, 16, 109-118 (2002)

[8] Q. Fang and M.A. Hanna, *Bioresour. Technol.*, 81, 187-192 (2002)

[9] S.W. Fitzpatrick, *Biofine Inc.*, *US Patent*, US 5608105 (2004)

[10] B. Girisuta, L.P.B.M. Janssen and H.J. Heeres, *Chem. Eng. Res. Des.,* 84 (A5), 339-349 (2006)
[11] B. Kamm, M. Kamm, P.R. Gruber and S. Kromus, '*Biorefenery – Industrial Process and Products,' Statuts Quo and Future Directions,* Vol. 1. ISBN 3-527-31027-4, Wiley-VCH Verlag GmbH & Co. KGaA, Weinheim Germany, 1 – 40 (2006)
[12] G.J. Mulder, *J. Prakt. Chem*., 21, 219 (1840)
[13] R.L. David, *CRC Handbook of Chemistry & Physics*, CRC Press, 88th Ed. **3**-408 – **3**-409 (2004)
[14] B.V. Timokhin, V.A. Baransky and G.D. Eliseeva, *Russ. Chem. Rev.,* 68 (1), 73-84 (1999)
[15] G. Cavinato and L. Toniolo, *J. Mol. Catal*., 58, 251-267 (1990)
[16] R.H. Leonard, *Ind.Eng. Chem*., 48, 1330-1341 (1956)
[17] B. Girisuta, L.P.B.M. Janssen and H.J. Heeres, *Green Chem.,* 8, 701-709 (2006)
[18] B. Girisuta, *Levulinic Acid from Lignocellulosic Biomass*, PhD dissertation of University of Groningen, 15-19 (2007)
[19] C. Chang, X. Ma and P. Cen, *Chin. J. Chem. Eng.,* 14, 708-712 (2006)
[20] L. Yan, N. Yang, H. Pang and B. Liao, *Clean: Soil, Air, Water* 36, 158-163 (2008)
[21] B. Girisuta, B. Danon, R. Manurung, L.P.B.M. Janssen and H.J. Heeres, *Bioresour. Technol.* ,99, 8367-8375 (2008)
[22] J. Hegner, K.C. Pereira, B. DeBoef and B.L. Lucht, *Tetrahedron Lett.,* 51, 2356-2358 (2010)
[23] C. Hongzhang, Y. Bin and J. Shengying, *Bioresour.Technol*., 102, 3568-3570 (2011)
[24] K.J. Zeitsch, *the Chemistry and Technology of Furfural and its Many By-Products*, Elsevier, London, UK, (2000)
[25] M. Otsuka, Y. Hirose, T. Kinoshita and T. Masawa, *US Patent,* US 37552849 (1973)
[26] L.M. Fuentes and G.L. Larson, *Tetrahedron Lett.,* 23 (3), 271-274 (1982)
[27] W.B. Edwards, *US Patent,* US 4,612,391 (1986)
[28] F. Csende, *Acta Chim. Slov.,* 49, 663-676 (2002)
[29] J. Nakas, S.W. Tanenbaum and T. Keenan, *WIPO*, No. 027076 A2 (2004)
[30] B. Doidge and D.J. Miller, *Strategic Market Management System Platform Chemicals*, Canadian Agriculturea New Uses Council, June 25 (2002)
[31] J. Groenestijn, C. Enzing, M. Dongen and J. Bossenbroek, *Biobased economy – Exploring the opportunities for the Netherlands: Overview of high value added applications of biomass and biorefenery,* TNO Report, September 30 (2008)
[32] D.J. Hayes, S. Fitzpatrick, M.H.B. Hayes and J.R.H. Ross, "The Biofine Process – Production of Levulinic acid, Furfural and Formic Acid from Lignocellulosic Feedstock", Biorefineries–Industrial Processes and Products, Vol. 1, ISBN 3-527-31027-4, Wiley-VCH Verlag GmbH & Co. KGaA, Weinheim, Germany, 139-164 (2006)
[33] J.J. Bozell, L. Moens, D.C. Elliott, Y. Wang, G.G. Neuenscwander, S.W. Fitzpatrick, R.J. Bilski and J.L. Jarnefeld, *Resources, Conservation and Recycling*, **28**, 227-239 (2000)

[34] H. Mehdi, A. Bodor, A. Tuba and I.T. Horvath, *Abstr. Pap. Am. Chem. S.*, 226, U721 (2003)
[35] H. Mehdi, V. Fábos, R. Tuba, A. Bodor, L.T. Mika and I.T. Horvath, *Top. Catal.*, 48, 49-54 (2008)
[36] G. Braca, A.M.R. Galletti and G. Sbrana, *J. Organomet. Chem,* 417, 41-49 (1991)
[37] H. Heeres, R. Handana, D. Chunai, C.B. Rasrendra, B. Girisuta and H.J. Heeres, *Green Chem.*, 11, 1247-1255 (2009)
[38] S.F. Paul, *US Patent*, US 5,697,987 (1996)
[39] I.T. Horvath, H. Mehdi, V. Fabos, L. Boda and L.T. Mika, *Green Chem.,* 10, 238-242 (2008)
[40] Y.M. Wang, A. Ikeda, N. Hori, A. Takemura, H. Ono, T. Yamada and T. Tsukatani, *Polymer*, 46, 9793-9802 (2005)
[41] G. Schmack, V. Gorenflo and A. Steinbüchel, *Macromol.,* 31, 644-649 (1998)
[42] V. Gorenflo, G. Schmack, R. Vogel and A. Steinbüchel, *Biomacromol.,* 2, 45-57 (2002)
[43] H.E. Valentin, A. Schönebaum and A. Steinbüchel, *Appl. Microbiol Biotechnol.*, 36, 507-514 (1992)
[44] R. Solaro, G. Canton and E. Chiellini, *Eur. Polym. J.*, 33(2), 205–211 (1997)
[45] C.W. Lee, R. Urakawa and Y. Kimura, *Eur. Polym. J.,* 34(1), 117-122 (1998)
[46] C.S. Marvel and C.L. Levesque, *J. Am. Chem. Soc.*, 61(7), 1682-1684 (1939)
[47] K. Jaszcz, J. Lukaszczyk and M. Smiga-Matuszowicz, *Reac. Funct. Polym.*, 68, 351-360 (2008)
[48] I. Bechthold, K. Bretz, S. Kabasci and R. Kopitzky, Springer A., *Chem. Eng. Technol.*, **31**(5), 647-654 (2008)
[49] W-J. Tsai, W-C. Chang, C-H. Chen, H-Y. Lu and M. Chen, *Europ.Polym.J.*, 44, 2339-2347 (2008)
[50] P. Zhang, L. Wu, Z. Bu and B-G. Li, *J. Appl.Polym. Sci.*, 108, 3586-3592 (2008)
[51] J.A. Moore and T. Tannahill, *High Perform. Polym.*, 13, S305-S316 (2001)
[52] M. Nakamoto and Y. Iwakuni-shi, *European Patent*, EP 1 632 469 A1 (2006)
[53] Website of *Live Journal*: http://saintbryan.livejournal.com/204109.html?thread=1210701, accessed June 22, 2011
[54] Website of *IDES - the Platics Web* : http://www.ides.com/articles/ oil.asp, accessed July 1, 2011
[55] G. Scott, *Pol. Degr. Stab.*, 68, 1-7 (2000)
[56] S.Y. Lee, S.J. Park, J.P. Park and Y. Lee, S.H. Lee, *Biopolymers, General Aspects and Special Applications*, Wiley-VCH, 10, 308-333, April 2003
[57] E. Gary, Wnek, "*Biopolymer*", in AccesScience@McGraw-Hill, **Fout! De hyperlinkverwijzing is ongeldig.**.accessscience.com/DOI10.1036/1097-8542.757239, accessed June 22, 2011
[58] D.P. Bloom, Venkitasubramanian and Padmesh, *US Patent,* US A1 20090018300 (2009)
[59] J.I. Brauman and A.J. Pandell, *J. Am.Chem. Soc.*, 89(21), 5421–5424 (1967)
[60] M. Node, K. Nishide, M. Ochiai, K. Fuji and E. Fujita, J. Org. Chem., 46 5163-5166 (1981)

[61] P.J. van den Brink, K.L.van Hebel, J.P. Lange and L. Petrus, *US Patent*, US 0162239 A1 (2006)
[62] J.P. Lange, J.Z. Vestering and R.J. Haan, *Chem. Comm.*, 3488-3490 (2007)
[63] H.E. Valentin, A. Schönebaum and A. Steinbüchel, *Appl. Microbiol. Biotechnol.*, 46, 261-267 (1996)
[64] W. Saiyasombat, R. Molloy, T.M. Nicholson, A.F. Johnson, I. M. Ward and S. Poshyachinda, *Polymer,* 39(23), 5581–5585 (1998)
[65] M. Teresa Pérez-Prior, A.M. Jose, M. del Pilar García-Santos, M. Calle and J. Casado, *J. Org. Chem.,* 70, 420-426 (2005)
[66] K.N. Houk, H.K. Arash Jabbari, Jr. Hall and Carlos Alema´n, *J. Org. Chem.*, 73, 2674-2678 (2008)
[67] W.J. McGraw, *US Patent,* US 2,624,723 (1953)
[68] D.R. Coulson, L.E. Manzer and N. Herron, *US Patent,* US 6,313,318 (2001)
[69] L.E. Manzer, *Appl. Catal. A-Gen.*, 272, 249-256 (2004)
[70] C.U. Pittman and H. Lee, *J. Polym. Sci.: Part A: Polym. Chem.*, *41*, 1759–1777 (2003)
[71] M. Arasa, X. Ramis, J.M. Salla, A. Mantecon and A. Serra, *Polym Degr. and Stab.*, 92, 2214–2222 (2007)
[72] M. Arasa, X. Ramis, J.M. Salla, A. Mantecon and A. Serra, *J. Polym. Sci. Pol. Chem.*, 45, 2129–2141 (2007)
[73] J.Q. Bond, D. Wang, D.M. Alonso, J.A. Dumesic, *J. Catal.*, 281, 290-299 (2011)
[74] H.N. Pham, Y.J. Pagan-Torres, J.C. Serrano-Ruiz, D. Wang, J.A. Dumesic, A.K. Datye, *Appl. Catal. A-Gen.*, 39 (1-2), 153–162 (2011)

Chapter 2
Experimental Studies on LA Hydrogenation using a Ru/C Catalyst in Water

Abstract

γ-Valerolactone (GVL) is considered a very attractive biomass derived compound with a broad application range. GVL is typically obtained from levulinic acid (LA) by catalytic hydrogenation. We here report an experimental study on the hydrogenation of LA in water using a Ru/C catalyst (5 wt%) in a batch reactor set-up. The effect of process conditions like temperature (50 °C – 140 °C), stirring rate (200-2000 rpm) and catalyst intake (0.05-3 wt% on LA intake) on the LA conversion rate and product selectivity (GVL versus 4-hydroxypentanoic acid (4-HPA)) was determined. Quantitative conversion of LA was observed after 30 min at 140 °C in water, with a GVL selectivity of 94%. The product selectivity may be steered by the temperature. At low temperatures 4-HVA is formed selectively, whereas higher temperatures favor the formation of GVL. Preliminary insights in catalyst stability were obtained by performing catalyst recycling experiments, showing that the activity of the recycled catalyst is slightly lower than that of the fresh catalyst. A possible reason is coke deposition on the catalyst as indicated by BET measurements on fresh (890 m^2/g) and spent catalyst (170 m^2/g)

2.1. Introduction

The conversion of biomass to higher added value bio-based chemicals is receiving a lot of attention worldwide. A potentially very powerful approach is the conversion of the cellulose and hemicellulose fraction into platform chemicals using either biochemical (fermentation or enzymatic) or metal catalyzed transformations.[1,2] An attractive top-12 platform chemical is levulinic acid (LA), obtainable from the C6-sugars of ligno-cellulosic biomass in good yields. LA may be converted to a number of derivatives with good application potential. An attractive derivative is γ-valerolactone (GVL).[3] GVL has existing applications in the food industry and is also used as a component in drug delivery systems.[3,4,5] Other potential applications are the use as an oxygenate in transportation fuels, as a co-monomer for the preparation of polymers like poly-hydroxyalkanoate,[6] and as a precursor for long chain alkanes to be used as hydrocarbon fuels.[7]

GVL is typically obtained from LA by catalytic hydrogenation processes using hydrogen or other hydrogen sources (e.g. formic acid) using homogeneous[8-14] or heterogeneous catalysts. An overview of heterogeneous catalyst and process conditions is given in Table 1.

Table 1. Overview of catalytic hydrogenations of LA to GVL using heterogeneous catalysts and hydrogen

Catalyst	Typical conditions	LA conversion, %[a]	Ref.
Raney-Ni	320 bar, 250 °C	84	[15]
Rhenium-Heptoxide	150 bar, 106 °C, 1080 min	71	[16]
Pd on Calgon C	Dioxane, 55 bar	15.7	[17]
TA-NaBr-Modified reduced Ni	100 °C, water, 90 bar	-	[18]
Ru/C	150 °C, 34 bar, 240 min, dioxane	100	[19]
Ru/C	130 °C, 12 bar, 120 min methanol	92	[20]
Ru-Starbon	100 °C, 10 bar, ethanol /water, 130 min	> 95[b]	[21]
Ru/C	150 °C, water, 35 bar, WHSV= 288 min^{-1}	96	[22]

a. GVL is the main product unless stated otherwise b. 4-hydroxyvaleric acid (4-HVA) is the main product.

The largest screening study for LA hydrogenation using supported metal catalysts was carried out by Manzer et al.[19] The reactions were carried out using Ir, Rh, Pd, Ru, Pt, Re and Ni as the active metal on a carbon support in dioxane (150 °C, 120 min reaction time, 55 bar). By far the highest GVL selectivity was obtained with Ru; Ir, Rh and Pd were also active but the selectivity to GVL was low. This has stimulated considerable interest in the use of supported Ru catalysts for the reaction (Table 1). Typically, the reactions with Ru/C are carried out at 100 – 150 °C, hydrogen pressures between 1 and 35 bar, and, reaction times between 20 min. and 4 hrs. At these conditions, the LA conversions are high (> 92%) and the main product is reported to be GVL. The only exception is the work of Clark, showing that in water/ethanol mixtures, 4-hydroxyvaleric acid (4-HVA) is the main product. Other possible reaction products are pentanoic acid, methyl-THF and 1,4-pentanediol. However, it appears that more severe conditions are required for these conversions and catalysts other than Ru/C are preferred.[3, 23]

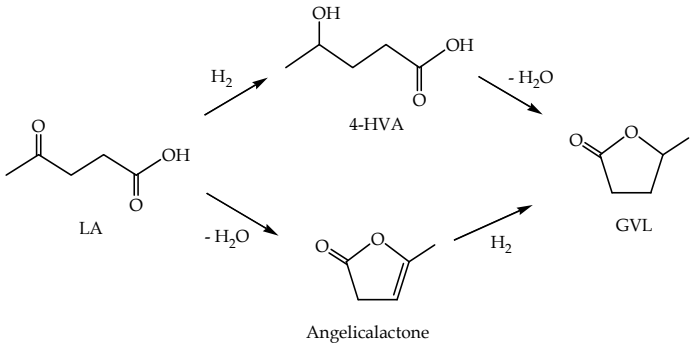

Scheme 1. Hydrogenation pathways for LA to GVL

The support of choice appears to be active carbon, most likely because it has a low acidity. It is well known that levulinic acid dehydrates at moderate temperatures to yield the corresponding cyclic product (α-angelicalactone, see Scheme 1). The latter is known to polymerize on acidic surfaces leading to deactivation of the catalyst.[22] A variety of solvents has been tested, ranging from dioxane to alcohols, alcohol water mixtures and pure water (Table 1). However, it is difficult to use the literature data to assess solvent effects on the reactions as different experimental conditions, reactor types and catalyst preparation procedures were applied.

The reaction typically involves the hydrogenation of LA to 4-hydroxypentanoic acid followed by ring-closure and the formation of GVL (Scheme 1). In acidic environments, α-angelicalactone may also be involved in the reaction sequence (Scheme 1).

The aim of this work is to study hydrogenation of levulinic acid to GVL with Ru/C as the catalyst. The effects of various solvents on the LA conversion and GVL yield were determined under comparable conditions, allowing us to draw conclusions on solvent effects. Furthermore, the effects of process conditions such as temperature and catalyst intake on the GVL yield in water were explored in more detail. Finally, catalyst deactivation was probed by performing catalyst recycling experiments in a batch mode.

2.2. Experimental

2.2.1. Materials

Levulinic acid (purity > 98 %), deuterium oxide, D_2O (purity > 99 %) and Ru/C (5 %-wt loading on coal char based-carbon active; 19μm average particle size; 900 m^2/g surface area was purchased from Aldrich. 1,4-Dioxane (purity 99.5 %) was purchased from ACROS. 1-Methyl-2-pyrrolidinone, NMP (purity ≥ 99.5%) and ethanol (purity ≥ 99.5%) were purchased from Sigma-Aldrich. Hydrogen and nitrogen gases were from Hoek-Loos (purity 99.5%-v). All chemicals were used without purification.

2.2.2. Analytical procedures

^1H- and ^{13}C-NMR spectra were recorded on a Varian AMS 200 MHz spectrometer using D_2O as the solvent and tetramethylsilane (TMS) as the internal reference.

X-ray diffraction (XRD) analysis was conducted using a D8 Bruker x-ray diffractometer (Germany) at ambient temperature with filtered CuKα_1 radiation and a wavelength of 1.5404 Å. The 2θ scanning rate was 0.02° min^{-1}; 2θ ranged from 5° to 80°

The BET specific surface area of the samples was measured by a multipoint nitrogen adsorption–desorption method at liquid nitrogen temperature (-196 °C) with a Micromeritics Tri Star 3000 surface area analyzer. Samples were out-gassed under vacuum to remove the physisorbed water immediately before analysis.

2.2.3. Reactor set-up for the hydrogenation experiments

The hydrogenation reactions were performed in a 350 ml stainless steel batch autoclave (Büchi GmBH). The mantel of the autoclave is equipped with (electrically operated) heating rods and a cooling coil (using water) to enable temperature control. The reactor content is well mixed using a magnetically induced overhead stirrer equipped with a Rushton type impeller. The temperature and pressure in the reactor are measured online using a pressure indicator and a thermocouple placed in the liquid. The reactor is equipped with a dip-tube to allow for liquid sampling during reaction.

2.2.4. Typical example of a hydrogenation experiment

The autoclave was charged with the selected solvent (100 mL). Subsequently, LA (7,370 mg, 63.5 mmol) and Ru/C (0.07 g, 1.0 wt% on LA) were added. The stirrer was started (2000 rpm) and the reactor was purged three times with nitrogen. The mixture was heated to 90 °C in about 30 min and subsequently hydrogen was charged to the reactor to a pressure of about 10 bars to saturate the solution with hydrogen. After 10 minutes, the pressure was increased to 45 bar by hydrogen addition and this point was taken as the start of the reaction. During reaction, hydrogen was admitted to the reactor to keep the pressure at 45 bar. After 60 minutes, a liquid sample was taken from the reactor. The sample was analyzed by ^{1}H-NMR to determine the conversion of LA and the amount of 4-HVA and GVL. Subsequently, the autoclave was cooled to room temperature and vented to atmospheric pressure.

2.2.5. Catalyst recycling experiments in water

The autoclave was charged with water (100 mL), LA (7.37 g, 63.5 mmol) and Ru/C (0.07 g, 1.0 wt% on LA). Subsequent reaction and analysis were performed as described above. After cooling down and depressurizing, the reaction mixture was allowed to settle and the Ru/C catalyst was filtered using filter paper (Ederol No. 2182). The catalyst was re-charged to the batch autoclave together with LA (7,370 mg, 63.5 mmol) dissolved in fresh water (100 ml). The reaction was performed under similar conditions as described above. After 60 min reaction, a liquid sample was taken from the reactor and subsequently analyzed by ^{1}H-NMR.

2.2.6. Concentration and conversion calculations from ^{1}H-NMR data

The concentrations of LA, 4-HVA and GVL in the reaction mixture were determined by ^{1}H-NMR. A sample was taken from the reactor and subsequently dissolved in D_2O. The characteristic peak intensities representing the methyl group of the three major components were used for this purpose. The three methyl group peaks are present as a singlet at δ 2.2 ppm, a doublet at δ 1.0 ppm and a doublet at δ 1.4 ppm for LA, 4-HVA and GVL, respectively. With this information and assuming that GVL and 4-HVA are the sole products *(vide infra*) the LA conversion (X_{LA}) may be calculated using eq. 1:

$$X_{LA} = \frac{c_{LA,0} - c_{LA}}{c_{LA,0}} = \frac{c_{GVL} + c_{HVA}}{c_{LA} + c_{GVL} + c_{HVA}} \quad (1)$$

Here c_i is concentration of component *i* in solution and $C_{LA,0}$ the initial concentration of LA.

The selectivities to GVL (S_{GVL}) and 4-HVA (S_{HVA}) were calculated using the following equation:

$$S_i = \frac{c_i}{c_{LA,0} - c_{LA}} \quad (2)$$

2.3. Results and discussion

2.3.1. Solvents screening

In the first stage of the project, four different polar solvents were tested (water, dioxane, ethanol and NMP) for the hydrogenation of LA with a Ru/C catalyst (5 wt% Ru on C). Experiments were carried out at 90 °C with 45 bar of hydrogen gas at a stirring speed of 2000 rpm for either 60 min or 330 min. An overview of the experiments and the composition of the reaction mixture after the reaction are given in Table 2.

Clearly, the highest conversion of LA was observed in water and essentially quantitative conversion was obtained after 60 min. The reactions are considerably slower when using ethanol (69% conversion) and dioxane (5% conversion), whereas activity in NMP is only 14% after 330 min. Liu *et al*.[20] reported a LA conversion of 92% when working in methanol as the solvent, using Ru/C as the catalyst and a reaction time of 160 min. More severe conditions (130 °C) and higher catalyst intakes (5 wt% on LA) were applied in the literature, indicating that water is a better solvent for the reaction than methanol when considering catalyst activity.

Table 2. Solvent effects on the hydrogenation of LA using a Ru/C catalyst[a].

No	Ru/C intake (%-wt on LA)	Solvent	t, min	X_{LA} (%)	S_{GVL} (%)
1	2.0	NMP	330	14	100
2	2.0	Dioxane	330	74	100
3	1.0	Dioxane	60	5	100
4	1.0	Ethanol	60	69	100
5	1.0	Water	60	99	78

[a]. solvent intake 100 ml, LA intake 7.37 g, 45 bar and 90 °C.

GVL was the sole product detected when working in all solvents, except when using water. Here, GVL was the main product, though considerable amounts of the intermediate 4-HVA were present as well (Scheme 1). A similar observation was made very recently by Clark et al,[21] for the hydrogenation of LA using Ru-Carbon catalysts in ethanol/water mixtures. For reactions at 100°C in a mixture of ethanol/water, 4-HVA was the major product (Table 2). Based on activity considerations and the possibility to steer the reaction to either GVL or 4-HVA, water was used as solvent for further investigation on the hydrogenation of LA with a Ru/C catalyst.

2.3.2. LA hydrogenations

In a subsequent study, the effect of process conditions on the LA hydrogenation in water with the Ru/C catalyst was investigated. An overview of experiments is given in Table 3.

For the reaction at base conditions, though a reaction time of 60 min, the concentration of the various components versus batch time was determined by ^{1}H-NMR (Figure 1). The labeling scheme for the hydrogen atoms is given in Scheme 2.

Table 3. Overview of experimental conditions for the hydrogenation of LA

Process Variable	Base Condition	Range
T, ^{0}C	90	50 - 140
P, bar	45	-
Agitation rate, rpm	2000	200 - 2000
Catalyst intake, %-wt on LA	1.0	0.05 - 3.00
LA intake, gram	7.37	-
Reaction time, min	30	0 - 60
Solvent	water	-

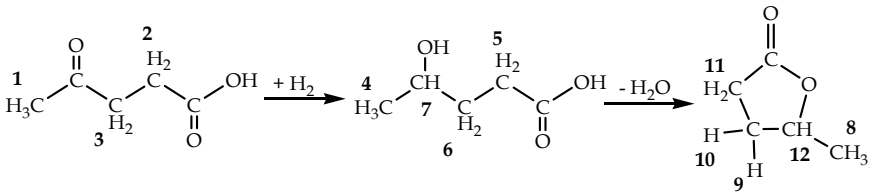

Scheme 2. Atom labeling scheme for LA, 4-HVA and GVL

The ^{1}H-NMR spectra indicate that the reaction proceeds via the intermediate 4-HVA with characteristic resonances at δ 1.04 ppm (Me group 4), δ 1.61 ppm (CH_2 group 5), δ 2.30 ppm (CH_2 group 6) and δ 3.70 ppm (CH group 7). Characteristic resonances of angelicalactone, e.g. at δ 3.17 ppm (CH_2 group), resulting from the dehydration of levulinic acid (Scheme 1) were not observed.

The concentration-time profiles were determined experimentally and the results for methyl base case are provided in Figure 2. The conversion of LA was complete within 50 min reaction time, giving an average turnover number of 298 g LA/g cat h. The highest concentration of 4-HVA was observed after 20 min (Figure 2). Prolonged reaction times resulted in an increase in the amount of GVL, a clear

indication that the reactions proceeded via a consecutive reaction pathway. The relatively high concentrations during a run of 4-HVA is likely caused by the presence of water, which is expected to reduce the rate of the reaction from 4-HVA to GVL due to equilibrium considerations.

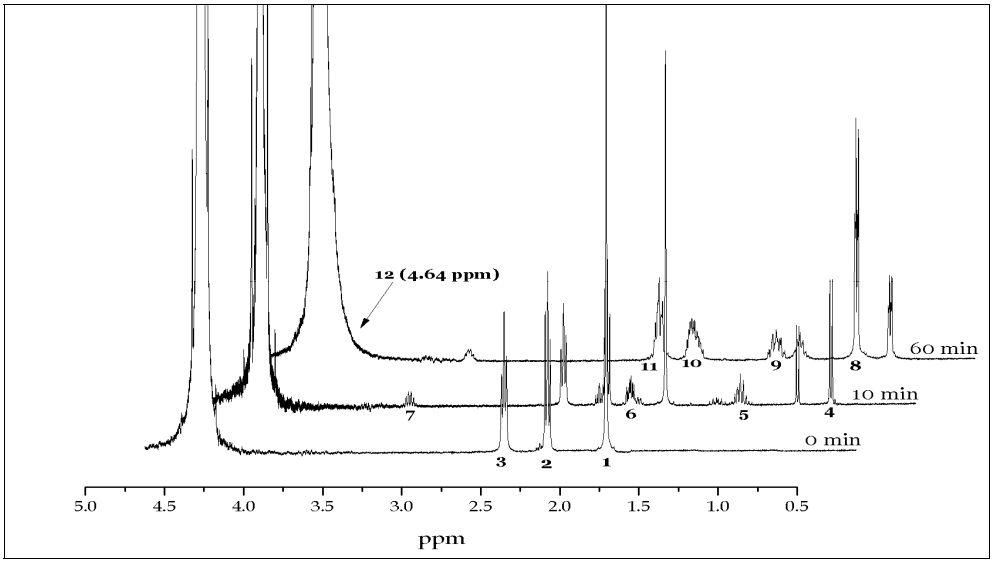

Figure 1. ^{1}H-NMR spectra (D_2O) at various reaction times for the hydrogenation of LA with Ru/C in water. Peak assignments are given in Scheme 2.

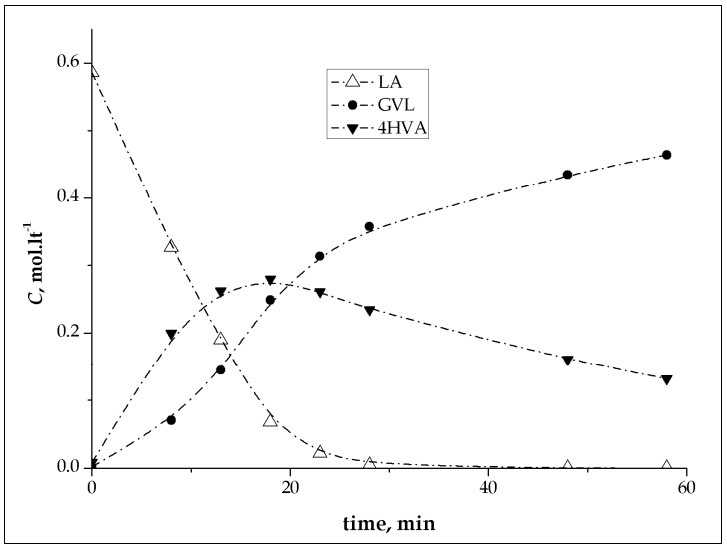

Figure 2. Reaction profile for the hydrogenation of LA in water using a Ru/C catalyst. Conditions: see Table 3 for base conditions, except 60 min reaction time instead of 30 minfor the base case.

Subsequent hydrogenation reactions of GVL to for instance 1,4-pentanediol or methyltetrahydrofuran (MTHF) were not observed under the conditions employed.[7, 24-25]

2.3.3. Optimization study of the LA hydrogenation

Effect of stirring rate. The catalytic hydrogenation of LA acid in water using a Ru/C catalyst is an example of a three phase gas-liquid-solid reaction. As such, the conversion rates and product selectivities may be biased by mass transfer limitations

of hydrogen and, though less likely, also by that of LA and products. To assure that the results are not affected by mass transfer limitations of hydrogen and particularly gas-liquid mass transfer, the effect of stirring rate on X_{LA} was determined at base case conditions. The results are given in Figure 3.

The graph clearly indicates that the conversion is a function of the agitation rate when the stirring rate is below 1400 rpm. Above 1400 rpm, the conversion is relatively constant. These results imply that the overall conversion rate is biased by mass transfer of hydrogen when the agitation rate is below 1400 rpm. Thus, to avoid such effects, the reactions need to be performed at stirring rates exceeding 1400 rpm and 2000 rpm was used throughout all subsequent experiments.

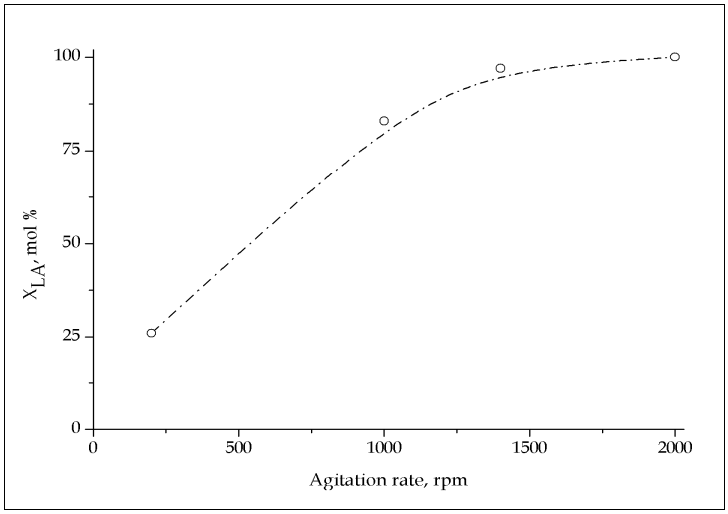

Figure 3. Effect of the stirring rate on the LA conversion. Conditions are given in Table 3 (base case).

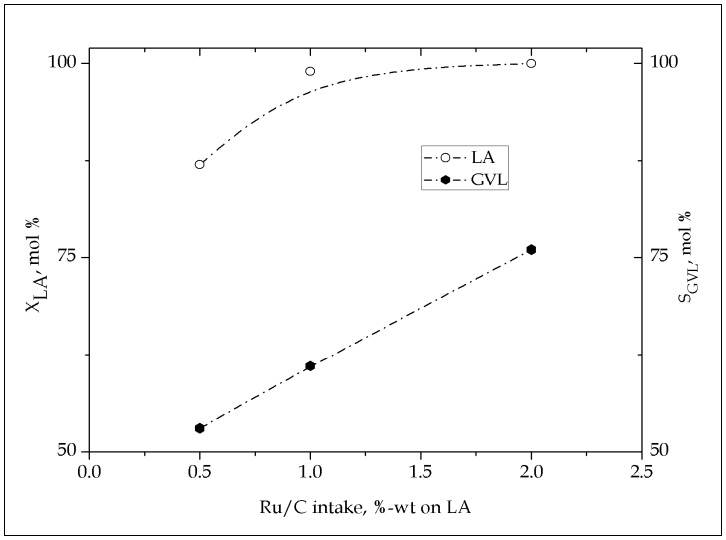

Figure 4. Effect of catalyst intake on X_{LA} and S_{GVL}. Conditions are given in Table 3

Effect of catalyst intake. The effect of catalyst intake on LA conversion and product selectivity was determined for three different catalyst intakes (0.5, 1 and 2 wt% on LA). All other conditions were set at the base conditions as given in Table 3. As expected, the conversion increased with higher catalyst intakes, though is

essentially quantitative for both 1 and 2 wt% catalyst intake (Figure 4). The selectivity for GVL is a clear function of the catalyst intake. At higher intakes, the GVL yield increases at the expense of 4-HVA, in line with the proposed consecutive reaction pathway.

Effect of temperature. Temperature effects on the LA conversion rate and product selectivity were determined for three temperatures in the range 50-140 °C. All other conditions were set at the base conditions as given in Table 3. The results are shown in Figure 5.

Figure 5 clearly implies that temperature has a strong effect on the conversion of LA into 4-HVA and GVL. When going from 50 °C to 140 °C, the LA conversion increases from 76 to 100%. On the basis of these experiments we can conclude that the hydrogenation reaction in water is already occurring at a reasonable rate at 50 °C, which indicates that Ru is a very efficient catalyst for the hydrogenation of ketone moieties. The product distribution is also a strong function of the temperature. At the lowest temperature in the range, 4-HVA is essentially the main product, whereas at 140 °C, the opposite holds and the selectivity for GVL increases to 100%. Thus, proper temperature selection allows for the near selective synthesis of either GVL or 4-HVA. As such, the catalytic hydrogenation of LA in water at low temperatures may be a very efficient synthetic methodology to synthesize 4-HVA.

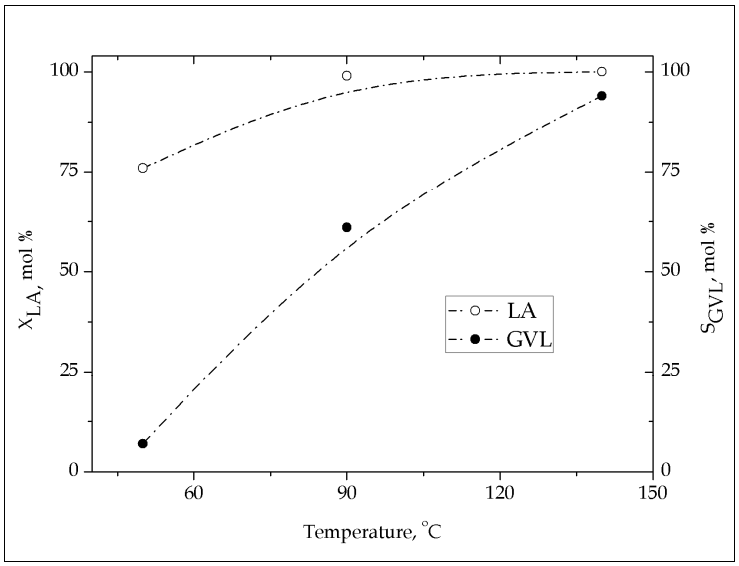

Figure 5. Effect of temperature on X_{LA} and S_{GVL}. See Table 3 for conditions.

The experimentally observed effect of the temperature on the product selectivity indicates that the activation energy for the hydrogenation reaction is considerably lower than for the subsequent cyclisation reaction. Detailed kinetic studies including activation energies for both the hydrogenation of LA to 4-HVA and the subsequent cyclisation reaction to support this statement are in progress.

2.3.4. Catalyst recycling

To gain insights in the stability of the Ru/C catalyst, a number of catalyst recycling experiments were performed. After the first reaction at standard

conditions (Table 3), the Ru/C catalyst was isolated from the reaction mixture and recharged to the autoclave. The autoclave was again filled with solvent and LA, and a second reaction was performed at similar conditions as for the first one. The results regarding LA conversion and GVL selectivity are given in Figure 6.

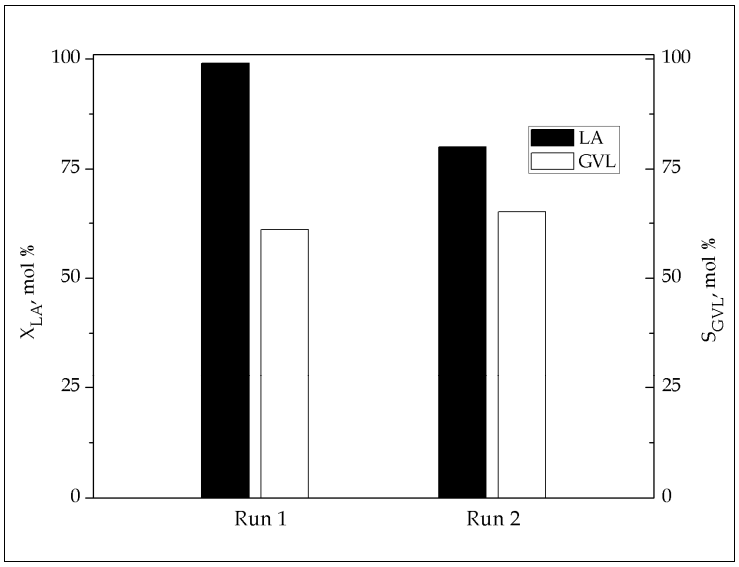

Figure 6. Catalyst recycling experiments. Conditions are given in Table 3 (base case).

The conversion of LA for the second run (80%) was lower than for the first run (99%). The selectivity for GVL in the first run was 54%, the only other product being the intermediate 4-HVA. For the second run, the selectivity was similar to that of the first run. The decrease in activity for the second run is indicative for some catalyst deactivation during the first run. These results are in line with recent data from Liu *et al.*[20] for the hydrogenation of LA to GVL in methanol using Ru/C as the catalyst. Here a drop in catalyst activity from 92% conversion for the first run to 61% conversion for the second run was observed in a batch reactor set-up. However, Manzer[19] reported that the Ru/C catalyst showed no sign of deactivation in recycling studies when using dioxane as the solvent, though no quantitative data were given. This indicates that the solvent may have an effect on possible deactivation pathways, though differences in support type (surface area, pore size distribution) and catalyst preparation procedures (metal dispersion, metal precursors and trace elements) cannot be excluded *a priori*.

A possible explanation for catalyst deactivation is the involvement of α- and β-angelicalactone in the reaction sequence. Though not visible in the liquid phase during reaction (*vide supra*), these may be formed in low amounts and have affinity for the carbon support. Angelicalactones are prone to polymerization and this may occur to a significant extent on the catalyst surface. An indication that this indeed is a possible pathway was obtained from BET measurements of the catalyst before and after reaction. The BET of the catalyst after reaction (170 m^2/g) is considerably lower than the fresh catalyst (900 m^2/g). XRD measurements before and after reaction do not show significant differences.

Further studies in a dedicated flow reactor will be required to establish the long term stability of the catalyst.

2.4. Conclusions

Ru/C is an active heterogeneous catalyst for hydrogenation of LA to GVL in water. The activities exceed those in alcohols and other polar solvents and the catalyst is even active at 50 °C. Quantitative conversion of LA was observed after 30 min at 140 °C in water, with a GVL selectivity of 94%. Mass transfer issues, and particularly gas-liquid mass transfer of hydrogen should be taken into account when working at elevated temperatures, as was shown by experiments with a variable stirring speed. Product selectivity may be tuned to 4-HVA or GVL by adjusting the experimental conditions.

Further ongoing activities in our research group focus on determining the kinetics of the reaction for a broad experimental window to allow selection of the best operating conditions to obtain either 4-HVA or GVL in high selectivity. In addition, catalyst stability will be evaluated in long duration tests in a continuous set-up.

2.5. References

1. A. Corma, S. Iborra and A. Velty, *Chem. Rev.*, 107, 2411–2502 (2007)
2. T. Werpy and G. Petersen, *the National Renewable Energy Laboratory and the Pacific Northwest National Laboratory - US*, August 2004
3. R.H. Leonard,*Ind. Eng. Chem.*, 48, 1330-1341 (1956)
4. H. Mehdi, V. Fábos, R. Tuba, A. Bodor, L.T. Mika and I.T. Horváth, *Top. Catal.*, 48, 49–54 (2008)
5. W. Saiyasombat, R. Molloy, T.M. Nicholson, A.F. Johnson, I.M. Ward and S. Poshyachinda, *Polym.*, 39(23), 5581–5585 (1998)
6. C. Woo Lee, R. Urakawa and Y. Kimura, *Eur. Polym. J.*, 34(1), 117-122 (1998)
7. J.C. Serrano-Ruiz, D.J. Braden, R.M. West and J.A. Dumesic, *Appl. Cat. B: Environ.*, 100, 184–189 (2010)
8. K. Osaka, T. Ikariya and S. Yoshikawa, *J. Organomet. Chem.*, 231, 79-90 (1982)
9. T. Ohkuma, M. Kitamura and R. Noyori, *Tetrahedron Lett.*, 31(38), 5509-5512 (1990)
10. S.A. King, *J. Org.Chem.*, 59, 2253-2257 (1994)
11. T. Saito, T. Yokozawa, T. Ishizakis, T. Moroi, N. Sayo, T. Miura and H. Kumabayashi, *Adv. Synth. Catal.*, 343, 264-267 (2001)
12. E.L. Stangeland and T. Sammakia, *J. Org. Chem.*, 69, 2381-2385 (2004)
13. V. Starodubtseva, O.V. Turova, M.G. Vinogradov, L.S. Gorshkova and V.A. Ferapontov, *Russ. Chem. Bull.* Int. Ed., 54(10), 2374-2378 (2005)
14. F.M.A. Geilen, B. Engendahl, A. Harwardt, W. Marquardt. J. Klankermayer and W. Leitner. *Angew. Chem.* Int. Ed., 49, 5510-5514 (2010)
15. B.A. Bruce, B. Woodrow and H.R. Henze, *J. Am. Chem. Soc.*, 61, 843-846 (1939)
16. H.S. Broadbent, G.C. Campbell, W.J. Bartley and J.H. Johnson, *J. Org. Chem.*, 24, 1847-1854 (1959)

17. L.E. Manzer, *WIPO*, WO 02/074760 A1 (2002)
18. T. Osawa, E. Mieno, T. Harada and O. Takayasu, *J. Mol. Cat. A; Chem.*, 200, 315-321 (2003)
19. L.E. Manzer, *Appl. Catal. A*, 272, 249–256 (2004)
20. Z-P. Yan, L. Lin and S. Liu, *Energ. Fuel.*, 23, 3853–3858 (2009)
21. R. Luque and J.H. Clark, *Cat. Comm.*, 11(10), 928-931 (2010)
22. J.C. Serrano-Ruiz, D. Wang and J.A. Dumesic, *Green Chem.*, 12, 574–577 (2010)
23. K. Folkerts and H. Adkins, *J. Am. Chem. Soc.*,54, 3570-3582 (1932)
24. L. Sun, D. Cao and G. Wang, *J. Appl Electrochem.*, 38, 1415-1419 (2008)
25. G. Lui, H. Zhang and J. Hu, *Electrochem.Comm.*, 9, 2643-2648 (2007)

Chapter 3
Experimental and kinetic modeling studies on the biphasic hydrogenation of LA to GVL using a homogeneous water-soluble Ru-(TPPTS) catalyst

Abstract

γ-Valerolactone (GVL) is considered a very attractive biomass derived platform chemical. This paper describes the use of biphasic homogeneous catalysis for the hydrogenation of levulinic acid (LA) to GVL using water soluble Ru-catalysts made in situ from $RuCl_3\,3H_2O$ and sodium-tris(*m*-sulfonatophenyl)phosphine (Na_3TPPTS) in dichloromethane/water biphasic mixtures. The hydrogenations were performed at mild conditions in a batch hydrogenation reactor and essentially quantitative GVL yields were obtained at 45 bar, 90 °C and 80 min reaction time (1 mol% catalyst). The effects of process variables like substrate concentration, hydrogen pressure, temperature, pH and the catalyst to substrate ratio on the LA conversion and GVL yield were determined. The experimental data were quantified by kinetic modeling and it was shown that the reaction is first order in LA. Catalyst recycle experiments show that the recycled catalyst is still active; though the activity is lower than for the first run (81% LA conversion for first run versus 55% for recycle experiment).

3.1. Introduction

Levulinic acid (LA) is considered an important bio-based platform chemical and may serve as a starting material for a wide range of interesting chemicals with a broad application range.[1] LA may be obtained in high yields by the acid catalyzed hydrolysis of the C6-sugars present in lignocellulosic biomass.[2]

A very attractive LA derivate is γ-valerolactone (GVL). It has potential as a solvent, as food additive[3,4] and as a biofuel, for instance as a substitute of ethanol in gasoline-ethanol blends.[4] GVL may also be converted to a number of interesting derivatives. Hydrogenation of GVL provides access to methyltetrahydrofuran (MTHF), which is a potential fuel additive.[5] The reaction with GVL and formaldehyde leads to the formation of α-methylene-γ-valerolactone (MGVL), a new acrylic monomer which may be converted to novel acrylic polymers with improved product properties (e.g. thermal stability).[6] Another interesting option is the ring-opening reaction of GVL with methanol followed by dehydration to produce (isomeric) methylpentenoates (MP)**.** These may be converted to well known bulk chemicals like caprolactone by hydroformylation, caprolactam by hydrocyanation or adipic acid by hydroxycarbonylation.[7] Recently, the conversion of GVL to 5-nonanone and subsequently to alkanes in the C_9 or C_{18}-C_{27} range has been reported.[8]

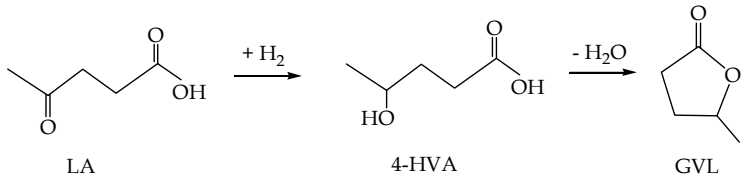

LA 4-HVA GVL

Scheme 1. Hydrogenation of LA to GVL

GVL is typically obtained from LA by stoichiometric reactions or catalytic hydrogenations.[8] The catalytic hydrogenation reactions, either starting with LA itself or its ester derivatives, may be carried out either using heterogeneous[10-14] or homogeneous catalysts. The intermediate 4-hydroxyvaleric acid (4-HVA) is not very stable and cyclisation to GVL occurs easily under mild reaction conditions (Scheme 1).

Excellent GVL yields (> 98%) have been reported for the hydrogenation of LA using a variety of Ru catalysts (Ru/C, [6,15] Ru/Al_2O_3.[16]) Recently, good results were obtained for catalytic transfer hydrogenation reactions with formic acid as the hydrogen source using Ru/C as the catalyst.[17]

Homogeneous catalysts have also been used for the hydrogenation of LA to GVL using both molecular hydrogen and formic acid as the reductants. Typically, ruthenium complexes with chelating phosphine ligands are applied. For hydrogen gas, Osakada *et al.* showed that $RuCl_2(PPh_3)_3$ is a good catalyst and 99% yield of GVL was obtained at 11.8 bar of H_2 pressure, 180°C during 24 hours.[18] Joo *et al.*[19,20] demonstrated the use of water-soluble homogeneous ruthenium catalysts (e.g. $HRuCl(Dpm)_3$, Dpm=diphenylphosphinobenzene-m-sulphonic acid) for the hydrogenation of oxo- and keto- acids. However, catalytic activity for the hydrogenation of keto-acids like LA was low. Chiral versions have also been

developed, e.g. by using Ru-BINAP complexes.[21,22] For instance, ethyllevulinate was converted to GVL using a Ru-BINAP complex obtained *in situ* from $Ru(acetate)_2BINAP$ with 2 equiv. of HCl at 25 °C in ethanol using 1000 bar of hydrogen in 96% chemical yield and >99% ee with only 0.1 mol% of catalyst. The latter example nicely illustrates the potential of homogeneous catalysts for the synthesis of GVL, i.e. the possibility to obtain high reaction rates and selectivities at less severe reaction conditions than needed for heterogeneous analogues.

Recently, the potential of homogeneous transfer hydrogenations with formic acid was also demonstrated. For instance, Horvath *et al.*[23] applied a homogeneous Ru compound $[(\eta^6\text{-}C_6Me_6)Ru(bpy)(H_2O)][SO_4]$ in water for the transfer hydrogenation of LA using formic acid as the hydrogen donor. Both GVL and 1,4-pentanediol were obtained in 25% yield. Improved GVL yields (up to 94%) were reported using $RuCl_3.3\ H_2O$ in combination with PPh_3 and a base (150-200 °C, solvent free).[24]

A drawback of the use of homogeneous catalysts with limited activity is the necessity for catalyst recycles to improve the economic viability of the process. A possible solution is the application of biphasic catalysis, where the catalyst is present in a second phase after and usually during reaction, and easily separated from the product and recycled.[25-27] A well known approach in homogeneous hydrogenation reactions is the use of aqueous/organic biphasic systems using water soluble ruthenium complexes with sulfonated phosphine ligands like tris(*m*-sulfonatophenyl)phosphine (TPPTS). Examples are the biphasic hydrogenation of α-β-unsaturated aldehydes,[28] aromatic and aliphatic nitriles,[29] alkenes and aromatics,[30] and model compounds of fast pyrolysis oil (vanillin, *iso*-eugenol and acetoguaiacone).[31] The biphasic hydrogenation of LA is to the best of our knowledge not reported in the literature. In this paper the feasibility of a biphasic hydrogenation of LA to GVL in a biphasic water/organic solvent system using the water soluble $RuCl_3$/TPPTS catalyst will be explored. The effect of process conditions on catalyst activity and stability has been determined and will be reported. Based on the experimental data, a kinetic model was developed. The possibility of effective catalyst recycling has also been studied.

3.2. Experimental

3.2.1. Materials

LA was purchased from Sigma Aldrich (purity > 98%). $RuCl_3.3H_2O$ (purity 99%) and Na_3TPPTS were provided by Riedel-de Haen and Strem, respectively. Dichloromethane (DCM) was obtained from Lab Scan (analytical grade, purity 99%). $Na_2HPO_4.12H_2O$, HCl and NaOH were obtained from Merck Chemicals. Hydrogen and nitrogen gas were purchased from Hoek-Loos (purity 99.5%-v). All chemicals were used without further purification.

Buffer solutions were prepared using standard procedures[32] by dissolving the appropriate amount of the phosphate salts in reverse osmosis water (pH 7.0 & 9.0: 0.1 M Na_2HPO_4 and 0.1 M HCl; pH 11.0: 0.1 M Na_2HPO_4 and 0.1 M NaOH). Experiments at neutral pH were performed in deionised water.

3.2.2. Analytical procedures

^{1}H- and ^{13}C-NMR spectra were recorded on a Varian 200 MHz spectrometer using $CDCl_3$ as the solvent and tetramethylsilane (TMS) as an internal reference.

The composition of the aqueous phase after the partitioning experiments (*vide infra*) was analyzed using HPLC. A HPLC apparatus consisting of a Hewlett Packard 1050 pump, a Bio-Rad organic acid column (Aminex HPX-87H) and a Waters 410 refractive index detector was used. The mobile phase consisted of an aqueous solution of sulfuric acid (5 mmol/l)) operated at a flow rate of 0.55 ml.min^{-1}. The column was operated at 60 °C. The amounts of LA and GVL were calculated using calibration curves obtained from standard solutions of known concentrations.

3.2.3. Reactor set-up for hydrogenation experiments

The hydrogenation reaction was performed in a 350 ml stainless steel batch autoclave (Buchi GmBH). The autoclave is electrically heated and, when appropriate, may be cooled using water. The reactor content is stirred with an overhead stirrer, equipped with a *Rushton* type impeller. The reactor is equipped with a pressure indicator and a thermocouple to measure the temperature inside the reactor.

3.2.4. Typical example of a catalytic hydrogenation reaction

The autoclave was charged with Na_3TPPTS (90.4 mg, 0.15 mmol) in DCM (100 mL). Subsequently, LA (1.5 ml, 1,740 mg, 15.0 mmol), $RuCl_3.3H_2O$ (38.1 mg, 0.15 mmol) and water (25 mL) were added. The stirrer was started (2000 rpm) and the reactor was purged three times with nitrogen. The mixture was heated to 90 °C (about 30 min) and then hydrogen was charged to the reactor to a pressure of about 10 bar to saturate the solution with hydrogen and to form the active catalyst from the precursors (TPPTS and $RuCl_3.3H_2O$).[28] After about 10 minutes, the pressure was increased to 45 bar by hydrogen addition and this point was taken as the start of the reaction. During reaction, hydrogen was admitted to the reactor to keep the pressure at 45 bar. After 60 minutes, a sample was taken from the reactor by a dip tube. The organic and water phase were allowed to settle and the organic phase was analyzed by NMR to determine the conversion of LA and the yield of GVL. Subsequently, the autoclave was cooled to room temperature and vented to atmospheric pressure.

3.2.5. Typical example for a kinetic hydrogenation experiment

The experiments were carried out as describe above. During the reaction, samples were withdrawn from the reaction mixture by a dip tube at pre-determined time intervals. The organic and water phase in the samples were allowed to settle and the organic phase was analyzed by NMR to determine the conversion of LA and the GVL yield.

3.2.6. Determination of the partitioning coefficient of LA and GVL in water/DCM mixture

The experiments were performed by addition of LA (1.5 ml, 1,740 mg, 15.0 mmol) or GVL (1.5 ml, 1,580 mg, 15.6 mmol) into a solvent mixture consisting of

water (25 mL) and DCM (75 mL) in a stainless steel batch autoclave equipped with an overhead stirrer and a dip-tube for sampling. The mixture was purged three times by nitrogen gas. The contents were heated to 90 °C, the nitrogen pressure was increased to 20 bar to avoid excessive solvent evaporation, and the mixture was stirred for 30 min under vigorous stirring (2000 rpm). After 30 min, the stirrer was stopped to induce phase separation. After 30 min, a sample of the aqueous phase was taken using the dip-tube and analyzed by HPLC to determine the LA (or GVL) content.

3.2.7. Catalyst recycling experiments

$RuCl_3.3H_2O$ (38.1 mg, 0.15 mmol) dissolved in water (25 mL) and LA (1.54 ml, 1,740 mg, 15 mmol) dissolved in DCM (75 ml) were charged to the batch autoclave. Subsequent purging, heating and hydrogen addition were performed as described above. After 60 minutes, a sample was taken from the reactor by a dip tube. The organic and water phase in the sample were allowed to settle and the organic phase was analyzed by NMR to determine the conversion of LA and the GVL yield. Subsequently, the autoclave was cooled to room temperature and vented to atmospheric pressure. Both phases were allowed to settle and the light-brown aqueous phase containing the Ru-TPPTS catalyst was collected. This solution was again charged to the batch autoclave together with LA (1.54 ml, 1,740 mg, 15 mmol) dissolved in DCM (75 ml). The reaction was performed under similar conditions as described above. After 60 min reaction, a sample was taken from the reactor and subsequently analyzed by ^{1}H-NMR.

3.2.8. Concentration and conversion calculations from ^{1}H-NMR data

The LA conversion and the concentration of LA in water were determined using the composition of the organic phase as determined by ^{1}H-NMR. The LA conversion (X_{LA}) is defined as:

$$X_{LA} = \frac{n_{LA,0} - n_{LA}}{n_{LA,0}} = \frac{n_{GVL,org}}{n_{LA,0}} = \frac{n_{GVL,org}}{n_{GVL,org} + n_{LA}} \quad (1)$$

Here $n_{LA,0}$ is the initial intake of LA (in mole), $n_{GVL,org}$ the number of moles of GVL in the organic phase and n_{LA} the sum of the number of moles of LA in the aqueous and organic phase. In here, it is assumed that 1 mole of LA is converted to 1 mole of GVL (in line with the stoichiometry and selectivity of the reaction, *vide infra*), that LA distributes between both phases and that the GVL resides only in the organic phase. The latter is justified by partitioning experiments carried out for GVL in water-DCM mixtures (*vide infra*). These experiments also show that LA is soluble in both the organic and the aqueous phase and distributes between both phases (*vide infra*). The conversion is calculated from ^{1}H-NMR spectra of the organic phase (*vide infra*). To eliminate the concentration of LA in the waterphase in eq. 1, the mol balance for LA over both phases (eq. 2) was combined with the definition of the partitioning coefficient of LA (m_{LA}) (eq. 3).

$$n_{LA} = n_{LA,org} + n_{LA,aq} \quad (2)$$

$$m_{LA} = \frac{n_{LA,org}.V_{aq}}{n_{LA,aq}.V_{org}} = \frac{n_{LA,org}}{n_{LA,aq}}.\theta \quad (3)$$

$$\text{where } \theta = \frac{V_{aq}}{V_{org}} \quad (4)$$

Elimination of $n_{LA,aq}$ by substitution of eq. (2) into (3) leads to:

$$n_{LA} = a.n_{LA,org} \quad (5)$$

$$\text{where } a = \left[\frac{m_{LA} + \theta}{m_{LA}}\right] \quad (6)$$

Thus the conversion of LA is as follows:

$$X_{LA} = \frac{n_{GVL,org}}{n_{GVL,org} + a.n_{LA,org}} \quad (7)$$

The $X_{LA}$was calculated by integration of the ^{1}H-NMR spectra of the organic phase by rewriting eq. 7:

$$X_{LA} = \frac{I_{GVL,org}}{I_{GVL,org} + a.I_{LA,org}} \quad (8)$$

where I_i is the normalized area of one of the H atoms of component *i*. The concentration of LA in water ($C_{LA,aq}$), which is important input for the kinetic modeling, was determined using the conversion definition (eq. 1) and the definition of the partitioning coefficient for LA (eq. 3). This leads to:

$$C_{LA,aq} = \frac{n_{LA,0}}{V_{aq}}\left[\frac{\theta}{\theta + m_{LA}}\right](1 - X_{LA}) \quad (9)$$

The initial rate of the reaction was determined from a plot of the concentration of LA in the aqueous phase versus reaction time. The profile was fitted by a fourth-order polynomial function using the *Polymath* software package. The initial rate was obtained by differentiation of the polynomial function and evaluation of this function at t = 0.

3.2.9. Kinetic modeling

The experimental concentration profiles were modeled using the Matlab® programming platform using the numerical integration toolbox *ode45*. The kinetic parameter values were determined by minimization of the sum of squared errors between all experimental data and the simulated data from the kinetic model.[22] Error minimization was performed using the Matlab® toolbox *fminsearch,* which is based on the Nelderl-Mead optimization method.

3.3. Results and Discussion

3.3.1. LA hydrogenation in a biphasic system using $H_{2hydrogen}$ and a Ru-TPPTS

All reactions were carried out in a biphasic system consisting of water and dichloromethane. The effect of important process variables (reaction temperature, pH, substrate concentration, catalyst concentration, hydrogen pressure) on the LA conversion was determined. An overview of the base case conditions and the range

of process variables studied are given in Table 1. The catalyst was made in situ by adding the individual components (RuCl3.3H2O and sodium-tris(m-sulfonatophenyl)-phosphine (Na3TPPTS)) to the reaction mixture instead of an ex-situ preparation procedure. This facilitates the experimental procedures considerably and has shown to lead to equal reactivity.31 The use of a co-solvent or phase transfer agent to transfer the LA from the organic to the water phase is not necessary as LA is partly soluble in water (vide infra). After reaction, the reaction mixture was biphasic in nature and consisted of a light brown water phase and a slightly yellow organic phase.

The conversion of LA in the course of the reactions was monitored by taking samples at regular time intervals and subsequent analyses of the organic phase by ^{1}H-NMR. A representative example of a typical experiment (at base conditions) is given in Figure 1. Clearly visible is the appearance of the methyl group of GVL as a doublet at δ 1.4 ppm and the disappearance of the characteristic methyl group adjacent to the ketone moiety of LA at δ 2.2 ppm.

Selectivity towards GVL appears to be very high and near quantitative, as confirmed by NMR and GC analyses of the organic phase and HPLC analyses of the aqueous phase. The intermediate 4-hydroxyvalericacid (4-HVA) was not observed (Scheme 1), a clear indication that the subsequent lactonisation of 4-HVA to GVL is very fast in the system.[33,34] Subsequent hydrogenation products like methyltetrahydrofuran and pentanoic acid were also not detected under the mild reaction conditions employed.

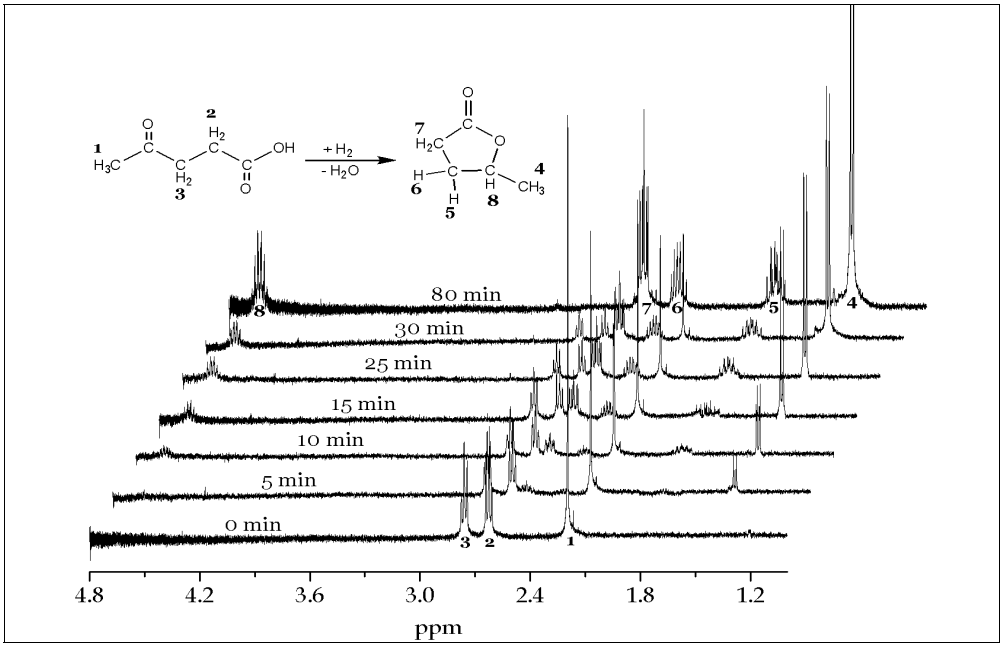

Figure 1. ^{1}H NMR spectra in $CDCl_3$ of a representative LA hydrogenation run in DCM/water using a Ru-TPPTS catalyst (base case Table 1)

The conversion of LA after 60 min for an experiment at standard conditions as in Table 1 was 82%. This corresponds with an average turnover frequency (TOF)

of about 100 mol.mol cat.$^{-1}$ h^{-1}. The initial turnover frequency was determined from the initial reaction rate and was about 170 mol mol cat^{-1} h^{-1}.

Table 1. Base case and ranges of process variables

Process Variable	Base Condition	Experimental Range
Pressure of H_2, bar	45	5 – 45
Reaction time, min	60	30-200
Phase ratio θ	0.25	-
Organic solvent	DCM	-
Stirring speed, rpm	2000	200 - 2000
Temperature, ^{0}C	90	50 – 115
Substrate/catalyst ratio, mmol/mmol	100	67 – 520
TPPTS/Ru ratio	1.0	-
pH	7	7.0 - 11.0

The reproducibility of the reaction was checked by performing the experiment at base conditions (Table 1) twice. The LA conversion was 82 and 81%, respectively, indicating that the reproducibility is good.

3.3.2. Optimization study of LA hydrogenation with RuTPPTS catalyst

Mass transfer limitations. The system under study is a three-phase G-L-L system, consisting of hydrogen gas, an aqueous phase with the homogeneous catalyst and an organic phase with the product. The LA distributes between both liquid phases (*vide infra*). In such a multiphase reactive system, the overall conversion rate may be limited by among others gas-liquid mass transfer of hydrogen gas and transfer of substrates between both liquid phases. To determine the intrinsic kinetics, it is advantageous to perform the experiments in the kinetic regime. To gain insights in possible mass transfer effects, some experiments were performed at different agitation rates while keeping all other variables at base conditions (Table 1). The conversion of LA for a 60 min reaction is given in Figure 2 as a function of the stirring speed.

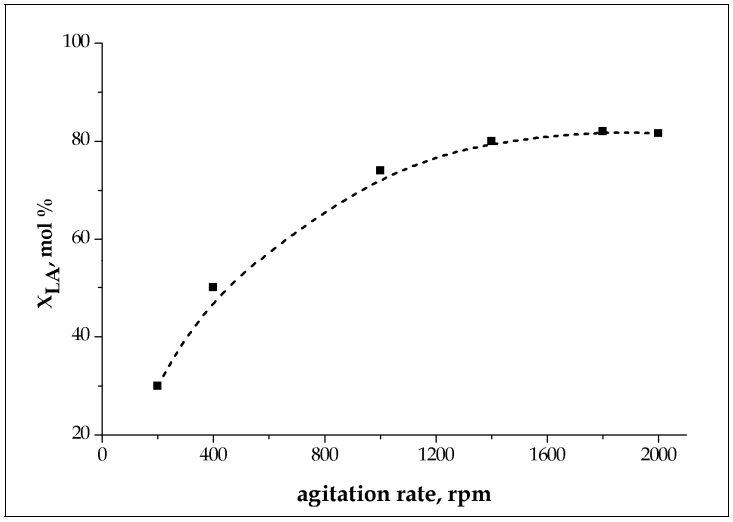

Figure 2. Conversion of LA at various agitation rates after 1 h. All other variables are at base conditions (Table 1).

The X_{LA} is evidently a function of the agitation rate when the agitation rate is below 1400 rpm. This implies that the reactions below 1400 rpm are affected by mass transfer effects. Above 1400 rpm, the $X_{LA}$is essentially independent of the stirring rate, an indication that these experiments were performed in the kinetic regime. All further experiments were performed at 2000 rpm to ensure that the hydrogenation reactions take place in the kinetic region.

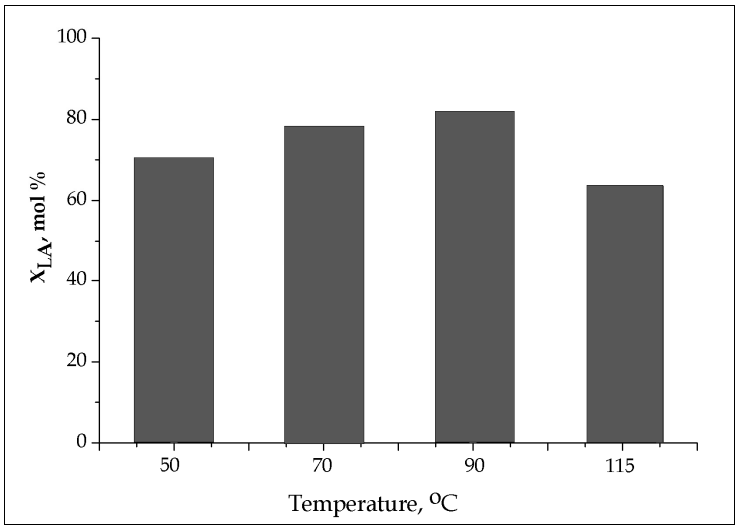

Figure 3. Effect of temperature on the conversion of LA after 60 min reaction time. Conditions: see Table 1 for base conditions.

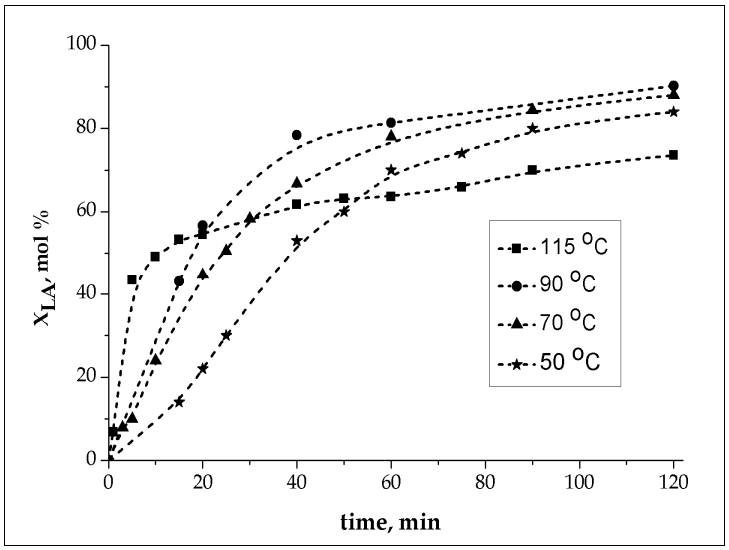

Figure 4. LA conversion versus time at different temperatures. Conditions: see Table 1 for base conditions

Effect of temperature. The effect of temperature on the X_{LA} was determined in the range 50-115 °C. All other conditions were set at base conditions as given in Table 1. The conversion of LA for a 60 min reaction time at different temperatures is given in Figure 3. It is clear that the hydrogenation reaction is very sensitive to the temperature. The LA conversion increases till about 90 °C (81%), at higher

temperatures the conversion is considerably lower. This is indicative for the occurrence of catalyst deactivation at elevated temperatures. This is further confirmed by considering the LA hydrogenation profile (Figure 4).The initial reaction rate is highest at the highest temperature in the range. However, after about 10 minutes, a rapid decay of catalyst activity is observed, likely due to catalyst deactivation. Similar observations were reported for related hydrogenations using the Ru-TPPTS system. Heinen *et al.*[35] studied the hydrogenation of D-fructose in aqueous systems and found that catalyst deactivation and the formation of Ru(0) particles (XRF) occurs easily above 90 °C. Mahfud *et al.*[31] reported the use of the Ru-TPPTS catalyst for the biphasic hydrogenation of vanillin to creosol in a water/DCM mixture and found that catalyst activity levels off above 60 °C. These examples indicate that the stability of the Ru-TPPTS catalysts is limited, though the temperature at which deactivation occurs to a considerable extent seems to be reaction-specific.

Effect of substrate concentration. The effect of the initial LA concentration on the reaction rate was determined at a fixed catalyst intake. All other experimental conditions were set at base conditions (Table 1), except that the temperature was set at 70°C to avoid excessive catalyst deactivation (Figure 4).

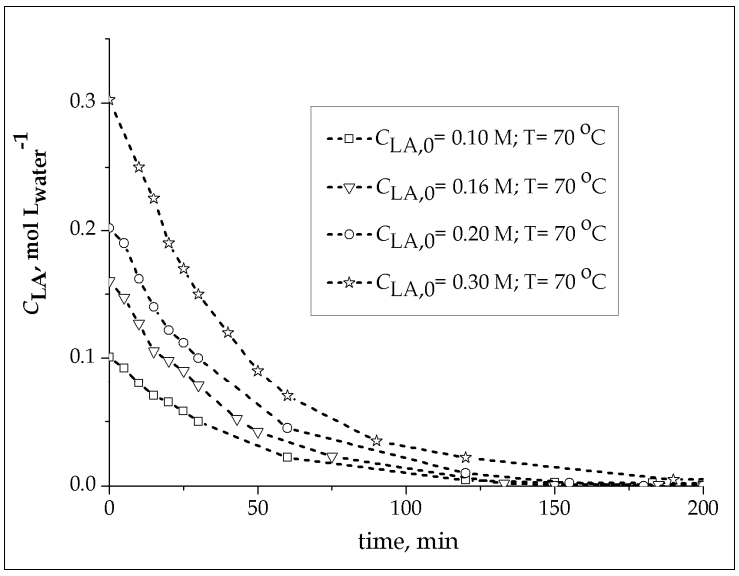

Figure 5. LA concentrations in water versus time for various initial LA concentrations. Conditions: see Table 1 for base conditions, except T = 70 °C

Typical concentration-time profiles are given in Figure 5 for four different initial LA concentrations. Four initial LA conversion rates may be determined from these profiles. This allows evaluation of the reaction order in LA by using the following equation:

$$R_{LA,water,0} = -k.C^{\alpha}_{LA,water,0} \quad (10)$$

Here, the subscript 0 is related to initial conditions, k is the observed kinetic constant and α the reaction order in LA. The concentrations and rates are evaluated for the water phase, as this is expected to be the locus of the chemical reaction (*vide infra*).

Equation 10 may be rewritten as:

$$\ln(-R_{LA,water,0}) = \ln k + \alpha.\ln(C_{LA,water,0}) \quad (11)$$

The experimental data for the hydrogenation at four initial LA concentrations at 70 °C, are plotted according to equation 10 and the results are given in Figure 6. The figure shows that the reaction is approximately first order in LA concentration with a k value of 0.025 min^{-1}.

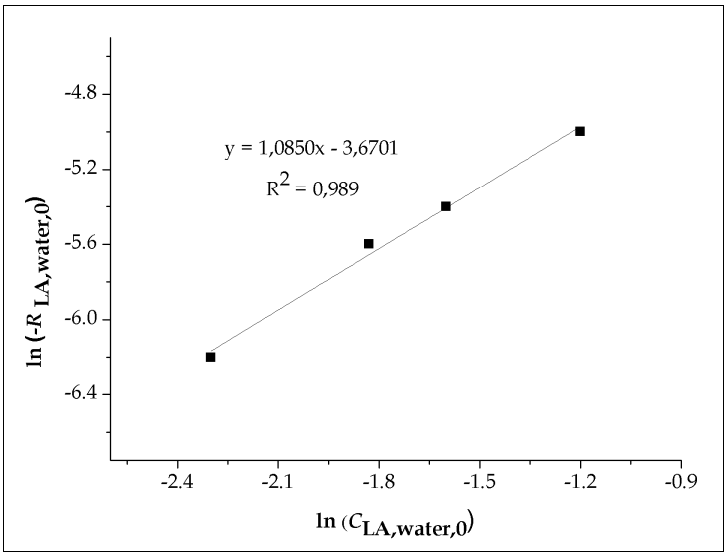

Figure 6. Determination of the order of reaction in LA (base conditions (70 °C))

Effect of catalyst concentration. The effect of catalyst intake on the initial LA reaction rate was studied by performing experiments with a variable catalyst intake at a fixed initial LA intake at base conditions (Table 1). The experimental results, as shown in Figure 7, suggest that the hydrogenation reaction is first order in catalyst for this hydrogenation system.

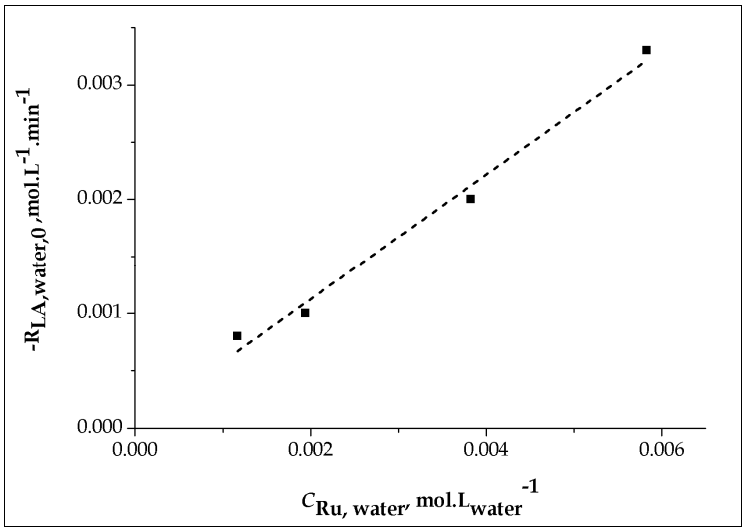

Figure 7. Effect of the catalyst intake on the initial rate of LA.
Conditions: see Table 1 for base conditions.

Effect of hydrogen pressure. Six experiments with hydrogen pressures ranging from 5 to 45 bar were performed at base conditions (Table 1) to determine the effect of hydrogen on the reaction rate of LA. The results are given in Figure 8. The figure indicates that the initial reaction rate of LA is independent of the hydrogen pressure when the pressure exceeds 15 bar. At lower pressures, a first order dependency is observed. Similar behavior has been observed for related hydrogenations using homogeneous Ru-systems.[36]

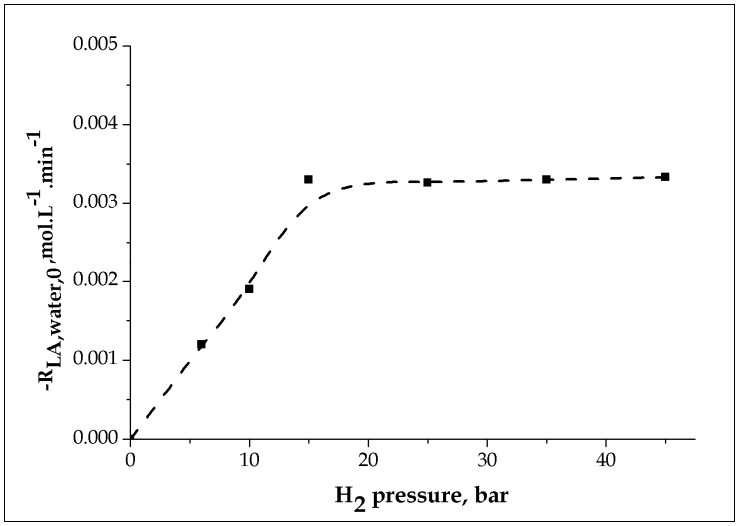

Figure 8. Hydrogen pressure effect on initial rate at base conditions (70 °C)

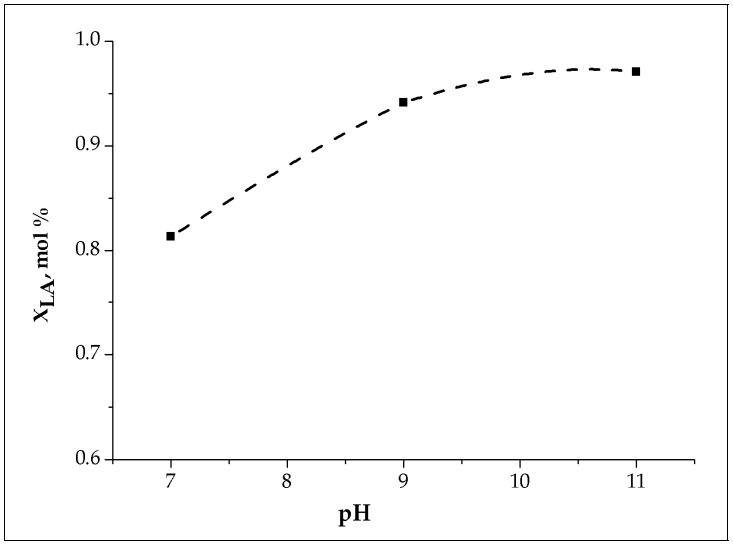

Figure 9. Conversion of LA after 1 h as a function of the pH.
Conditions: see Table 1 for base conditions.

Effect of the pH of the aqueous phase. A number of experiments in buffer solutions at different pH values in the range 7-11 were performed while keeping all other conditions at base conditions (Table 1). The results are given in Figure 9 for a 1 h reaction time. Clearly the conversion of LA is a function of the pH and the highest conversions were found at pH=11.The pH of the aqueous phase for biphasic organic-aqueous phase hydrogenations with water soluble Ru-based catalysts is known to affect the catalytic activity and selectivity of the reactions. For instance, Joo *et al.*[37]

showed that the rate and selectivity of the hydrogenation reaction of unsaturated aldehydes using well defined Ru-TPPTS compounds is a strong function of the pH of the solution. These findings were rationalized by assuming the existence of various Ru complexes in solution, of which the concentration is a function of the pH. However, other studies suggest that the reactions are not catalyzed by homogeneous Ru-species but by Ru-colloids.[38] The rate of colloid formation is assumed to be a function of the pH. In addition, the pH will also affect the distribution of LA between the organic and water phase and this may also affect the overall reaction rate. Further studies, beyond the scope of this paper, will be required to draw definite conclusions on the origin of pH effects on catalytic performance.

3.3.3. Kinetic modeling

A kinetic model was developed for the biphasic hydrogenation of LA to GVL on the basis of the following considerations and assumptions:

1. It is assumed that the water phase is the reactive phase and the organic phase is the transport phase. This is rationalized by the high solubility of the Ru-TPPTS catalyst in water.[28,39] The substrates and product participate between the two liquid phases, see Figure 10 for a schematic representation.

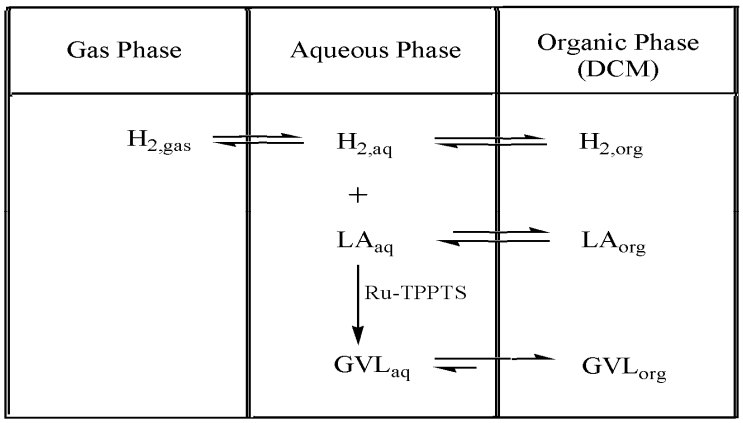

Figure 10. Schematic representation of LA biphasic hydrogenation with the water-soluble Ru-TPPTS catalyst

2. To avoid possible mass transfer effects and to measure intrinsic kinetics, all experiments were performed at an agitation rate of 2000 rpm (Figure 2).
3. The reaction rate for the hydrogenation of LA in the water phase is expressed by the following general equation:

$$R_{LA,water} = -k.C^{\alpha}_{LA,water}.P^{\beta}_{H_2,water} \quad (12)$$

where α and β are the order in LA and H_2, respectively.

The reaction rate constant is defined in terms of a modified Arrhenius equation which combines both the effects of temperature and the Ru-TPPTS concentration:

$$k = C^{\gamma}_{RuTPPTS}.k_R.\exp\left[\frac{-E_a}{R}\left(\frac{1}{T}-\frac{1}{T_R}\right)\right] \quad (13)$$

Here k_R is the kinetic constant at reference temperature T_R, arbitrarily set at 70 °C, and γ, the order in catalyst.

The orders in LA and catalyst were determined experimentally (Figures 6 and 7) and shown to be about 1. The kinetic experiments were carried out at constant hydrogen pressure (45 bar) through continuously feeding from a high pressure reservoir, meaning that the effect of hydrogen was not evaluated in the kinetic model. However, it was shown experimentally that the order in hydrogen is zero when the pressure exceeds 15 bar. Thus, the kinetic model presented here is valid at hydrogen pressures above 15 bar. A more extensive model, including a more complex relation for the hydrogen pressure will be required to model the complete pressure range.

With the orders in substrates and catalyst taken into account, eq. 11 and 12 simplify to eq. 13 and 14.

$$R_{LA,water} = -k.C_{LA,water} \tag{14}$$

$$k = C_{RuTPPTS}.k_R.\exp\left[\frac{-E_a}{R}\left(\frac{1}{T}-\frac{1}{T_R}\right)\right] \tag{15}$$

A mass balance equation for LA for a batch reactor (eq. 13) completes the mathematical description of the model.

$$\frac{dC_{LA,water}}{dt} = R_{LA,water} \tag{16}$$

4. The kinetic model is set up for the waterphase and involves LA waterphase concentrations. LA is expected to partition between both phases. The partitioning coefficients of LA and GVL (m_i with i = LA and GVL) as a function of the temperature (50-115 °C) were determined experimentally for the water-DCM system. Here m_i is defined as:

$$m_i = \frac{C_{i,DCM}}{C_{i,water}} \tag{17}$$

Table 2. Estimated kinetic parameters for the biphasic hydrogenation of LA with Ru-TPPTS [a]

Parameter	Estimate
E_a (kJ.mol^{-1})	61 ± 2
k_R (l_{aq}.mol^{-1} min^{-1})	64 ± 1

[a] Reference temperature (T_R) of 70 °C

Within the experimental window, good linear correlations were observed for the equilibrium concentrations of LA in water and dichloromethane. The experimental values for m_{LA} are between 0.9 and 2.2 and indicate that LA has affinity for both phases. Similar experiments were performed for GVL. The amount of GVL in the water phase of the water/DCM biphasic system appeared to be very low and the value of m is below 10^{-6} in the experimental temperature range. Thus, it is assumed that GVL is not present in the water phase.

To determine the kinetic parameters, a total of 6 batch experiments were performed at 50, 70 and 90 °C at different initial LA concentrations and provided a total of 76 data points. All other conditions were as for the base case given in Table 1. The experimental concentration profiles were modeled using Eq. (14) – (16) using the Matlab® programming platform. The optimized kinetic parameters and their 95% confidence limits are shown in Table 2. Agreement between model and experiment is good, as is clearly seen when comparing the experimental and the modeled data (Figure 11). The value of the activation energy (61 kJ/mol) implies that the kinetic data are not biased by mass transfer effects. In such cases, activation energies below 20-30 kJ/mol are expected.[40]

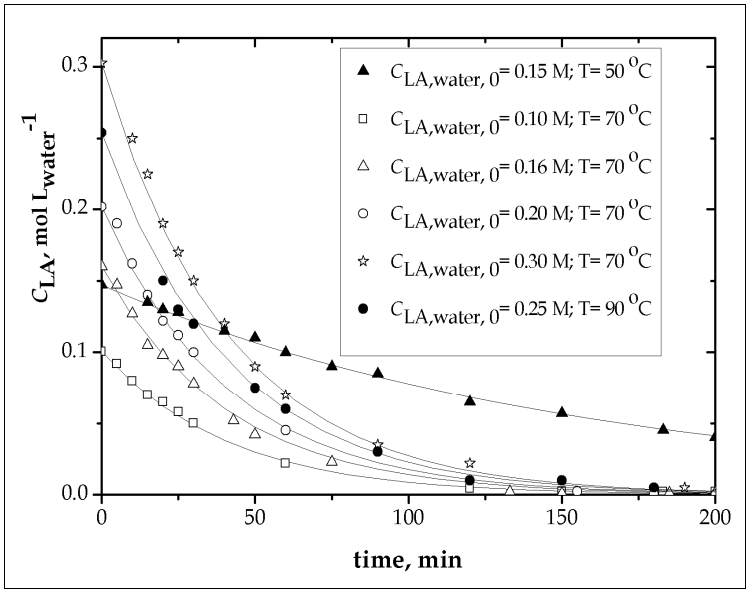

Figure 11. Experimental and modeling results for the hydrogenation of LA
Conditions: see Table 1 for base conditions at various temperatures and substrate concentrations

3.3.4. Catalyst recycling

The feasibility for catalyst recycling was determined by performing a hydrogenation experiment at standard conditions (Table 1). The LA conversion after 1h was 81%. The aqueous phase with catalysts was separated from the organic phase and charged to the reactor together with a fresh solution of LA in DCM. The LA conversion after the second run at standard conditions (Table 1) was 55%. This value is considerably lower than the first run, though clearly indicates the proof of concept for catalyst recycle. Further optimization experiments (i.e. experiments at lower temperatures to avoid catalyst deactivation during a run and work-up of the aqueous phase after reaction under the rigorous exclusion of air) will be required to improve the recyclability.

3.4. Conclusions

It has been shown that biphasic catalysis in DCM/water using homogeneous Ru-catalysts made in situ from $RuCl_3.3H_2O$ and sodium-tris(*m*-sulfonatophenyl)phosphine (Na_3TPPTS) allows the synthesis of GVL in quantitative

yields at mild conditions. Catalyst recycle by phase separation is possible, though further studies are required to reduce loss of activity in subsequent recycles. The kinetics in the biphasic system were determined using chemical reaction engineering models and it was shown that the reaction is first order in LA, zero order in hydrogen at hydrogen pressures above 15 bar and first order below 15 bar.

3.5. References

1. R.H. Leonard, *Ind.Eng. Chem.*, 48, 1330-1341 (1956)
2. B. Girisuta, L.P.B.M. Janssen and H.J. Heeres, *Green Chem.*, 8, 701–709 (2006)
3. P. Dunlop and J. W. Madden, *US Patent*, 2786852 (1957)
4. T. Horvath, H. Mehdi, V. Fábos, L. Boda and L.T. Mika, *Green Chem.*, 10, 238–242 (2008)
5. J. Bozell, L. Moens, D.C. Elliott, Y.Wang, G.G. Neuenschwander, S.W. Fitzpatrick, R.J. Bilski and J.L. Jarnefeld, *Resour. Conserv.Recycl.*, 28, 227-239 (2000)
6. E. Manzer, *Appl. Catal. A*, 272, 249–256 (2004)
7. J.P. Lange, J. Z. Vestering and R. J. Haan, *Chem. Commun.*, 3488–3490 (2007)
8. J.C. Serrano-Ruiz, D. Wang and J.A. Dumesic, *Green Chemistry,* 12, 574-577 (2010)
9. H.A. Schuette and P.T. Sah, *J. Am. Chem. Soc.*, 48, 3163-3165 (1926)
10. B.A. Bruce, B. Woodrow, and H.R. Henze, *J. Am. Chem. Soc.*, 61, 843-846 (1939)
11. H.S. Broadbent, G.C. Campbell, W.J. Bartley, and J.H. Johnson, *J. Org. Chem.*, 24, 1847-1854 (1959)
12. L.E. Manzer, *World Intellectual Property Organization*, WO 02/074760 A1 (2002)
13. T. Osawa, E. Mieno, T. Harada and O. Takayasu, *J. Mol. Cat. A; Chem.*, 200, 315-321 (2003)
14. P.J. van den Brink, K.L. Van Hebel, J.P. Lange and L. Petrus, *US Patent*, 0162239 A1 (2006)
15. Zhi-pei Yan, Lu Lin and Shijie Liu, *Energy & Fuels,* 23, 3853–3858 (2009)
16. R.A. Bourne, J.G. Stevens, J. Ke and M. Poliakoff, *Chem. Comm.*, 4632-4634 (2007)
17. H. Heeres, R. Handana, D. Chunai, C.B. Rasrendra, B. Girisuta and H.J. Heeres, *Green Chem.*, 11, 1247–1255 (2009)
18. K. Osakada, T. Ikariya, and S. Yoshikawa, *J. Organo. Chem.*, 231, 79-90 (1982)
19. F.Joo and M.T. Beck, *React. Kinet. Catal. Lett.*, 2, 257-263 (1975)
20. F.Joo, Z. Toth and M.T. Beck, *Inorg. Chim. Acta,* 25, L61-L62 (1977)
21. T. Ohkkuma, M. Kitamura and R. Noyori, *Tetrahedron Lett.*, 31(38), 5509-5512 (1990)
22. E.V. Starodubtseva, O.V. Turova, M.G. Vinogradov, L.S. Gorshkova and V.A. Ferapontov, *Russ. Chem. Bull., Int. Ed.*, 54(10), 2374-2378 (2005)
23. H. Mehdi, V. Fabos, R. Tuba, A. Bodor, L.T. Mika and I.T. Horvath, *Top Catal.*, 48, 49-54 (2008)
24. L. Deng, J. Li, D. Lai and Y. Fu, Q.Guo, *Angew. Chem. Int. Ed.*, 48, 6529-6532 (2009)
25. B. Cornils, *J. Mol. Cat. A: Chem.,* 143, 1-10 (1999)
26. E. Fache, C. Santini, F. Senocq and J.M. Basset, *J. Mol. Cat., Part II & III*, 72, 331-350 (1992)
27. K. Nuithiktikul and M. Winterbottom, *Cat. Today*, 128, 74-79 (2007)

28. M. Grosselin, C. Mercier, G. Allmang and F. Grass, *Organometallics*, 10, 2126-2133 (1991)
29. Y.P. Xie, J. Men, Y.Z. Li, H. Chen, P.M. Cheng and X.J. Li, *Cat. Comm*., 5, 237-238 (2004)
30. D.U. Parmar, S.D. Bhatt, H.C. Bajaj and R.V. Jasra, *J. Mol. Cat. A: Chem*., 202, 9-15 (2003)
31. F.H. Mahfud, S. Bussemaker, B. Kooi, F.G. ten Brink and H.J. Heeres, *J. Mol. Cat. A: Chem*., 277, 127–136 (2007)
32. J. Lambert and T.A. Muir, *Practical Chemistry* 3rd. Ed. Heinerman, London (1996)
33. W. Saiyasombat, R. Molloy, T.M. Nicholson, A.F. Johnson and I.M. Ward, *Polym*., 39, 5581-5585 (1998)
34. J.J. Bozell, *Conserv. Recycling*., 28, 227-239 (2000)
35. A.W. Heinen, G. Papadogianakis, R.A. Sheldon, J.A. Peters and H. Bekkum, *J. Mol. Cat. A: Chem*., 142, 17-26 (1999)
36. S.I. Fujita, Y. Sano, B.M. Bhanage and M. Arai, *J. Chem. Eng. Jap*., 36(2), 155–160 (2003)
37. F. Joo, J. Kovacs, A. Cs. Benyei and A. Katho, *Angew. Chem. Int. Ed*., 37, No. 7, 969–970 (1998)
38. C. Daguenet and P.J. Dyson, *Catal. Comm*., 4, 153–157 (2003)
39. R.V. Chaudari, A. Bhattacharya and B.M. Bhanage, *Cat. Today*, 24, 123–133 (1995)
40. C. de Bellefon, N. Tanchoux and Caravieilhes, *J. Organomet. Chem*., 567, 143–150 (1998)

Chapter 4
Ring-opening reactions of GVL with mono- and di-amines

Abstract

A novel route for the ring-opening of γ-Valerolactone (GVL) using mono- and di-amines to give γ-hydroxy-amide compounds was developed. The products were analyzed using ^{1}H-NMR, ^{13}C-NMR, FTIR and elemental analyses. Bulk reactions between GVL and some model compounds representing ammonia, primary- and secondary amines, showed that steric hindrance and partial charge at the nitrogen atom, i.e. base-strength, have a significant effect on the reactivity of the amino compounds. The following reactivity order was found: ammonia > 2-aminoethanol > 2-phenylethylamine > morpholine. Reactions between GVL and some di-amine model compounds indicate that steric hindrance is the most important factor. This is shown by the order of amine-conversion: 1,2-diaminoethane> 1,2-diaminopropane > piperazine, and the amine-selectivity to the di-addition product: 1,2-diaminoethane > 1,2-diaminopropane > piperazine. Furthermore, the reaction of GVL and 1,2-diaminoethane (EDA) was studied to optimize the yield of the desired difunctional products. Experiments showed that the highest yield was obtained at 100 °C and a GVL to EDA molar ratio of 9. These variables appeared to be the determining factors, while the use of catalyst and solvent polarity seemed to have limited effects on the product yields.

4.1. Introduction

The ever increasing demand for consumer products such as polymeric materials and the foreseeable shortage and depletion of crude oil as the major feedstock for the chemical industry has prompted studies on the use of biomass as a renewable source for platform chemicals. LA is an example of a promising green basechemical that can be obtained from biomass in good yields.[1-4] Its hydrogenation to GVL and subsequent ring-opening[5,6] has been studied as a route for the synthesis of novel co-polymers.[7-9] Unfortunately however, the lactone has a very low reactivity due to a very low ring strain[10-12] and direct polymerization resulted in relatively low molecular weight products.[7-9] Two main approaches have been applied for the ring-opening of lactones such as GVL, *viz*. bond cleavage at the γ-carbon-oxygen position and opening of the ester-function at the carbonyl carbon-oxygen bond (as shown in Scheme 1). As discussed in Chapter 1, some ring-opening pathways produce polymer precursors, others just provide functional molecules.

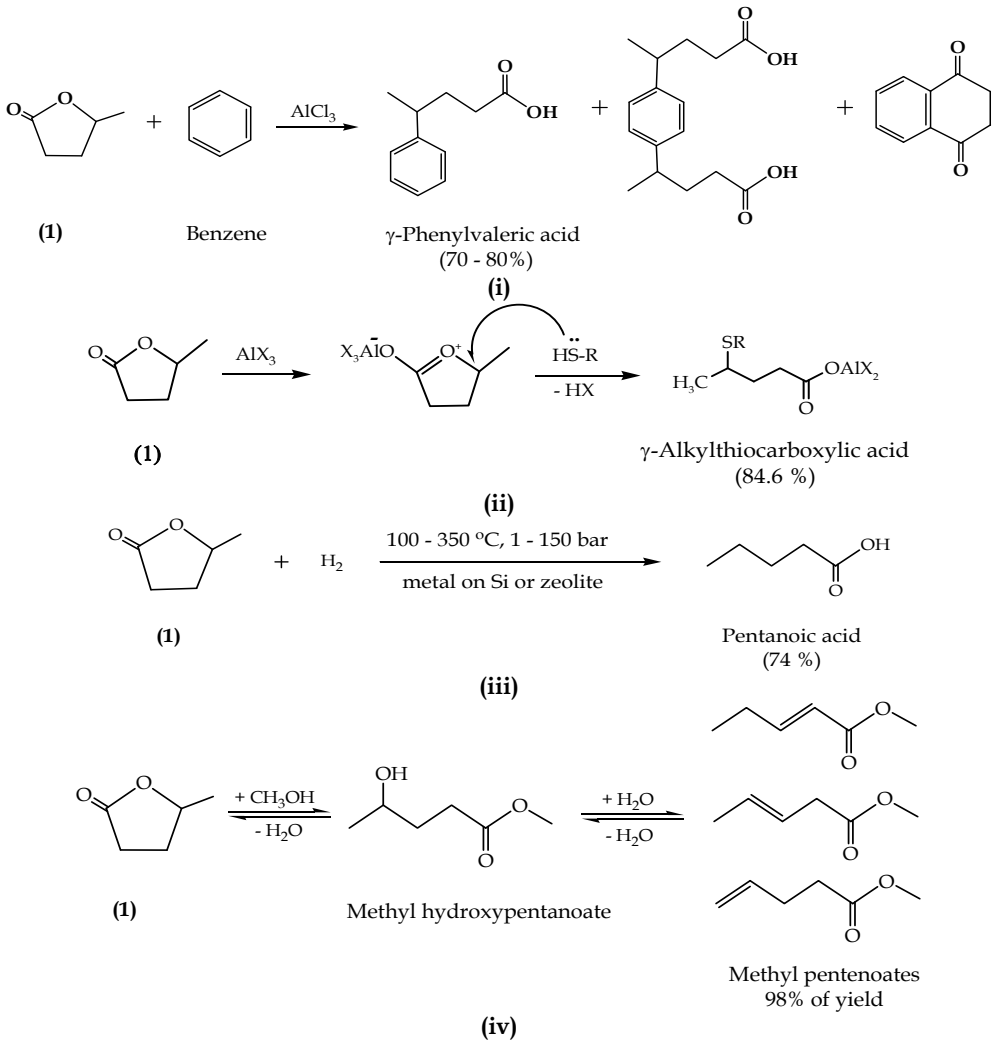

Scheme 1. Approaches for γ-valerolactone ring-opening. (i) ref.[13], (ii) ref.[14], (iii) ref.[15], (iv) ref.[16]

Brauman *et al.* reported the ring-opening reaction of GVL with benzene using Friedel-Crafts methodology at 60 °C for 2 hours to produce γ-phenylvaleric acid.[13]

Node *et al.* reported the formation of γ-alkylthio or γ-arylthio carboxylic acids by ring opening of GVL with a thiol using an aluminum halide catalyst at room temperature.[14] Van den Brink *et al.*[15] performed the hydrogenation of GVL into pentanoic acid using a strong acidic heterogeneous catalyst comprising of a hydrogenating metal such as Pt and Ni on silica or zeolite at a temperature in the range of 100 – 350 °C and pressures until 150 bar.

GVL ring-opening reactions to obtain polymerizable monomers have also been reported. Lange *et al.* reported the esterification and subsequent dehydration of GVL into mixtures of methyl pentenoates using catalytic distillation at 200°C.[16] These compounds are promising nylon precursors.

However, reaction conditions for these conversions are rather severe and product mixtures are formed. Therefore, selective chemistry to produce reactive intermediates from levulinic acid by the ring-opening of GVL is desired for the synthesis of high molecular weight polymers. Nelson *et al.* reported that the chemoselectivity of bond cleavage reactions for β-butyrolactone depends on the nucleophilicity of the reagent.[17] Addition of "soft" nucleophiles (such as azides and sulfonamide anions) leads to bond cleavage at the γ-carbon-oxygen whereas "hard" ones (such as primary and secondary amines) attack the carbonyl group (*see* Scheme 2).

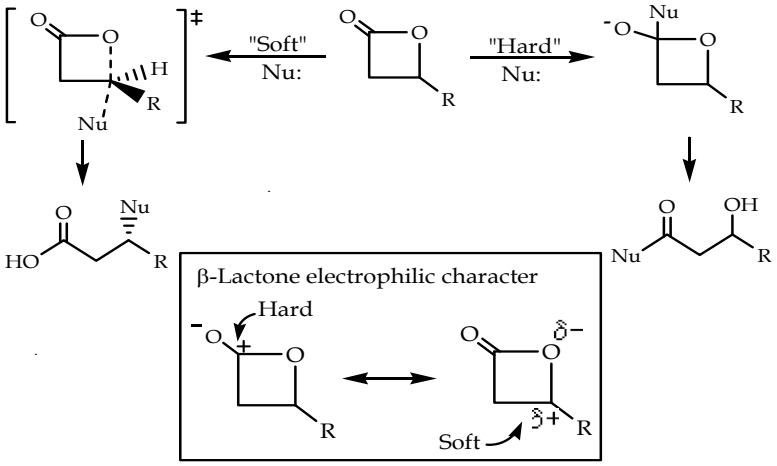

Scheme 2. Mechanism of addition reactions to β-lactones (taken from[17]).

Scheme 2 suggests that amino compounds, as examples of hard nucleophiles, should be able to open GVL to form γ-hydroxy(amino)amide compounds under mild conditions. This is indeed the case as shown by Burba *et al.*. They synthesized an amino-amide containing a free hydroxyl-group by the addition of di-amine compounds to caprolactone.[18] This ring-opening reaction applied to GVL could deliver a promising polymer engineering pathway by properly selecting the structure of the amino compound, e.g. by selecting the proper backbone structure or the presence of functional groups (*see* Scheme 3). As such, the novel pathway is expected to deliver co-monomers useful in polymer synthesis, and suitable for the manufacture of polymers such as polyurethanes, polyesters and polyethers.

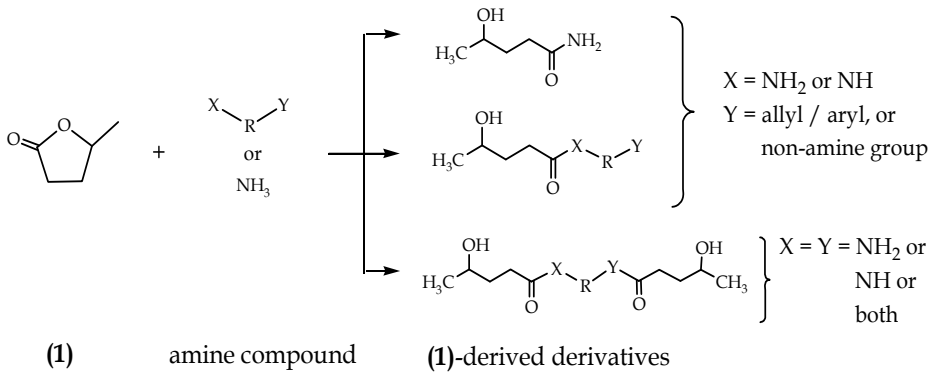

Scheme 3. Product design based on GVL ring-opening by varying the structure of the amine compound

In this work, the reactivity of amino compounds has been explored for the ring-opening of GVL. Both mono- and di-amino compounds were reacted with GVL under different reaction conditions and the effect of process variables on the conversion and product selectivity was studied. For the addition of monoamine compounds such as ammonium hydroxide, 2-aminoethanol, 2-phenylethylamine and morpholine, it is expected that the partial charge and steric hindrance around the nucleophilic centre will affect the reactivity of the amines. Furthermore, the addition of di-amines such as 1,2-diaminoethane, piperazine, and 1,2-diaminopropane was tested to investigate whether steric hindrance has a stronger effect on the reactivity than the partial charge at the nitrogen atom. Process variables such as the presence of an acid catalyst, solvent polarity, temperature, and molar ratio of lactone to amine were studied to understand and optimize the reactivity of the ring-opening of GVL.

4.2. Experimental

4.2.1. Materials (*Chemicals coded as in Scheme 4 and 6*)

GVL **(1)** (purity ≥ 98%), 2-aminoethanol **(3)** (purity ≥ 99%), Triphenylphospine (purity ≥ 99%), and 1,2-diaminoethane **(10)** (purity ≥ 99%) were purchased from Sigma Aldrich. N,N-dimethylacetamide DMA (purity ≥ 99%) was purchased from Sigma. Ytterbium(III)trifuoromethanesulfonate, $Y(OTf)_3$ (purity ≥ 99.99%) was purchased from Aldrich. Tin (II)-2-ethylhexanoate, TEH (purity ≥ 95%). 2- phenylethylamine, **(4)** (purity ≥ 99.99%) and **(11)** (purity ≥ 95%) were purchased from Fluka. Aluminum(III)trichloride, $AlCl_3$ (purity ≥ 98%) and ammonia **(2)** (98 vol-% in water) were purchased from Merck. $SnCl_2.2H_2O$ (purity 98%) and morpholine **(5)** (purity ≥ 99+ %) were respectively provided by Riedel-de Haen and Janssen Chemica. Dimethylsulfoxide, DMSO, (purity ≥ 99.7%) and 1,2-diaminopropane **(12)** (purity ≥ 99%) were provided by ACROS. Diethyl ether (analytical grade, purity ≥ 99.5%), methanol (analytical grade, purity ≥ 99%) and n-hexane (analytical grade, purity ≥ 99%) were obtained from Lab Scan. Silica gel Davisil®, grade 633 with pore size 60Å and 200-425 mesh was purchased from Aldrich. All chemicals were used without purification.

4.2.2. Analyses & characterizations

^{1}H- and ^{13}C-NMR spectra were recorded with tetramethylsilane (TMS) as the internal reference on a Varian AMS 100 spectrometer (400 MHz NMR) using D_2O as the solvent. Multiplicities of proton resonance were designated as single (s), doublet (d), triplet (t), and multiplet (m).

FT-IR spectra were recorded on a Perkin Elmer FT-IR spectrometer (Spectrum 2000 series, resolution 2.0 cm^{-1}, 100 scans). Spectra of solids were recorded using KBr pellets. Vibrational transition frequencies are reported in wave number (cm^{-1}). Band intensities are assigned as weak (w), medium (m), shoulder (sh), strong (s) and broad (br).

Elemental analyses were carried out using a Flash EA 1112 from CE Instruments.

4.2.3. Procedure for the ring opening of GVL with mono-amines

An amount of 20.75 mmoles of GVL **(1)** was mixed with an amount of 16.25 mmoles of mono-amino compound (**(2)**, **(3)**, **(4)**, or **(5); see Scheme 4**) without solvent, and the mixture was stirred at room temperature for 5 hours. Separation of the reaction product from the remaining reactants was conducted by adding a mixture of n-hexane and diethyl ether (1/1 v/v) and stirring. The precipitate was decanted and then washed three times using the same solvent mixture. Finally, the precipitate was dried under vacuum for about 5 hours at 70 °C to remove the remaining solvents. The weight of products was determined to calculate the yield of the reactions. The products were characterized by ^{1}H- and ^{13}C-NMR analysis, FTIR and elemental analysis.

4.2.4. Procedure for the ring-opening of GVL with di-amines

20.75 mmoles of GVL **(1)** was mixed with 8.125 mmoles of di-amine compound (**(10)**, **(11)** or **(12);** *see* Scheme 6), and the mixture was stirred at 50 °C for 3 hours. Samples were withdrawn from the reaction mixture at the end of the reaction and directly characterized by ^{1}H-NMR analysis to determine the conversion of the di-amine, the selectivity towards the mono- and di-adduct, and the yield. Calculation of both parameters was performed by assuming that the proton integration values (I) of the di-amine ($I_{di\text{-}amine}$), the mono-adduct ($I_{mono\text{-}adduct}$) and the di-adduct ($I_{di\text{-}adduct}$) is equivalent to their molar amount (n). The conversion of the di-amine ($X_{di\text{-}amine}$) and the selectivity of both mono- ($S_{mono\text{-}adduct}$) and di-adduct ($S_{mono\text{-}adduct}$) were calculated using Eq. 1, 2 and 3, respectively:

$$X_{di-amine} = \frac{I_{mono-adduct} + I_{di-adduct}}{I_{di-amine} + I_{mono-adduct} + I_{di-adduct}} \quad (1)$$

$$S_{mono-adduct} = \frac{I_{mono-adduct}}{I_{mono-adduct} + I_{di-adduct}} \quad (2)$$

$$S_{di-adduct} = \frac{I_{di-adduct}}{I_{mono-adduct} + I_{di-adduct}} \quad (3)$$

The separation of the final product from the remaining reactants and the intermediate product, and the characterization of the final product were performed by the same procedure as used in the ring-opening experiments of **(1)** with mono-amines. The reaction product **(16)** was further separated from the mixture by chromatography using silica gel (200-425 mesh) with methanol and water mixture (1/1 v/v) as the eluent.

4.2.5. Optimization procedure for the ring-opening of GVL with di-amines

In a typical procedure as shown in Table 1, (**1**) was mixed with 1,2-diaminoethane **(10)** (dissolved in a solvent), and the mixture was stirred at 50 °C for 3 hours. To investigate the selectivity of the di-amine compound in the ring-opening at various temperatures, the ring-opening of **(1)** was also performed by mixing **(1)** with 1,2-diaminepropane **(12)**, as shown in Table 1 (exp. 14-17).

Samples were withdrawn from the reaction mixture at the end of the reaction, and directly characterized by ^{1}H-NMR analysis to calculate the conversion and selectivity of di-amine addition according Eq. 1 – 3.

Table 1. Experimental overview

Exp	(1), mmole	(10), mmole	(12), mmole	Catalyst*)	Solvent*)	Temp, °C	Time, hr
1	20.75	8.13	-	-	-	50	0.5
2	20.75	8.13	-	TEH	-	50	0.5
3	20.75	8.13	-	AlCl3	-	50	0.5
4	20.75	8.13	-	SnCl2	-	50	0.5
5	20.75	8.13	-	Yb(OTf)3	-	50	0.5
6	20.75	8.13	-	-	DMA	50	3.0
7	20.75	8.13	-	-	DMSO	50	3.0
8	20.75	8.13	-	-	Methanol	50	3.0
9	20.75	8.13	-	-	Water	50	3.0
10	20.75	8.13	-	-	-	25	3.0
11	20.75	8.13	-	-	-	50	3.0
12	20.75	8.13	-	-	-	75	3.0
13	20.75	8.13	-	-	-	100	3.0
14	20.75	-	8.13	-	-	25	3.0
15	20.75	-	8.13	-	-	50	3.0
16	20.75	-	8.13	-	-	75	3.0
17	20.75	-	8.13	-	-	100	3.0
18	40.65	8.13	-	-	-	50	3.0
19	56.91	8.13	-	-	-	50	3.0
20	73.17	8.13	-	-	-	50	3.0

*) Amounts of catalyst and solvent are 0.08 mmoles (1.0 %-mole of EDA) and 12 ml, respectively

4.2.6. Typical kinetic experiment of the ring opening of GVL with 1,2-diaminoethane

The experiments were carried out as described above. During the reaction, samples were withdrawn from the reaction mixture at pre-determined time intervals

using a pipette. The samples were allowed to settle and analyzed by NMR to determine the amount of GVL and products.

4.3. Results & discussion

4.3.1. Addition of mono-amines to GVL

The ring-opening reaction of **(1)** with mono-amines was performed using selected mono-amino compounds, namely ammonia **(2)**, aliphatic primary **(3** and **4)** and secondary amines **(5)**. The ring-opening reactions are schematically shown in Scheme 4.

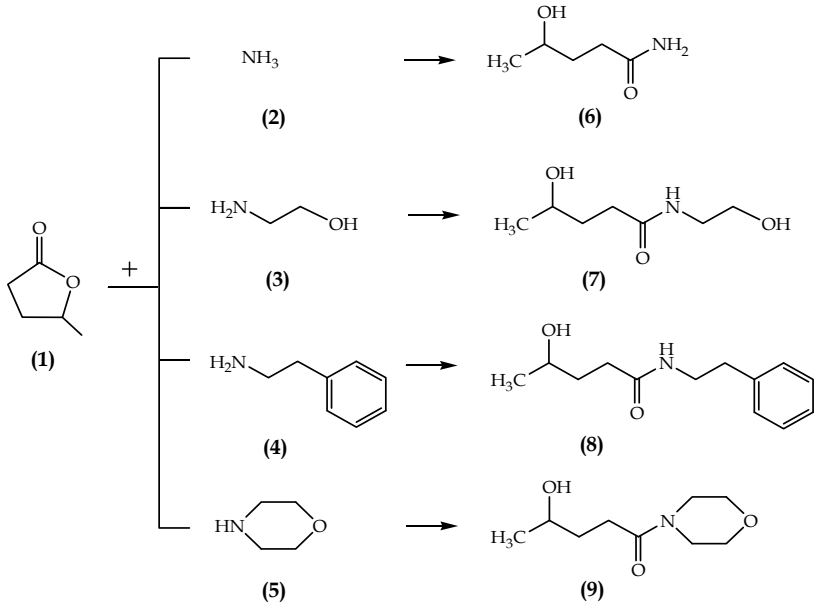

Scheme 4. Synthesis of GVL**(1)**-derived γ-hydroxy-amides by reaction with mono-amino compounds

The ring-opening reactions resulted in the production of γ-hydroxy-amides with methyne, amide and methyl functions. Characterization of the compounds was performed by ^{1}H- and ^{13}C-NMR, FTIR and elemental analysis. The representative ^{1}H- and ^{13}C-NMR spectra for adduct **(8)** are shown in Figure 1 as an example.

In the ^{1}H-NMR spectra the chemical shifts of the typical methyl (1 in Figure 1) and methyne group (6 in Figure 1) appear at δ 0.96 and δ 3.47 ppm, respectively. In the ^{13}C-NMR spectra, the chemical shifts of the typical methyl (1 in Figure 1), methyne group (6 in Figure 1), and C=O (11 in Figure 1) of the amide group in **(8)** appear at δ 21.79, δ 67.02 and δ 176.26 ppm, respectively.

The structural assignments are confirmed by the FTIR spectrum. The υ_{NH} (the amine bonds) appear at 2929 – 3311 cm^{-1}, while the υ_{CONH} (the amide groups) appear at 1633 cm^{-1}. Elemental analysis further supports the composition of the compound. The analytical data for the ring-opening products **(6)–(9)** are shown in Appendix 4.5.1.

To investigate the reactivity of the amines with **(1)**, yields (based on NMR analysis of reaction mixtures) after 5 hours reaction at room temperature were compared. The yields were as follows: **(2)** (95 %) > **(3)** (62 %) > **(4)** (54 %) > **(5)** (22 %).

Nucleophilicity of the amines appears to play an important role in the ring-opening chemoselectivity of **(1)**. Scheme 4 and the analytical support for the

structures summarized in Figure 1 and Appendix 4.5.1 indicate that the amines act as hard nucleophiles (See Scheme 2 for reference) as they show a preference for addition to the lactone carbonyl. This elicits ring-opening via the carbonyl addition pathway.[17] This conclusion is confirmed by NMR analysis which indicates no further adduct formation through a second addition of the newly formed amide function of **(6)**. This absence of further reaction by the amide can be explained by the soft nucleophilic nature of the amide. Besides, NMR spectra of the reaction mixture before and after purification also do not indicate a reaction product resulting from the amine attack at the gamma position. This behavior implies that the mono-amines are "hard" nucleophiles, as reported by Pearson *et al*.[19] A mechanism for this ring-opening is given in Scheme 5.

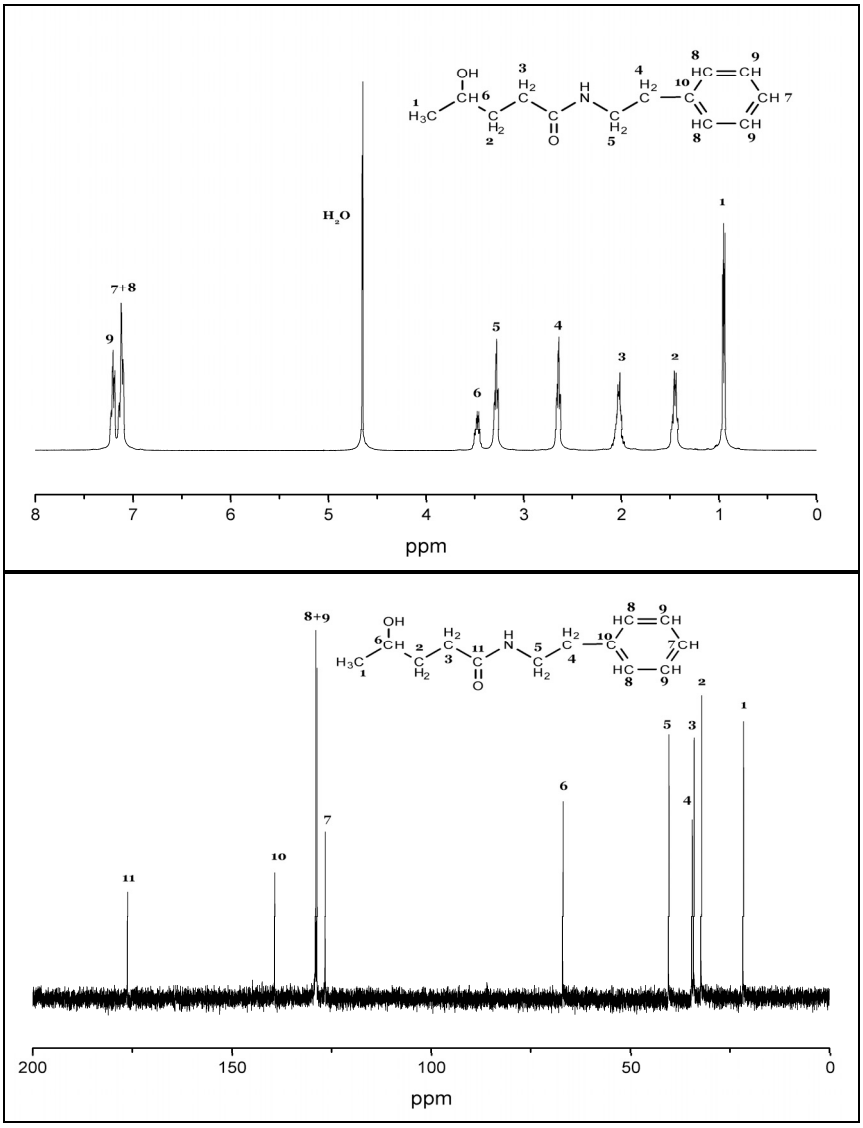

Figure 1. ^{1}H-NMR and ^{13}C-NMR spectra of **(8)** in D_2O at 25 ^{0}C

NMR based yields and the chemoselectivity of ring opening shown in Scheme 5 suggest that steric hindrance at the nitrogen atom and partial charge, i.e. the level of hardness, determine the reactivity of the amines. Steric hindrance at the nitrogen

atom for selected mono-amines was calculated using *Molecular Modeling Pro Plus Software for Windows* released by ChemSW®, Inc. The sequence for the increase of the steric hindrance at and around the nitrogen atom is **(2) < (3) ≈ (4) < (5)**. By using the same software, partial charges (i.e. the degree of polarization in the sigma bonds around the nitrogen atom) (**DelRe's** *method*) at the nitrogen atom in the selected mono-amines lead to the following ranking: **(2) < (3) < (4) < (5)**. Same trend with the sequence of these calculated partial charges was also reported by Del Re[20] and Rizzo *et al*.[21]. Values of both parameters for various amines are represented in Table 2.

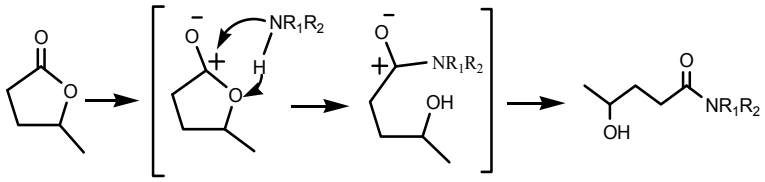

Scheme 5. Addition mechanism of ammonia, and the aliphatic primary and secondary amines to GVL **(1)**

Table 2. Calculated partial charge and steric hindrance at the nitrogen atom

No	Amine compound	Partial charge	Steric hindrance[a], %	Yield, %
1	**(2)**	- 0.8772	35	95
2	**(3)**	- 0.6519	37	62
3	**(4)**	- 0.6527	38	54
4	**(5)**	- 0.4407	42	4

[a] For reference: replacing the N-H proton in dimethylamine by methyl, ethyl, i-propyl and t-butyl increases the steric hindrance at the N-atom from 37.2 to 39.5, 41.9, 43.4 and 45.4, respectively.

Comparison of the yields obtained for this set of **(1)** ring-opening reactions suggests that both the partial charge and the steric hindrance at and around the N-atom (or a combination of the two) can be correlated with yield. However, from these data it is difficult to conclude which of the two parameters is dominant. For that reason a study was conducted to understand which parameter is the major factor determining the amine reactivity in the ring-opening reaction of GVL **(1)**.

4.3.2. Addition of di-amines to GVL

To extend the synthetic procedure and to obtain highly functionalized monomers, experiments were performed with a number of diamines **(10)**, **(11)** and **(12)** (Scheme 6). In addition, these studies also provide further insights and a better understanding of the influence of both steric hindrance and partial charge on amine reactivity. The amines in this study were selected such that steric hindrance and partial charge at the nitrogen atom were varied in a controlled manner. Scheme 6 shows that theoretically at least two products can be formed (a mono- and a di-adduct). Similar to the ring-opening of **(1)** with mono-amines, the products contain alcohol and amide groups as typical units.

As for the ring-opening reactions with the mono-amines, the identification of the adducts was supported by ^{1}H- and ^{13}C-NMR, FTIR and elemental analysis. ^{1}H- and ^{13}C-NMR spectra for the di-adduct **(16)** are shown in Figure 2 as an example.

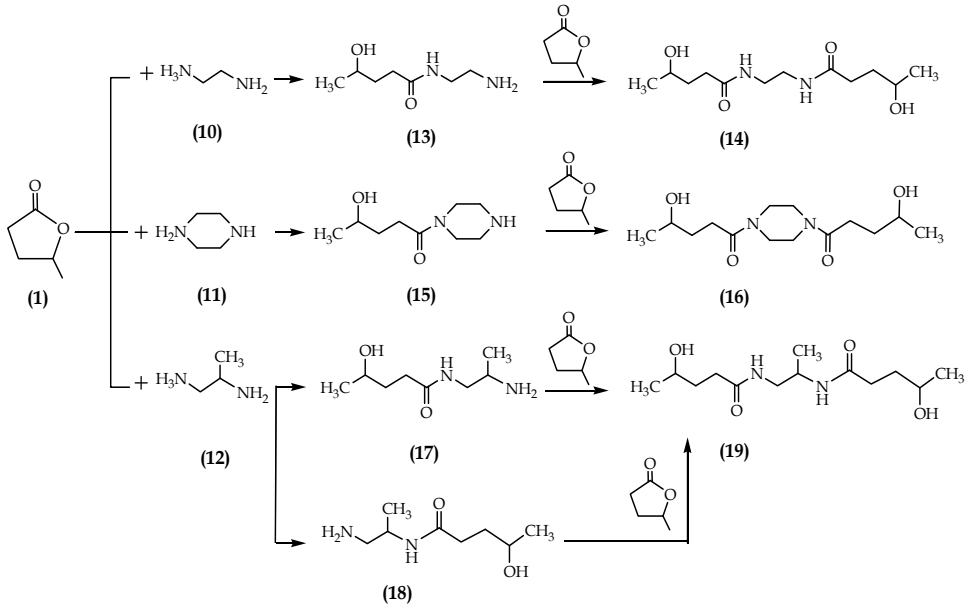

Scheme 6. Synthesis of GVL**(1)**-derived bis-hydroxy-amides through the addition of di-amines

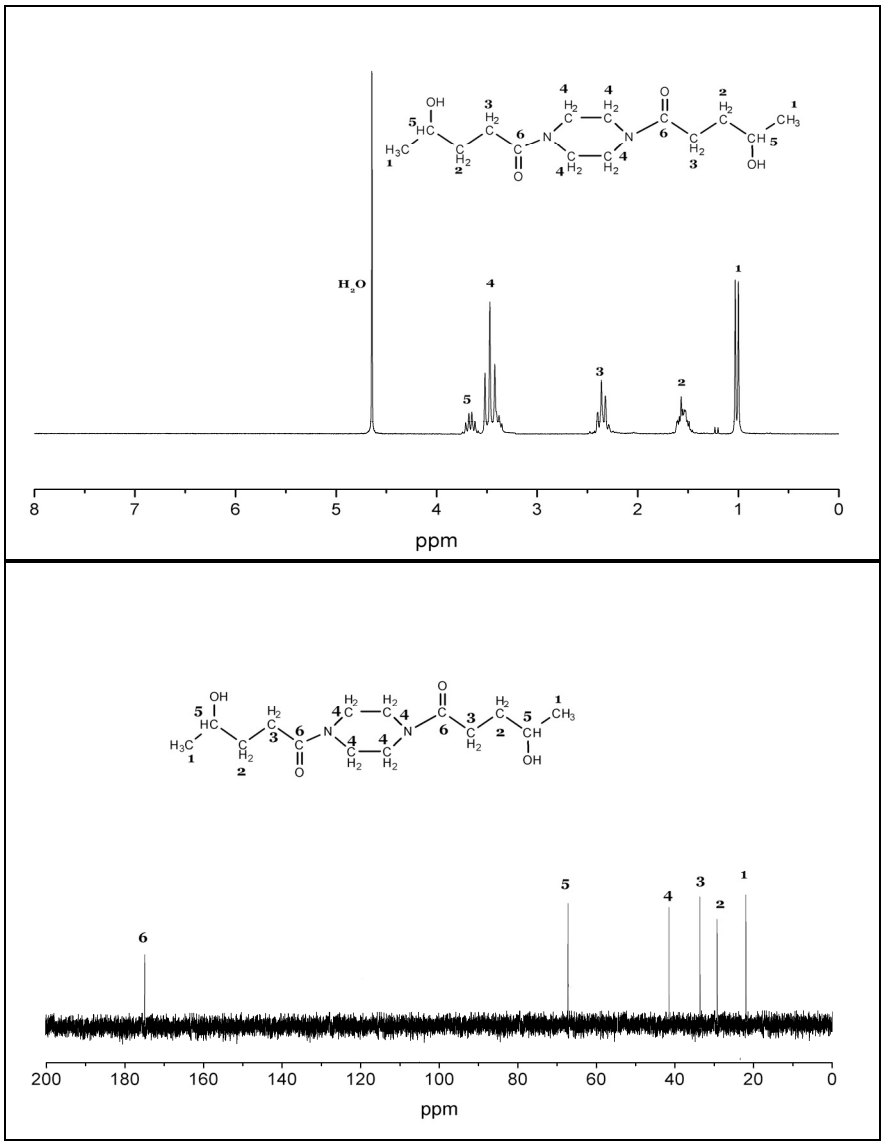

Figure 2. ^{1}H-NMR and ^{13}C-NMR spectra of **(19)** in D_2O at 25 °C

The structural assignments are confirmed by the FTIR spectra. The amine bonds appear at 2970 – 3384 cm^{-1}, while the υ_{CONH} of the amide groups appear at 1614 cm^{-1}. Elemental analysis further supports the elemental composition of the compound. Detailed analytical data for the di-adducts **(14) – (19)** are shown in Appendix 4.5.2.

NMR data and Equations 1 – 3 enable a comparison of conversion and selectivity for the ring-opening with di-amines. Figure 3 summarizes the data showing a sequence of 1.00; 0.90; and 0.57 for the conversion of **(10), (11)** and **(12)**, respectively, and 0.70; 0.60; and 0.50 for the selectivity to **(14), (16)** and **(19)**. It is important to note that product **(18)**, i.e. the mono-addition product obtained by the reaction of the sterically hindered amine in **(12)**, was not observed during NMR measurement before and after purification of the reaction mixture. The conversion results suggest that the di-amine reactivity increases according to the sequence: **(10) > (11) > (12)**.

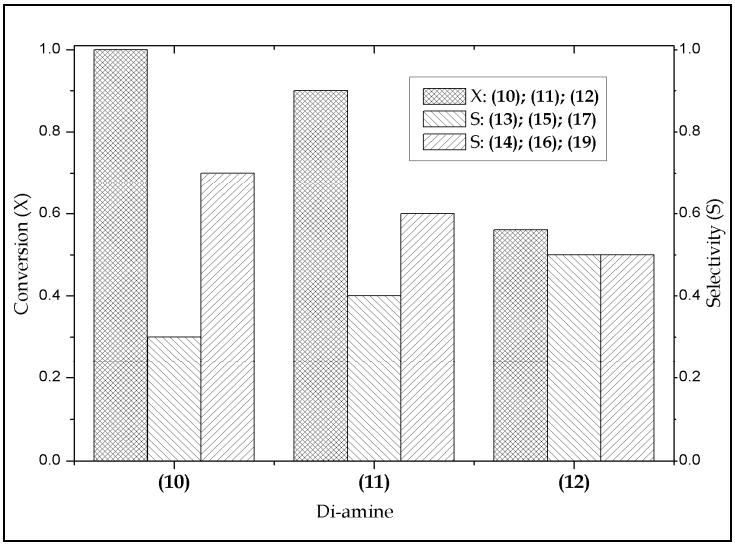

Figure 3. Comparison of the ring-opening reaction for **(1)** with a range of di-amines. (*See* Table 1 for the experimental conditions)

Table 3. Calculated partial charge and steric hindrance at the nitrogen atoms

No	Amine compound	Chemical structure	Partial charge		Steric hindrance[a], %	
			N_a	N_b	N_a	N_b
1	**(10)**		- 0.6527	-	38	-
2	**(11)**		- 0.4421	-	41	-
3	**(12)**	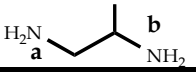	- 0.6529	- 0.6544	39	53

Furthermore, the electron densities (DelRe's *method*) and the steric hindrance for the selected di-amine compounds at both nitrogen atoms were calculated by using *Molecular Modeling Pro Plus Software for Windows* released by *ChemSW®, Inc* (*see* Table 3). Referring to the structure of the di-amines shown in Scheme 6 and the calculated data in Table 3, a sequence of reduced steric hindrance can be constructed as **(10) < (11) < (12)**.

Comparison of the conversion data (Figure 3) and the molecular parameters calculated for the di-amines **(10)** and **(12)** (Table 3) clearly indicates that the steric hindrance has a stronger effect than the partial charge on the reactivity of the evaluated di-amino compounds.

4.3.3. Reaction profile for the ring opening of (1) with a typical diamine (1,2-diaminoethane)

Before studying the optimization of the reaction of **(10)** with **(1)**, the formation of the products **(13)** and **(14)** during the reaction was monitored by measuring NMR spectra at regular time intervals. The ^{1}H-NMR spectra can also be used as additional evidence for the sequential formation of the mono- and the di-adduct during the reaction (*see* Figure 4).

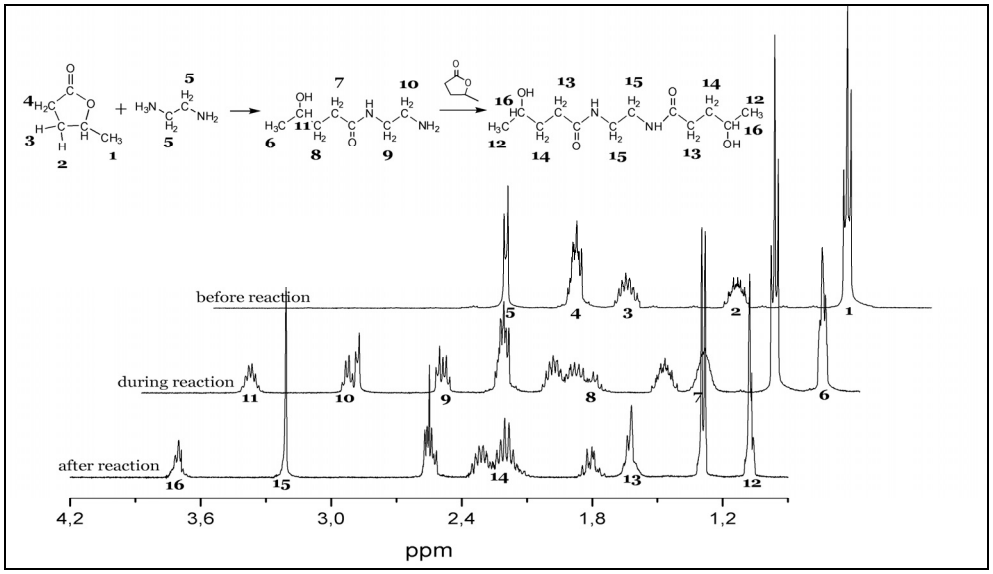

Figure 4. ^{1}H-NMR spectra for the reaction of diaminoethane **(10)** [8.125 mmoles] and GVL **(1)** [41.5 mmoles] at 25 °C

During the reaction, samples were withdrawn from the reaction mixture consisting of **(1)**, **(10)** and the products, and the actual composition was directly determined by ^{1}H-NMR analyses. Based on these spectra, a reaction profile can be constructed by calculating the ratio of prominent peak integrations (*see* Eq. 1 – 3 and Figure 5).

Figure 5 shows that the reaction of **(1)** and **(10** proceeds by a two step sequence, i.e., initial formation of the mono-adduct **[13]** followed by the formation of the di-adduct **[14]**. Rates of the reactions can be expressed as,

$$\frac{d[10]}{dt} = -k_1[10]^a[1]^b \tag{4}$$

$$\frac{d[13]}{dt} = k_1[10]^a[1]^b - k_2[13]^c[1]^d \tag{5}$$

$$\frac{d[14]}{dt} = k_2[13]^c[1]^d \tag{6}$$

Assuming first order for the reactions, simplifying the kinetics to pseudo-first order by taking an excess of **(1)** (5 to 1 molar ratio) and referring to literature,[22] the equations above can be transformed into equations (7) – (9):

$$[10] = [10]_0 . e^{-k_1'.t} \tag{7}$$

$$[13] = [10]_0 . k_1' \left(\frac{e^{-k_1'.t}}{k_2' - k_1'} - \frac{-e^{-k_2'.t}}{k_1' - k_2'} \right) \tag{8}$$

$$[14] = [10]_0 \left(1 + \frac{k_2' . e^{-k_1'.t}}{k_1' - k_2'} + \frac{k_1' . e^{-k_2'.t}}{k_2' - k_1'} \right) \tag{9}$$

Values of k_1' and k_2' were determined by modeling the experimental data given in Figure 5. Modeling was performed using *Mathcad* software, and resulted in values of k_1' and k_2' of 0.0108 mmoles per minute and 0.0026 mmoles per minute, respectively. Even though the applied molar ratio of 5 to 1 does not represent true pseudo first-order conditions, comparison of both rate constants shows that the first addition step is somewhat faster than di-adduct formation.

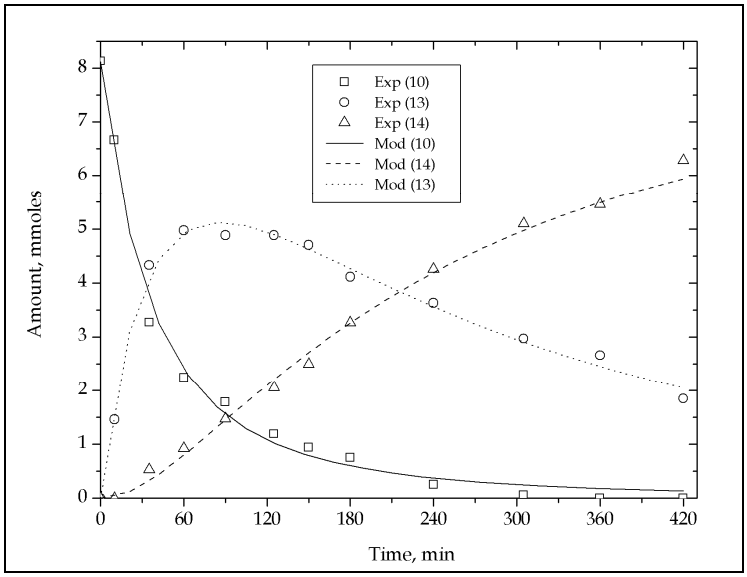

Figure 5. The reaction profile for reaction of diaminoethane **(10)** and GVL **(1)** (5 to 1 ratio) at 25 °C

As the di-adduct is the desired product, an investigation to enhance its formation rate appeared justified, and a number of experiments was conducted to investigate the effect of process variables on the yield and rate of the reaction between **(1)** and **(10)**.

4.3.4. Optimization study of the reaction of (1) and (10)

As the di-adducts are considered for the use in subsequent polymer synthesis, a high yield is desired. For this reason, several process variables such as type of catalyst, solvent polarity, temperature and molar ratio of **(10)** to **(1)** were varied.

Effect of catalyst. Different catalysts were selected on the basis of available literature. Saiyasombat *et al.* reported that the ring-opening of β-butyrolactone is

catalyzed by Lewis acid catalysts.[10] Considering a similar reactivity for GVL, this study was carried out with a set of Lewis acid catalysts, such as $AlCl_3$, $SnCl_2.2H_2O$, Ytterbium (III)trifuoromethanesulfonate ($Yb(OTf)_3$) and Tin(II)-2-ethylhexanoate (TEH). Triphenylphosphine (TP) was used as a typical example of a Lewis base.

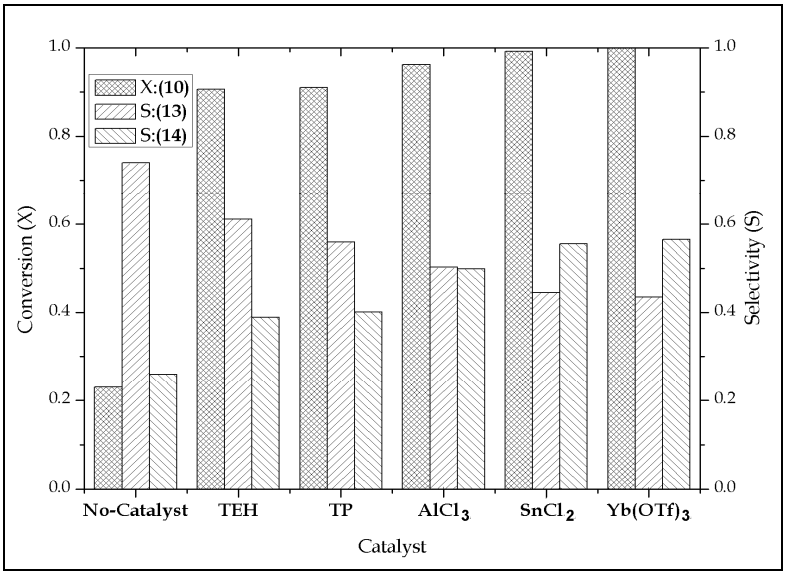

Figure 6. The effect of various Lewis acids on the reaction of **(1)** with **(10)**. *See* Table 1 for the experimental conditions

The experiments were conducted by mixing 20.75 mmoles of **(1)**, 8.125 mmoles of **(10)** and 1 %-wt of the catalyst and the mixtures were stirred at room temperature for 25 minutes. The effect of the catalyst on the reaction was quantified by measuring the conversion of **(10)** and the selectivity for **(13)** and **(14)**, as shown in Figure 6. This figure shows that catalysts enhance the conversion considerably, but have a less pronounced effect on the selectivity of the reaction.

Effect of solvent. The proposed reaction mechanism for the ringopening of lactones (Scheme 2) involves a polar intermediate. This suggests that the use of solvents which stabilize polar transition states and polar intermediates should have a positive effect on the reaction rates.[23] Solvent effects on the reactions were studied by comparing various polar solvents as diluents for the ring-opening of **(1)**. For this purpose, methanol, DMA, DMSO and water were investigated and the obtained results are presented in Figure 7. Clearly, both the conversion rate and the selectivity are a function of the reaction medium. Highest values for the conversion of the di-amine were found for water, whereas DMA gave the lowest value (Table 4).

Figure 7 and Table 4, show that the conversion of **(10)** is a function of the solubility parameter, with higher values for the solubility parameter leading to higher conversion rates. It is well possible that the higher conversions in methanol and water compared to DMA and DMSO are related to the hydrogen bonding capability of the former two solvents.[25] This behavior also may be the reason for the significant improvement in di-amine conversion found in methanol, which, compared to DMSO, only has a slightly higher solubility parameter.

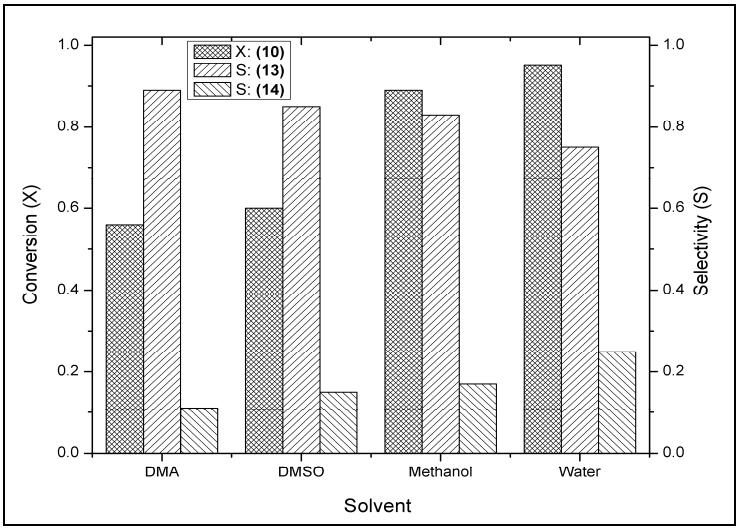

Figure 7. The effect of the various solvents on the reaction of **(1)** with **(10)**. Conditions: *see* exp 6-9 in Table 1 for the experimental conditions

Table 4. Values of solubility parameters (the Hildebrand) of the solvents[24]

Solvent	Solubility parameter, $MPa^{1/2}$	Diamine conversion
DMA	22.7	0.56
DMSO	26.6	0.60
Methanol	29.7	0.89
Water	47.9	0.95

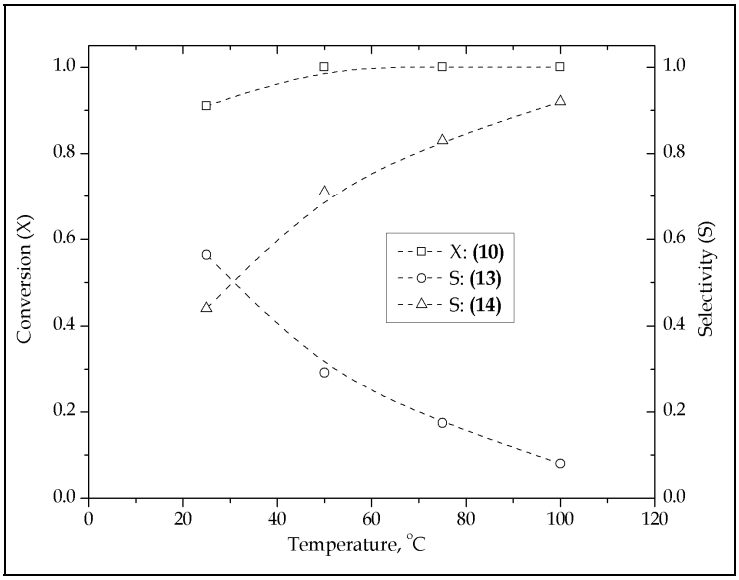

Figure 8. The temperature effect on the reaction of **(1)** and **(10)**. Conditions: *see* Table 1 for the experimental conditions

Effect of temperature. The reaction of **(10)** with **(1)** at various temperatures in bulk conditions and without catalysts was explored. The conversion of **(10)** and the selectivity for **(13)** and **(14)** versus temperature are shown in Figure 8. As expected, the temperature has a significant effect on the rate of the reaction. For di-amine **(10)**

high conversions can be obtained at temperatures of 50 - 60 °C and a further increase to around 100 °C enables quantitative conversion of (**1**) with 90% selectivity to the di-adduct **(14)**. When aiming for quantitative di-adduct yield, a slightly longer reaction time and a temperature just above 100 °C should be sufficient.

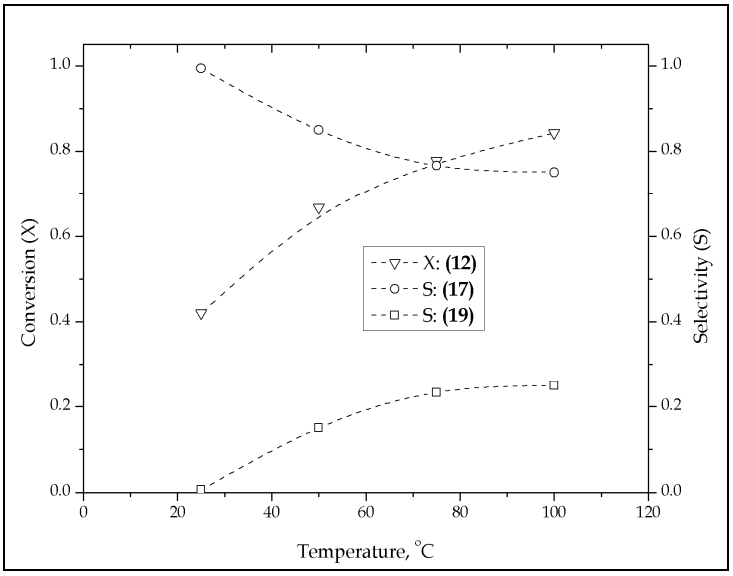

Figure 9. The temperature effect on the reaction of **(1)** and **(12)**. Conditions: *see* Table 1 for the experimental conditions.

A similar trend was found for the addition of **(1)** to **(12)**, as shown in Figure 9. A difference in rate of the reaction between both reactions, i.e. **(1)** and **(10)** *versus* **(1)** and **(12)**, was expected on the basis of the mono-amine chemistry discussed earlier in this chapter. A slower reaction is observed for the more sterically hindered amine function in the molecule, while the absence of intermediate **(18)** proves that the selectivity in this case is steered by the presence of a methyl substituent in the amine backbone (*see* Table 3).

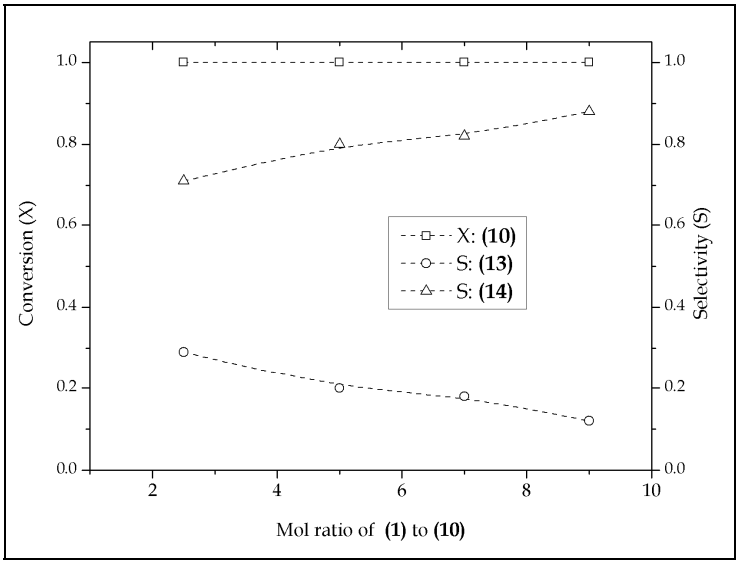

Figure 10. The effect of mole ratio of **(1)** to **(10)** on the conversion for reaction of **(1)** and **(10)**. Conditions: *see* Table 1 for the experimental conditions

Effect of mol ratio of GVL (1) to (10). On the basis of the results described above, it is expected that an increase in the mol ratio of **(1)** to **(10)** will have a positive effect on the conversion and selectivity of the reaction. This parameter was studied by performing some reactions at different amounts of **(1)** and a fixed intake of **(10)**. The conversions and selectivities for reactions carried out at 50 °C for 3 hours are shown in Figure 10.

The data indeed show that an increase in the amount of **(1)** at a fixed intake of **(10)** has a significant effect on the selectivity. At the applied reaction conditions a mol ratio of **(1)** to **(10)** of 2 is sufficient to achieve full conversion of the di-amine **(10)** while the selectivity for **(14)** steadily increases with an increase in mol ratio from 2 till 9.

4.4. Conclusions

γ-Valerolactone **(1)** undergoes ring-opening at mild conditions into various γ–hydroxy-amides by reaction with mono- or di-functional aliphatic primary- or secondary amines. The lactone ring opens *via* a nucleophilic addition of the "hard" amine to the lactone carbonyl and results in the cleavage of the cyclic ester with the formation of an amide.

To gain more insight in the amine-lactone reactivity, model compounds representing mono- and di-amines were applied to determine the reactivity of the amines. Steric hindrance around the nucleophilic nitrogen centre was found to be more important than partial charge at the nitrogen atom.

The ring-opening of GVL with 1,2-diaminoethane **(10)** was studied in more detail to optimize the yield of the desired difunctional monomers. Of the process parameters studied, the reaction temperature, reaction time and molar ratio of the reactants appeared to be the determining factors. These parameters were found to be more important than the use of catalysts and solvent polarity.

In conclusion it may be stated that ring-opening of GVL is a promising novel pathway to prepare di-functional monomers suitable for polymer synthesis. Product design through varying the structure of the amines, such as backbone structure and presence of secondary functional groups, appears to be a promising polymer engineering pathway. The application of the novel monomers for the synthesis of new polymers will be discussed in Chapter 5.

4.5. Appendices

4.5.1. Analytical data for reaction products of (1) with mono-amines

Product	Chemical Structure Appearance & Elemental analysis	^{1}H-Chemical Shift (ppm)	^{13}C-Chemical Shift (ppm)	FTIR (cm^{-1})
(6) 95% (yield)	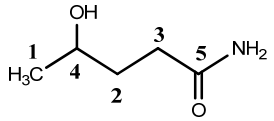 ***4-hydroxy-pentanamide*** $C_5H_{11}NO_2$, white solid (waxy) Anal. Calcd: 51.26% C; 9.46% H; 11.96% N Found: 50.98% C; 9.58% H; 11.87% N.	(H-1) 1.02 (H-2) 1.58 (H-3) 2.17 (H-4) 3.67	(C-1) 21.83 (C-2) 31.54 (C-3) 33.93 (C-4) 67.16 (C-5) 179.77	3346 (free N-H, br) 2969-2953 (H-bonded N-H, m) 1663 (C=O in amide, s) 1563 (stretched C-N & bended N-H, s)
(7) 62% (yield)	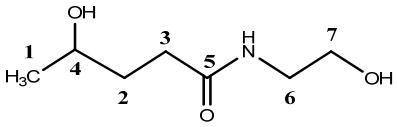 ***4-hydroxy-N-(2-hydroxyethyl)-pentanamide*** $C_7H_{15}NO_3$, brownish viscous liquid Anal. Calcd.: 52.16% C; 9.38% H; 8.69% N Found: 51.90% C; 9.45% H; 8.47% N.	(H-1) 1.03 (H-2) 1.57 (H-3) 2.16 (H-4) 3.64 (H-6) 3.17 (H-7) 3.49	(C-1) 24.50 (C-2) 34.90 (C-3) 36.70 (C-4) 44.14 (C-5) 179.46 (C-6) 62.65 (C-7) 69.77	3286 (free N-H, br) 2873-2965 (H-bonded N-H, m) 1633 (C=O in amide, s) 1548 (stretched C-N & bended N-H, s)
(8) 54% (yield)	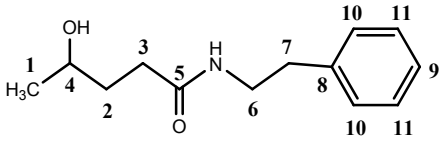 ***4-hydroxy-N-(2-phenylethyl)-pentanamide*** $C_{13}H_{19}NO_2$, brownish solid (waxy) Anal. Calcd: 70.56% C; 8.65% H; 6.33% N Found: 70.32% C; 8.67% H; 6.29% N	(H-1) 0.96 (H-2) 1.45 (H-3) 2.03 (H-4) 3.47 (H-6) 3.28 (H-7) 2.65 (H-9 &10) 7.12 (H-11) 7.21	(C-1) 21.79 (C-2) 32.32 (C-3) 34.18 (C-4) 67.02 (C-5) 176.26 (C-6) 40.49 (C-7) 34.64 (C-8) 139.37 (C-9) 67.02 (C-10) 128.75 (C-11) 129.07	3311 (free N-H, br) 3065-2929 (H-bonded N-H, m) 1633 (C=O in amide, s) 1543 (stretched C-N & bended N-H, s)
(9) 4% (yield)	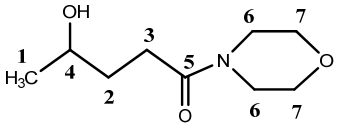 ***4-hydroxy-N,N-(diethylenoxide)-pentanamide*** $C_9H_{17}NO_3$, brownish viscous liquid Anal. Calcd: 57.73% C; 9.15% H; 7.48% N Found: 57.64% C; 9.22% H; 7.60% N.	(H-1) 1.05 (H-2) 1.58 (H-3) 2.36 (H-4) 3.69 (H-6) 3.45 (H-7) 3.59	(C-1) 21.96 (C-2) 29.08 (C-3) 33.93 (C-4) 67.21 (C-5) 174.74 (C-6) 44.31 (C-7) 66.46	3383 (free N-H, br) 2854-2970 (H-bonded N-H, m) 1633 (C=O in amide, s) 1435 (stretched C-N & bended N-H, s)

4.5.2. Analytical data for reaction products of (1) with di-amines

Product	Chemical Structure Appearance & Elemental analysis	^{1}H-Chemical Shift (ppm)	^{13}C-Chemical Shift (ppm)	FTIR (cm^{-1})
(14) 98% (yield)	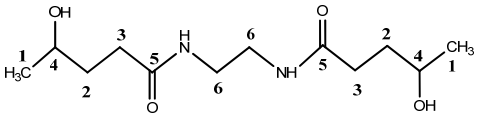 *N,N'-1,2-ethanediylbis-(4-hydroxy-pentanamide)* $C_{12}H_{24}N_2O_4$, white powder Anal. Calcd: 55.36% C; 9.29% H; 10.76% N. Found: 55.38% C; 9.33% H; 10.71% N.	(H-1) 1.03 (H-2) 1.58 (H-3) 2.15 (H-4) 3.65 (H-6) 3.17	(C-1) 21.85 (C-2) 32.37 (C-3) 34.16 (C-4) 67.19 (C-5) 176.89 (C-6) 38.72	3276 (free N-H, br) 2907-2964 (H-bonded N-H, m) 1639 (C=O in amide, s) 1555 (stretched C-N & bended N-H, s)
(16) 86% (yield)	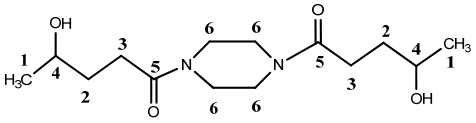 *N,N'-1,2-diethanediylbis-(4-hydroxy-pentanamide)* $C_{14}H_{26}N_2O_4$, brownish viscous liquid Anal..Calcd: 58.72% C; 9.15% H; 9.78% N. Found: 57.39% C; 9.11% H; 9.14% N	(H-1) 1.02 (H-2) 1.54 (H-3) 2.36 (H-4) 3.60 (H-6) 3.47	(C-1) 21.93 (C-2) 29.25 (C-3) 33.62 (C-4) 67.20 (C-5) 174.93 (C-6) 41.62	3384 (free N-H, br) 2970-2926 (H-bonded N-H, m) 1614 (C=O in amide, s) 1423 (stretched C-N & bended N-H, s)

(19) 44% (yield)	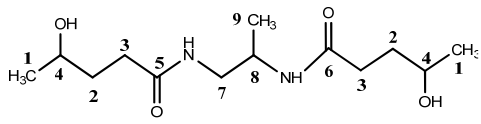 *N,N'-1,2-propanediylbis-(4-hydroxy-pentanamide)* $C_{13}H_{26}N_2O_4$, yellowish viscous liquid Anal. Calcd: 56.91% C; 9.55% H; 10.21% N. Found: 56.22% C; 9.72% H; 10.33% N	(H-1) 1.01 (H-2) 1.54 (H-3) 2.12 (H-4) 3.67 (H-7) 3.02 (H-8) 4.87 (H-9) 0.96	(C-1) 21.92 (C-2) 32.45 (C-3) 34.50 (C-4) 67.16 (C-5) 176.73 (C-6) 176.03 (C-7) 45.29 (C-8) 43.99 (C-9) 17.15	3274 (free N-H, br) 2970-2927 (H-bonded N-H, m) 1633 (C=O in amide, s) 1539 (stretched C-N & bended N-H, s)

4.6. References

[1] R.H. Leonard, *Ind.Eng. Chem.*, 48 (8), 1331-1341 (1956)

[2] B.V. Timokhin, V.A. Baransky and G.D. Eliseeva, *Russ. Chem. Rev.*, 68(1), 73-84 (1999)

[3] J.J. Bozell, L. Moens, D.C. Elliott, Y. Wang, G.G. Neuenscwander, S.W. Fitzpatrick, R.J. Bilski and J.L. Jarnefeld, *Resour. Conserv. Recy.*, 28, 227–239 (2000)

[4] B. Girisuta, L.P.B.M. Janssen and H.J. Heeres, *Chem. Eng. Res. Des.*, 84(A5), 339–349 (2006)

[5] I.T. Horvath, H. Mehdi, V. Fabos, L. Boda, and L.T. Mika, *Green Chem.*, 10, 238-242 (2008)

[6] A. Corma, S. Iborra, and A. Velty, *Chem. Rev.*, 107, 2411-2502 (2007)

[7] H.E. Valentin, A. Schönebaum, A. Steinbüchel, *Appl. Microbiol. Biotechnol.*, 36, 507-514 (1992)

[8] C.W. Lee, R. Urakawa and Y. Kimura, *Eur. Polym. J.*, 34 (I), 117-122 (1998)

[9] R. Solaro, G. Canton and E. Chiellini, *Eur. Polym. J.*, 33 (2), 205-211 (1997)

[10] W. Saiyasombat, R. Molloy, T.M. Nicholson, A.F. Johnson, I.M. Ward and S. Poshyachinda, *Polymer*, 39 (23), 5581–5585 (1998)

[11] M.T. Pérez-Prior, J.A. Manso, M.P. García-Santos, E. Calle, and J. Casado, *J. Org. Chem.*, 70, 420-426 (2005)

[12] K.N. Houk, A. Jabbari, H.K. Hall, Jr, and C. Alemán, *J. Org. Chem.*, 73, 2674--2678 (2008)

[13] J.I. Brauman and A.J. Pandell, *J. Am. Chem. Soc.*, 89 (21), 5421-5424 (1967)

[14] M. Node, K. Nishide, M. Ochiai, K. Fuji and E. Fujita, *J. Org. Chem.*, 46, 5163-5166 (1981)

[15] P.J. van den Brink, K.L van Hebel, J.P. Lange and L. Petrus, *US Patent*, No. 0162239 A1 (2006)

[16] J.P. Lange, J.Z. Vestering and R.J. Haan, *Chem. Comm.*, 3488-3490 (2007)

[17] S.G. Nelson, K.L. Spencer, W.S. Cheung and S.J. Mamie, *Tetrahedon,* 58, 7081-7091 (2002)

[18] C. Burba and H.G. Volland, *US Patent* No. 4,156,779 (1979)

[19] R.G.Pearson, *J. Am. Chem. Soc.*, 85, 3533-3543 (1963)

[20] O. Levenspiel, *Chemical Reaction Engineering*, 3rd ed.; Wiley, 53–55 (1998)

[21] C. Reichardt, *Solvents and Solvent Effect in Organic Chemistry*, 3rd ed.; Wiley-VCH: Weinheim, 237-273 (2003)

[22] G. Del Re, *J. Chem. Soc.*, 4031-4040 (1958)

[23] R.C. Rizzo and W.L. Jorgensen, *J. Am. Chem. Soc.*, *121,* 4827-4836 (1999)
[24] J. Brandrup, E.H. Immergut and E.K. Grulke, *Polymer Handbook*, 4th ed.; John Wiley & Sons Inc., VII/675–VII/711 (1999)
[25] Web site of Sigma Aldrich: *www.sigmaaldrich.com/etc/medialib/docs /Aldrich/General_Information/polymer_solutions.pdf*, accessed on July 29th, 2011

Chapter 5
From GVL to novel polyurethanes: synthetic aspects

Abstract
In the preceding chapter, the ring opening of GVL with amine compounds was reported as a promising molecular engineering tool to synthesize precursors for new bio-based polymers. In this chapter experimental work on the synthesis of polymers based on GVL/1,2-ethanolamine and GVL/1,2-diaminoethane adducts, and di-isocyanates (1,4-phenylene-di-isocyanate (PDI) 2,4-toluene-di-isocyanate (TDI) and hexamethylene-di-isocyanate (HDI)) is described. The polymers were characterized by FTIR, ^{1}H-NMR, ^{13}C-NMR, elemental analysis and GPC. The best polymerization results were obtained using TEA as the catalyst, DMA as the solvent and a temperature of 140°C for the reaction of the GVL/1,2-aminoethanol adduct with TDI. A polymer with a molecular weight (Mw) of 156 KDalton was produced in 97% yield.

5.1. Introduction

Polyurethane chemistry has been studied intensively and is well developed. Typically, polyurethanes are obtained by the reaction of a di-isocyanate with bifunctional or multifunctional reagent such as diols or polyols. The wide range of chemical structures available to build polyurethanes led to the design of materials that easily can meet the functional product demands and to the extraordinary spreading of these materials in the market.[1] Material design is achieved by varying the chemical structures and molecular weights of both the poly-ol and the di-isocyanate compounds as the polymer precursors. As a result, polyurethanes have been designed and developed for many product applications, such as elastomers, foams, coatings, adhesives, fibers, synthetic leathers and electrical insulators.[2,3]

Mechanical and physical properties of the obtained polymers are related to the chemical structure of the polyurethane backbone. Several studies have been performed to modify the chemical structures through varying the backbone of the monomers for both the di-isocyanates and the polyols. Some studies explored the relation between soft domains and thermal and mechanical properties of polyurethanes.[3-8] Other studies focused on the effect of the di-isocyanate structure on thermal and mechanical properties.[7-13] Soft domains in the backbone, such as aliphatic chains, contribute to flexibility and low temperature transitions like glass transition (T_g). Hard domains, such as functional groups and aromatic chains, contribute, to stiffness and high temperature transitions, such as the melting points of the polyurethanes.

Special techniques have been developed for the synthesis of high molecular weight polyurethanes. They are mainly based on the reaction of properly functionalized prepolymers with functionalized chain extenders.[14-17] For instance, prepolymers such as polyesters,[18] polyethers[19,20] and both polyethers and polyesters,[21] were reacted with iso-cyanates to build higher molecular weight polyurethanes. Another technique consists of the polymerization of high molecular weight monomers.

A number of polyurethanes prepared from biomass-based monomers have been reported. So far, these polymers were synthesized by using several stages, such as pre-polymerization followed by chain extension, [16,18,19,22] and have relatively low molecular weights.[23,24] Also the direct polymerization of relatively high molecular weight monomers is a promising approach to obtain high molecular weight polyurethanes.

γ-Valerolactone (GVL) is a chemical intermediate obtained from biomass-based levulinic acid by catalytic hydrogenation[25-28] and is considered to be a suitable building block for bio-based polymers. Some studies regarding direct polymerization of γ–valerolactone have been reported but most of the polymerizations resulted in polymers with relatively low molecular weights.[29-31] Alternatively, making a more reactive monomer from GVL through ring opening is a new versatile route to produce polymer precursors with relatively high molecular weights.

In the previous chapter we described the ring-opening of GVL by the addition of amine compounds to yield diols under mild reaction conditions. Using

this approach enables product design through varying the structure of the amine compound, such as backbone structure and presence of functional groups, and appears to be an attractive and promising polymer engineering pathway.

In this work, a novel route for the synthesis of high molecular weight polyurethanes has been investigated. Two γ-valerolactone-derived diols, i.e. N,N'-1,2-ethanediylbis-(4-hydroxy-pentanamide) **(1)** and 4-hydroxy-N-(2-hydroxyethyl)-pentanamide **(2)** obtained by the ring-opening of γ-valerolactone with ethylenediamine and aminoethanol, respectively, were reacted with di-isocyanate compounds. Both diols differ significantly in structure and molecular weight and were selected to evaluate the influence of chain composition on the polymerization reaction and the properties of the products. The synthesis of the diols, as shown in Scheme 1, was discussed in Chapter 4.

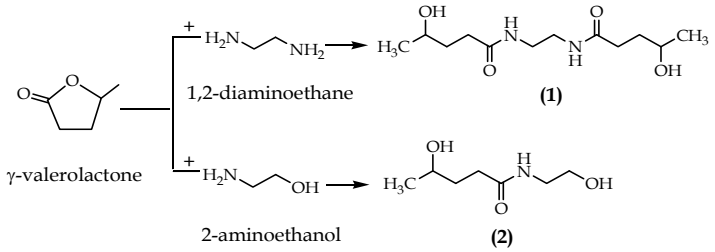

Scheme 1. Syntheses of γ-valerolactone-based diols

To test the feasibility of making polymers from these diols, **(1)** was reacted with phenyl isocyanate **(3)** using a Lewis base catalyst. Subsequent experiments were performed by reacting the diols **(1)** and **(2)** with different di-isocyanates to obtain novel polyurethanes. To study the effect of chemical structure on the properties of the products, an aliphatic di-isocyanate i.e. hexamethylene-di-isocyanate **(6)** and two aromatic di-isocyanates i.e. 1,4-phenylene-di-isocyanate **(5)** and 2,4-toluene-di-isocyanate **(7)** were selected.

To gain more insight in the polymerizations, the effect of process variables such as the use of a Lewis base catalyst, temperature variation and solvent composition, were evaluated.

5.2. Experimental

5.2.1. Materials

N,N'-1,2-ethanediylbis-(4-hydroxy-pentanamide) **(1)** and 4-hydroxy-N-(2-hydroxyethyl)-pentanamide **(2)** were obtained by a procedure described in Chapter 4. Triethylamine, TEA (purity ≥ 99 %), pyridine (purity ≥ 99%), (N,N-dimethylformamide, DMF(purity ≥ 99.8%), 1-Methyl-2-pyrrolidinone, NMP (purity ≥99.5%) and DMSO (purity ≥99.9%) were purchased from Sigma-Aldrich. N,N-dimethylacetamide, DMA (purity ≥ 99 %) was purchased from Sigma. 1,4-Phenylene-di-isocyanate, PDI **(5)** (purity ≥ 99%) and phenyl isocyanate **(3)** (purity ≥ 98%) were purchased from Aldrich. 2,4-Toluene-di-isocyanate, TDI **(7)** (purity ≥ 95%) and hexamethylene-di-isocyanate, HDI **(6)** (purity ≥ 98%) were purchased from Fluka.

Diethyl ether (analytical grade, purity ≥ 99.5 %), and n-hexane (analytical grade, purity ≥ 99%) were purchased from Lab Scan. All chemicals were used without purification, except DMA, NMP, TEA and pyridine which were dried over BaO and then distilled under reduced pressure. Chemical codes are given in Scheme 2 and 3.

5.2.2. Analyses & characterizations

^{1}H- and ^{13}C-NMR spectra were recorded with tetramethylsilane (TMS) as the internal reference on a Varian 400 MHz spectrometer using DMSO-d_6 as the solvent. Multiplicities of proton resonance were designated as single (s), doublet (d), triplet (t), and multiplet (m).

FT-IR spectra were recorded on a Perkin Elmer FT-IR spectrometer (Spectrum 2000 series, resolution 2.0 cm^{-1}, 100 scans). Spectra of solids were carried out using KBr pellets. Vibrational transition frequencies are reported in wave number (cm^{-1}). Band intensities are assigned as weak (w), medium (m), shoulder (sh), strong (s) and broad (br).

Elemental analyses were determined using a Flash EA 1112 from CE Instruments.

Gel permeation chromatograms were acquired at 70 °C with a *Viscotek GPC Max* instrument equipped with a PL-mixed C Column (*Polymer Labs*) at 70°C. DMF containing LiBr (10^{-2} M) was used as eluent and calibration was made against polymethylmethacrylate (PMMA) standards.

5.2.3. Preparation of model compound (4)

An amount of 367 mmoles of **(1)** dissolved in 2 ml of the dried-distilled DMA, was mixed with 734 mmoles of phenyl-isocyanate **(3)** and then 0.4 mmoles of TEA was added in a 10-ml Schlenk-tube. The mixture was saturated with nitrogen gas under vacuum condition to prevent intrusion of moisture. This mixture was stirred under nitrogen atmosphere for 2 hours at 25 °C, followed by 3 hours at 60 °C, and then 5 hours at 140 °C. Separation of the reaction product from the remaining reactants was conducted by adding a mixture of n-hexane and diethyl ether (1/1 v/v) followed by stirring to precipitate the product and to dissolve the reactants in the solvent mixture. The precipitate was decanted and re-precipitated using the same procedure (three times). Finally the precipitate was dried under vacuum for about 5 hours at 70 °C to remove the remaining solvents. The weight of the product was determined to calculate the yield. The product was characterized with ^{1}H- and ^{13}C-NMR analysis, FTIR and elemental analysis. The results of these analyses are shown in Appendix 5.5.1.

5.2.4. Preparation of novel polyurethanes

930 mmoles of **(1)** or **(2)** dissolved in 2 ml of purified DMA or NMP, was mixed with 930 mmoles of di-isocyanate (PDI, TDI or HDI) and 0.5 mmoles of a Lewis base catalyst (TEA or pyridine) in a 10-ml Schlenk-tube. The solution of the diol was saturated with nitrogen gas to prevent intrusion of moisture. The mixture was stirred under nitrogen atmosphere for 2 hours at 25 °C. The polymerization was

conditioned at 60 °C for 3 hours, and then left to react at a final reaction temperature (60, 90 or 140 °C) for 5 hours. The reaction mixture as viscous solution was added drop-wise into 200 mL of water to terminate polymerization and to separate the product as a precipitate. The solid was filtered and washed with methanol and water (1/1 v/v). The product was dried under vacuum condition for 10 hours at 80 °C.

The weight of the product was determined to calculate the yield. The products were then characterized using ^{1}H- and ^{13}C-NMR analysis, FTIR and elemental analysis. The results of these analyses are shown in Appendix 5.5.2.

5.3 Results & discussions

5.3.1. Model compound study

N,N'-1,2-ethanediylbis-(4-hydroxy-pentanamide) **(1)** and 4-hydroxy-N-(2-hydroxyethyl)-pentanamide **(2)** (both γ-valerolactone-derived products as discussed in Chapter 4) were initially tested as polymer precursors by reaction with mono-isocyanate. When diol **(1)** was reacted with excess phenyl-isocyanate **(3)** (*see* Scheme 2) in DMA as the solvent, 1,2-bis-(n-phenylamidocarbonyl)-N,N'-1,2-ethanediylbis-(4-hydroxy-pentanamide) **(4)** was obtained in high yield (90%). Product **(4)** was characterized with ^{1}H-NMR and ^{13}C-NMR, as shown in Figure 1.

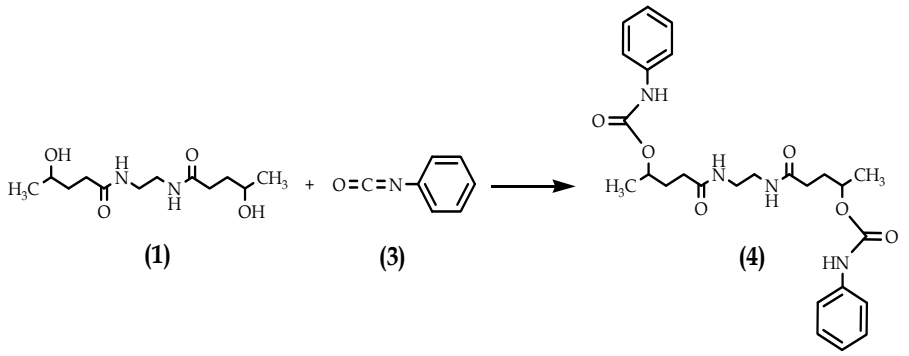

Scheme 2. Synthesis of model compound **(4)**

The reaction of **(1)** and phenylisocyanate occurs through the addition of the reactive hydroxyl groups of **(1)** to the isocyanate group to form a urethane group, as shown in Scheme 2. The chemical shift for the urethane C=O group (7 in Figure 1) is found at δ 153.9 ppm in the ^{13}C-NMR spectrum, while the N-H bond (13 in Figure 1) appears at δ 9.72 ppm in the ^{1}H-NMR spectrum. The amide group (5 and 12 in Figure 1) is assigned at δ 172.3 ppm in ^{13}C-NMR and at δ 7.83 ppm in ^{1}H-NMR.

The FTIR spectrum of **(4)** shows a υ_{NH} of the amide N-H bonds at 2944 – 3308 cm^{-1}, while the υ_{OCONH} (the urethane group) and the υ_{CONH} (the amide group) appear at 1695 cm^{-1} and 1641 cm^{-1}, respectively. Elemental analysis confirms the formation of compound **(4)**. More details about the characterization (^{1}H- ^{13}C-NMR, FTIR and elemental analysis) are provided in Appendix 5.5.1.

The successful reaction of **(1)** with the mono-isocyanate confirms that γ-valerolactone-derived diols are potential green polymer precursors. The remainder of the chapter focuses on the conversion of the diols into novel polyurethane polymers

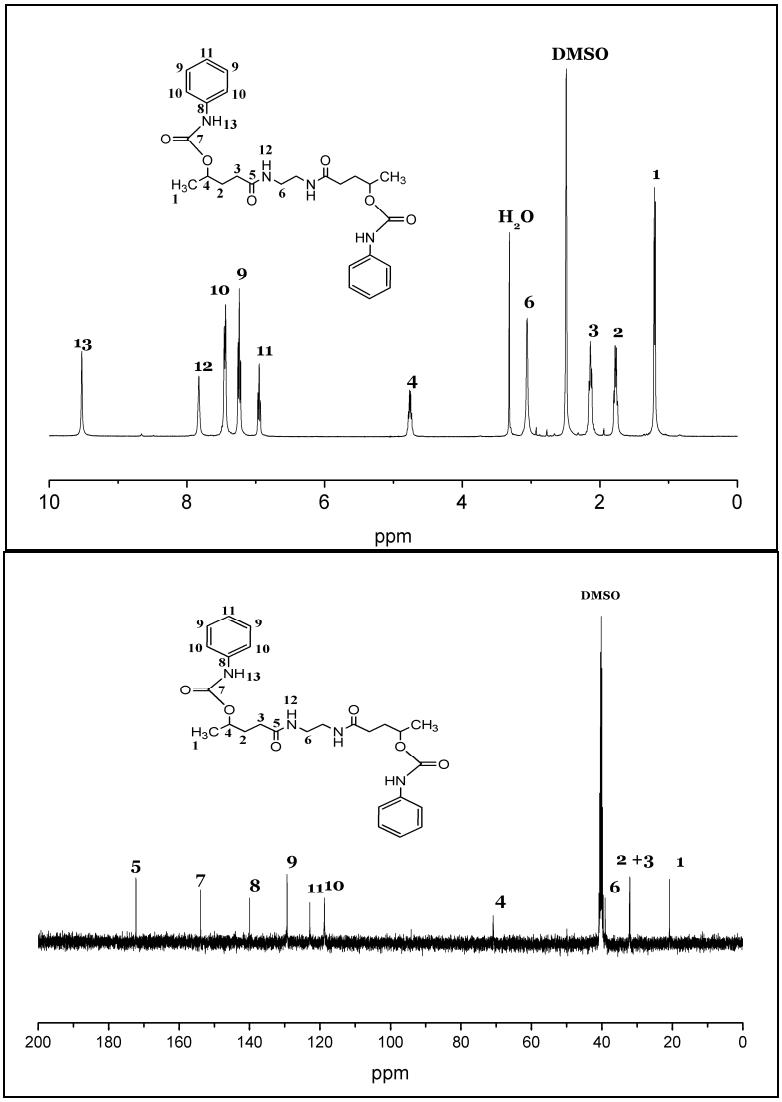

Figure 1. ^{1}H-NMR and ^{13}C-NMR spectra of model compound **(4)**

5.3.2. Synthesis and characterization of novel polyurethanes

The diols **(1)** and **(2)** were reacted with an equimolar amount of a di-isocyanate in a water free solution in the presence of a Lewis base catalyst to deliver novel polyurethanes in a one-step reaction. The polymerization reaction is depicted in Scheme 3.

As both diols contain an amide group, polymers with both urethane and amide groups are formed as shown in Scheme 3. Characterization of the polymers was performed by ^{1}H- ^{13}C-NMR, FTIR and elemental analyses. A representative ^{1}H- and ^{13}C-NMR spectrum for **(P1-7)** as one of the novel polyurethanes is shown in Figure 2.

The urethane C=O group in **(P1-7)** (14 in Figure 2) appears at δ 154.7 ppm in the ^{13}C-NMR spectra, and the urethane groups (16 and 17 in Figure 2) appear at δ 8.65 and δ 9.42 ppm in the ^{1}H-NMR spectra. Meanwhile the chemical shift of the amide groups (5 and 15 in Figure 2) appear at δ 172.3 ppm in the ^{13}C-NMR spectrum for the C=O and at δ 7.82 ppm in the ^{1}H-NMR spectrum for the NH.

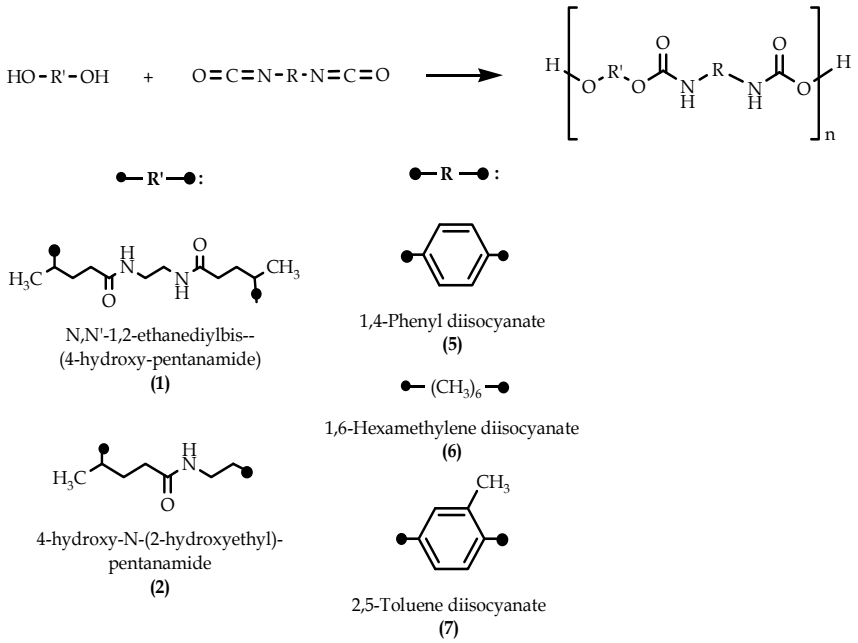

Scheme 3. Polymerization of the γ-valerolactone-derived diols with di-isocyanates.

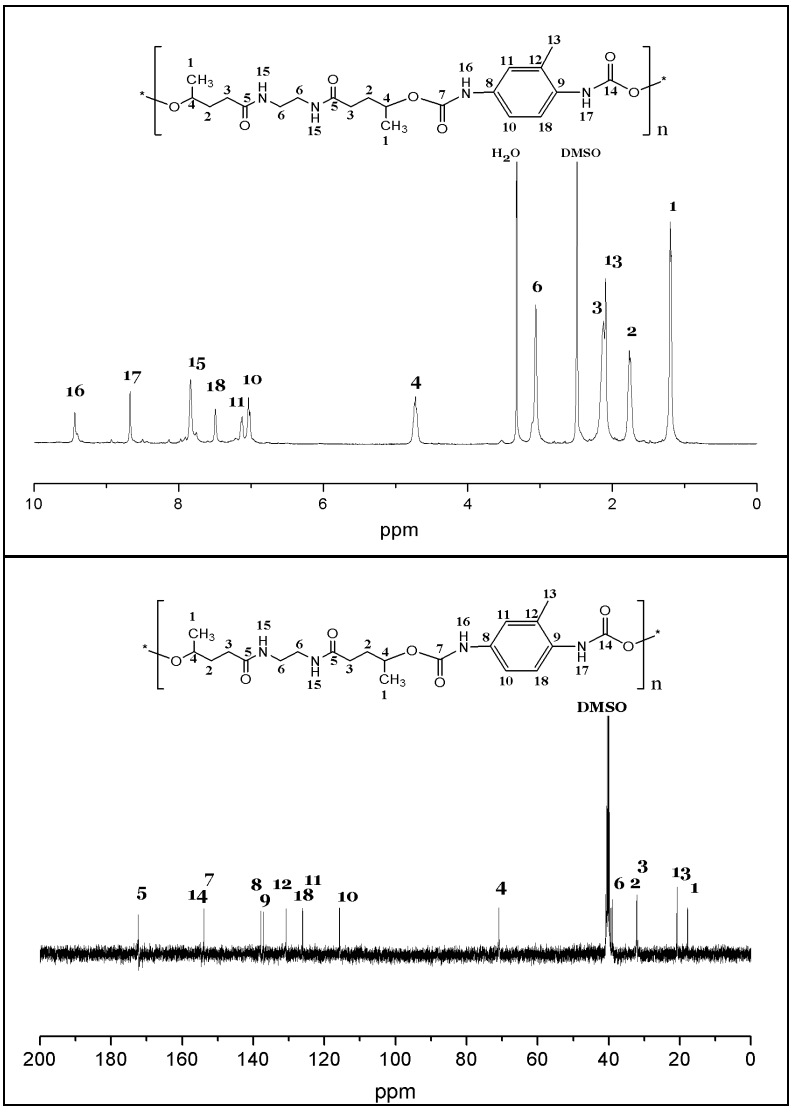

Figure 2.[1]H-NMR and [13]C-NMR spectra of (**P1-7)**

The structure of the polymer is also confirmed by FTIR spectrum. The presence of the v_{CONH} (the amine bonds) appears at 2891 – 3266 cm^{-1}, while the v_{OCONH} (the urethane group) and the v_{CONH} (the amide group) appear at 1703 cm^{-1} and 1621 cm^{-1}, respectively. Detailed analytical data for all novel polyurethanes are shown in Appendices 5.5.2. and 5.5.3.

5.3.3. Process optimization study for the polymerizations

A reaction optimization study was performed to determine the effects of process variables such as solvent, catalyst and temperature. In this study the yield, determined by NMR analysis of the reaction product, and the molecular weight of the polymer products were used as performance indicators. Furthermore the coding of the polymer products is shown in Scheme 4.

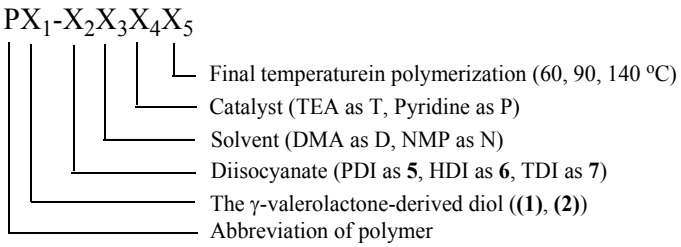

Scheme 4. Coding of polyurethane products

Effect of catalysts. Two catalysts were tested, TEA and pyridine. Both have a positive effect on the polymerization reaction; see Table 1 for details. TEA has a stronger catalytic effect than pyridine on the polymerization rate; compare experiment **P1-7DT140** with experiment of **P1-7DP140**. A similar but less pronounced catalytic effect is found by comparing the polymerization yields and molecular weights in experiments **P1-7NT90** and **P1-7NP90**. At the lower temperature, the effect is less prominent, but this may also be attributed to the differences in solvent and reaction temperature. In both cases, however, TEA provides the best results in terms of yield and molecular weight.

Table 1. Catalyst effect on polymer yield and polymer molecular weight
Experimental conditions: *see* product codes

Catalyst	Product Code	Yield, %	$\overline{M}_n$ (kDalton)	$\overline{M}_w$ (kDalton)
TEA	**P1-7DT140**	97	59	156
Pyridine	**P1-7DP140**	71	64	144
TEA	**P1-7NT90**	45	33	91
Pyridine	**P1-7NP90**	43	21	90

Van Maris *et al.*[32] reported a reaction mechanism to explain the role of tertiary amine as Lewis base catalyst in polyurethane synthesis (Scheme 5). This mechanism implicitly indicates that steric hindrance at the nitrogen atom and the ability of the

nitrogen atom to donate electrons (basicity) play important roles in the formation of the transition state.

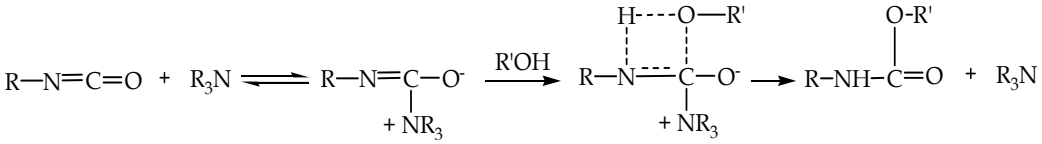

Scheme 5. Reaction mechanism for polymerization catalyzed by tertiary amine[32]

When comparing the yields of the polymer products using triethylamine and pyridine as the catalyst, the results suggest that catalyst basicity plays a dominant role. As reported by Shim *et al.*, the Gutmann donor number (D_N) of TEA (10.75 kcal/mol), a measure of Lewis basicity, is higher than that of pyridine (5.21 kcal/mol).[33] It indicates that the electron donor ability of TEA is relatively high which explains the higher yield of product, as shown in Table 4. Furthermore, Denmark *et al.*,[34] reported scales of Lewis basicity based on an enthalpy advantage for the formation of an active adduct as transition state. These studies indicate that the enthalpy for the formation of an adduct with TEA is higher than that for pyridine.

Effect of temperature. The effect of temperature was investigated by performing experiments in a temperature range of 60 – 140 °C. The polymerizations resulted in polyurethanes with yields and molecular weights as shown in Figure 3 – 5 and Table 2.

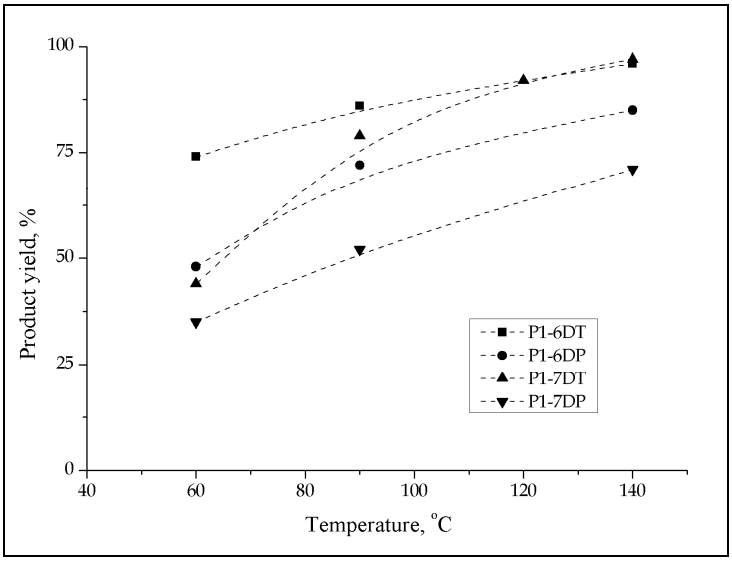

Figure 3. Temperature effect on product yield for polymerizations of **(1)** with **(6)** and **(7)**. Experimental conditions: *see* product codes

Figure 3 shows that temperature has a strong effect on the polymerization rate. All reactions of **(1)** with **(6)** and **(7)** with TEA or pyridine as catalyst in DMA solvent resulted in higher yields at higher temperatures.

The effect of temperature on molecular weight is shown in Figure 4 and Table 2. Higher temperatures lead to polymers with higher molecular weights.

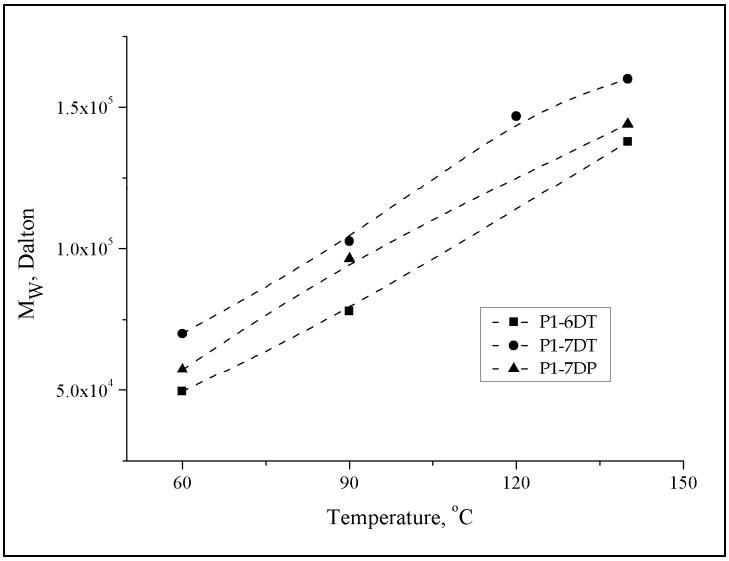

Figure 4. Temperature effect on polymer molecular weight for polymerizations of **(1)** with **(6)** and **(7)**. Experimental conditions: *see* product codes

Table 2. Result forthe polymerizations of **(1)** with **(6)** and **(7)**. Experimental conditions: *see* product codes

Product	**Yield,** %	$\overline{M}_n$ (kDalton)	$\overline{M}_w$ (kDalton)	$\overline{M}_w / \overline{M}_n$
P1-7DT60	44	8	70	8.4
P1-7DT90	79	23	103	4.5
P1-7DT120	92	41	147	3.6
P1-7DT140	97	59	156	2.6
P1-7DP90	52	46	96	2.2
P1-7DP140	71	64	144	2.3
P1-6DT60	74	49	7	7.4
P1-6DT90	86	78	12	6.7
P1-6DT140	96	137	51	2.7

A correlation between product yield and the molecular weight of the polyurethanes exists (*see* Figure 5). This figure shows the effect of di-isocyanate structure and catalyst on the kinetics of the polymerization. The presence of TEA (experiment of P1-7DT) leads to a faster reaction than the presence of pyridine (experiment of P1-7DP) at the same temperature. The polymerization in the P1-7 experiment shows a higher reaction rate than the P1-6 experiment. Due to its aromatic structure, TDI (7) is expected to be more reactive than HDI (6) in the polymerization at the same temperature. This observed reactivity indeed confirms that the reactivity of TDI is higher than that of HDI.[35]

Table 2 summarizes the molecular weights and polydispersity, defined as $\overline{M}_w / \overline{M}_n$, for the polymers. Increasing the polymerization temperature reduces the polydispersity. This tendency may be explained by a better homogeneity of the polymerization medium due to the higher temperatures.[36,37]

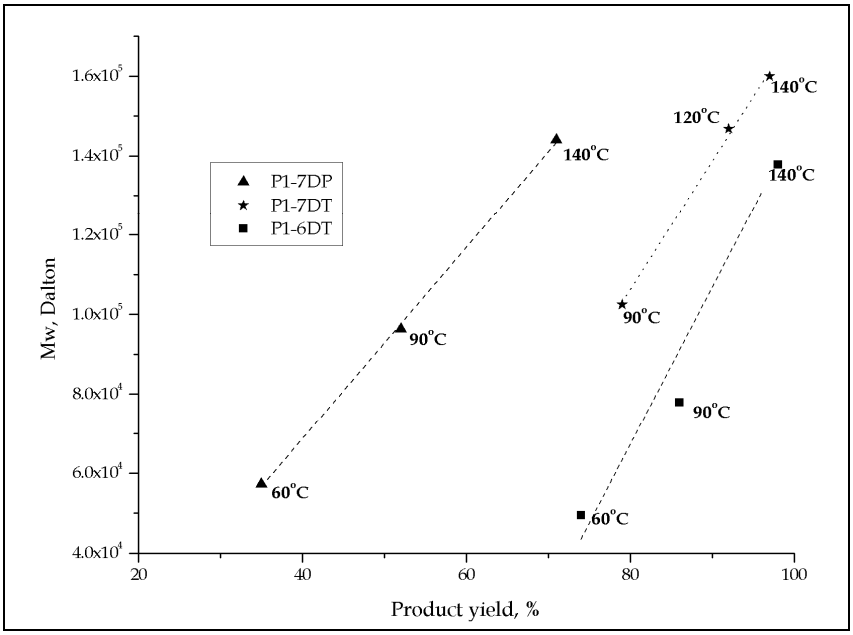

Figure 5. Correlation between molecular weight and product yield for polymerizations of **(1)** with **(6)** and **(7)** at various temperatures. Experimental conditions: *see* product codes

Effect of solvent. To study the effect of solvent on the polymerization, several experiments were performed for the reaction of **(1)** with **(7)** in both NMP and DMA solvent at 140 °C (Table 3).

Table 3. Solvent effect on polymer yield and molecular weight
Experimental conditions: *see* product codes

Product	**Yield,** %	$\overline{M}_n$ (kDalton)	$\overline{M}_w$ (kDalton)	$\overline{M}_w / \overline{M}_n$
P1-7DT140	97	59	156	2,6
P1-7NT140	54	43	96	2,2
P1-7DP140	71	64	144	2,3
P1-7NP140	67	48	100	2,1

Table 3 indicates that the use of DMA (**P1-7DT140** and **P1-7DP140** experiments) leads to the highest yields and molecular weights. (NMP experiments: **P1-7NT140** and **P1-7NP140**).

Scheme 5 shows that the proposed reaction mechanism for the polymerization involves polar intermediates. Therefore solvent polarity such as dielectric constant may be an important parameter. The dielectric constants for DMA and NMP are 37.8 and 32.0, respectively.[38,39] Therefore the higher yield and higher molecular weight in DMA, as shown in Table 3, are likely due to the higher polarity of DMA. The results are in line with research by Mallakpour *et al.*. They showed that the synthesis of polyureas *via* the polymerization of 4-(1-naphtyl)-1,2,4-triazolidine-3,5-dione with di-isocyanates gives higher yields in DMA than in NMP.[40]

5.3.4. Comparison of polyadditions

The last section showed that the best yield and the highest molecular weight for diol **(1)** were obtained at the highest temperature *viz.* 140 °C, using DMA as the solvent and TEA as the catalyst. This result triggered a comparison of the addition of **(1)** respectively **(2)** with **(6)** and **(7)** when performing the reaction at optimum conditions. The yield and molecular weights are depicted in Figure 7.

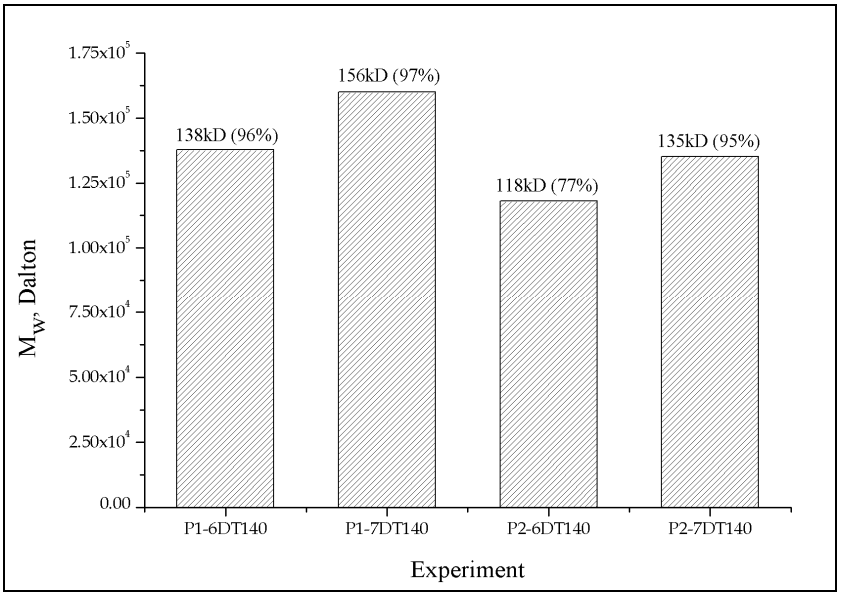

Figure 7. Molecular weight and product yield comparison at optimum polymerization conditions. Experimental conditions: *see* product codes

The figure shows that the polymerization of N,N'-1,2-ethanediylbis-(4-hydroxy-pentanamide) **(1)** and 4-hydroxy-N-(2-hydroxyethyl)-pentanamide **(2)** with the aliphatic **(6)** and aromatic **(7)** di-isocyanate at the best conditions resulted in polyurethanes with a yield in the range of 77 % (with 118 kD as molecular weight) to 97 % (with 156 kD as molecular weight).

Reaction of **(1)** with both di-isocyanates results in higher yields and higher molecular weight polymers than the reaction with precursor **(2)**. There may be two possible explanations for this behavior, viz. higher molecular weight and higher reactivity of monomer **(1)**. Scheme 5, which shows the reaction mechanism of these polymerizations, suggests that catalyst basicity is important. Referring to Scheme 1, the reagents **(1)** and **(2)** contain two nitrogen atoms and one nitrogen atom in the backbone, respectively. These nitrogen atoms may play a role and assist in forming the transition state. On the basis of this explanation, **(1)** is expected to be more reactive than (**2**), in line with the experimentally observed reactivity.

Figure 7 also depicts that molecular weights and yields obtained for the addition of the γ-valerolactone-based diols to the aromatic di-isocyanate **(7)** are higher than to the aliphatic di-isocyanate **(6**). The di-isocyanate structure affects the NCO group reactivity, which increases by substituents that stabilize the positive load on the NCO group carbon. This is why HDI, as aliphatic di-isocyanate, is less

reactive than the aromatic TDI. The latter will be more reactive when substituents on the aromatic ring stabilize the transition state of the reacting system.[35]

5.4. Conclusions

Ring opening of biomass-based γ-valerolactone through reaction with (di)-amine compounds resulted in interesting novel diols, which can be applied as green polymer precursors. Using the monomers in condensation reactions with di-isocyanates resulted in a set of new polyurethanes. The approach offers a novel polymer engineering pathway to produce new polymers starting with a bio-based chemical.

Process variables such as solvent, catalyst, and temperature were varied to determine their effects on the polymerization reaction. The best results were obtained at 140°C with TEA as the catalyst and DMA as the solvent for the reaction of TDI with the precursor made by ring-opening GVL with 1,2-diaminoethane. In general, all experiments performed within this study gave polyurethanes with relatively high molecular weights for all starting materials.

The structure of the polymer backbone has a dramatic effect on relevant polymer product properties, such as thermal and mechanical properties. Further investigations of these properties will be discussed in Chapter 6.

5.5. Appendices:

5.5.1. Analyticaldata for model compound

Product	Chemical Structure Appearance & Elemental analysis	^{1}H-Chemical Shift (ppm)	^{13}C-Chemical Shift (ppm)	FTIR (cm^{-1})
(4) 90% (yield)	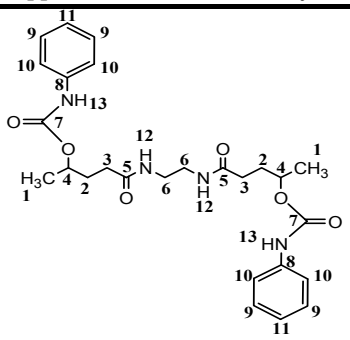 *1,2-bis-(n-phenylamidocarbonyl)-N,N'-1,2-ethanediylbis-(4-hydroxy-pentanamide)* $C_{26}H_{34}N_4O_6$, white powder Calcd: 62.6, C; 6.9, H; 11.2, N% Found: 62.8, C; 6.8, H; 11.3, N%	(H-1) 1.21 (H-2) 1.78 (H-3) 2.16 (H-4) 4.78 (H-6) 3.14 (H-9) 7.26 (H-10) 7.43 (H-11) 6.96 (H-12) 7.83 (H-13) 9.72	(C-1) 20.83 (C-2) 32.07 (C-3) 32.18 (C-4) 70.91 (C-5) 172.26 (C-6) 39.06 (C-7) 153.92 (C-8) 139.97 (C-9) 129.37 (C-10) 118.79 (C-11) 122.90	3308 (free N-H, br) 2944-2976 (H-bonded N- H, m) 1695 (C=O in urethane, s) 1641 (C=O in amide, s) 1538 (stretched C-N & bended N-H, s) 1243 (C-O-C, s)

5.5.2. Analytical data for polyurethane products

Product	Chemical Structure Appearance & Elemental analysis	^{1}H-Chemical Shift (ppm)	^{13}C-Chemical Shift (ppm)	FTIR (cm^{-1})
(P1-5)	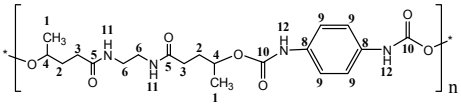 $C_{20}H_{28}N_4O_6$, white solid Calcd.: 57.1, C; 6.7, H; 13.3, N % Found: 57.9, C; 6.6, H; 14.6, N %.	(H-1) 1.21 (H-2) 1.78 (H-3) 2.16 (H-4) 4.78 (H-6) 3.14 (H-9) 7.32 (H-11) 7.82 (H-12) 9.49	(C-1) 20.84 (C-2) 32.09 (C-3) 32.21 (C-4) 70.91 (C-6) 39.06 (C-5) 172.30 (C-8) 134.99 (C-9) 119.46 (C-10) 154.01	3302 (free N-H, br) 2856-2976 (H-bonded N-H, m) 1694 (C=O urethane, s) 1643 (C=O in amide, s) 1527 (stretched C-N & bended N-H, s) 1260 (C-O-C, s)
(P1-6)	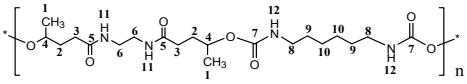 $C_{20}H_{36}N_4O_6$, white solid Calcd: 56.1, C; 8.5, H; 13.1, N % Found: 55.8, C; 8.8, H; 14.1, N %	(H-1) 1.11 (H-2) 1.68 (H-3) 2.08 (H-4) 4.49 (H-6) 3.06 (H-8) 2.92 (H-9) 1.32 (H-10) 1.19 (H-11) 7.80 (H-12) 6.95	(C-1) 21.05 (C-2) 30.81 (C-3) 32.25 (C-4) 70.98 (C-5) 172.30 (C-6) 39.06 (C-7) 158.25 (C-8) 32.30 (C-9) 30.01 (C-10) 26.40	3302 (free N-H, br) 2855-2927 (H-bonded N- H, m) 1682 (C=O urethane, s) 1641 (C=O in amide, s) 1531 (stretched C-N & bended N-H, s) 1256 (C-O-C, s)
(P1-7)	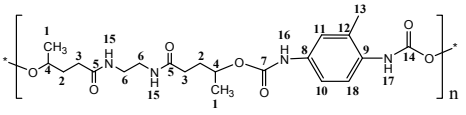 $C_{21}H_{30}N_4O_6$, white solid Calcd.: 58.1, C; 6.9, H; 12.9, N % Found: 57.6, C; 6.8, H; 13.3, N %	(H-1) 1.19 (H-2) 1.78 (H-3) 2.12 (H-4) 4.78 (H-6) 3.06 (H-10)7.02 (H-11) 7.12 (H-13) 2.09 (H-15) 7.82 (H-16) 8.65 (H-17) 9.42 (H-18) 7.52	(C-1) 17.84 (C-2) 32.11 (C-3) 32.15 (C-4) 71.53 (C-5) 172.32 (C-6) 39.07 (C-7&14) 154.69 (C-8) 137.19 (C-9) 137.95 (C-10) 115.74 (C-11&18) 126.36 (C-12) 130.86 (C-13) 20.81	3266 (free N-H, br) 2891-2965 (H-bonded N-H, m) 1703 (C=O urethane, s) 1621 (C=O in amide, s) 1531 (stretched C-N & bended N-H, s) 1236 (C-O-C, s)

(P2-6)	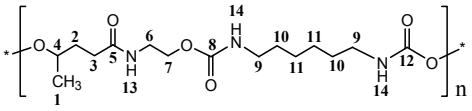 $C_{15}H_{27}N_3O_5$, brownish solid Calcd.: 54.7, C; 8.3, H; 12.8, N % Found: 54.8, C; 8.6, H; 13.8, N %	(H-1) 1.11 (H-2) 1.68 (H-3) 2.08 (H-4) 4.61 (H-6) 3.21 (H-7) 3.89 (H-9) 2.92 (H-10) 1.35 (H-11) 1.21 (H-13) 6.95-7.06 (H-14) 7.91	(C-1) 20.83 (C-2) 30.70 (C-3) 32.03 (C-4) 69.99 (C-5) 172.47 (C-6) 38.88 (C-7) 62.56 (C-8&12) 156.76 (C-9) 32.30 (C-10) 30.07 (C-11) 26.71	3312 (free N-H, br) 2856-2929 (H-bonded N-H, m) 1693 (C=O urethane, s) 1634 (C=O in amide, s) 1531 (stretched C-N & bended N-H, s) 1241 (C-O-C, s)
(P2-7)	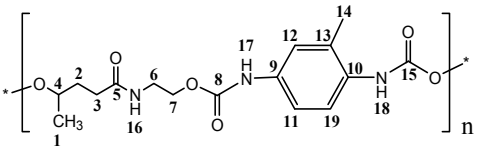 $C_{16}H_{21}N_3O_5$, brownish solid Calcd.: 57.3, C; 6.3, H; 12.5, N % Found: 57.6, C; 6.3, H; 13.2, N %	(H-1) 1.19 (H-2) 1.78 (H-3) 2.12 (H-4) 4.75 (H-6) 3.32 (H-7) 4.33 (H-11)7.02–7.12 (H-12) 7.52 (H-14) 2.09 (H-19) 7.91	(C-1) 17.84 (C-2) 32.04 (C-3) 32.22 (C-4) 71.53 (C-5) 172.53 (C-6) 38.79 (C-7) 62.56 (C-8&15) 155.65 (C-9) 138.16 (C-10) 136.29 (C-11) 115.53 (C-12&19) 126.54 (C-13) 130.81 (C-14) 20.731	3278 (free N-H, br) 2927-2975 (H-bonded N-H, m) 1703 (C=O in urethanes) 1622 (C=O in amide, s) 1531 (stretched C-N & bended N-H, s) 1230 (C-O-C, s)

*) Yield data depend on experimental condition and are given in Appendix 5.5.3.

5.5.3. Yields and molecular weights of polyurethane products

Product	Yield, %	$\overline{M}_n$, (kDalton)	$\overline{M}_w$, kDalton)	$\overline{M}_w / \overline{M}_n$
P1-5DT120	90	58	150	2.6
P1-6DT60	74	7	46	7.4
P1-6DT 90	86	12	78	6.7
P1-6DT120	90	31	121	3.9
P1-6DT140	96	51	138	2.7
P1-7DT90	79	23	103	4.5
P1-7DT120	92	41	147	3.6
P1-7DT140	97	59	156	2.6
P1-7DP60	35	14	57	4.2
P1-7DP90	52	45	96	2.2
P1-7DP140	71	64	144	2.3
P1-7NP90	43	21	89	4.3
P1-7NP140	67	48	100	2.1
P1-7NT90	45	33	91	2.8
P1-7NT140	54	43	96	2.2
P2-6DT90	55	20	61	3.1
P2-6DT120	68	41	100	2.4
P2-6DT140	77	58	118	2.0
P2-7DT120	94	19	134	7.2
P2-7DT140	95	21	135	6.4

5.6. References:

[1] G.A. Howarth, *Surf. Coat. Int.: Part B: Coat. Trans.*, 86, 11-118 (2003)

[2] X. Wang, X. Luo and X. Wang, *Polymer Testing*, 25, 18-24 (2005)

[3] H. Yeganeh, Razavi-Nouri and M. Ghaffari, *Polym. Adv. Technol.*, 19, 1024-1032 (2008)

[4] Y. Nori and I. Hideaki, *The Textile Machinery Society of Japan*, 54(2),T29-T36 (2001)

[5] N. Kébir, I. Campistron, A. Laguerre, J-F. Pilard, C. Bunel, J-P Couvercelle and C. Gondard, *Polymer.*, 46, 6869–6877 (2005)

[6] Y.M. Lee, J.C. Lee and B.K. Kim, *Polymer*, 35(5), 1095 (1994)

[7] D.J. Hourston, G. Williams, R. Satguru, J.D. Padget and D. Pears, *J. App. Polym. Sci.*, 66, 2035–2042 (1997)

[8] B.K. Kim and Y M. Lee, *Colloid Polym Sci.*, 270, 956-961 (1992)

[9] J.B. Lee, T. Kato, S. Ujiie, K. Iimura and T. Uryu, *Macromolecules*, 28**,** 2165-2171 (1995)

[10] B. Bengtson, C. Feger, W.J. Macknight and N.S. Schneider, *Polymer*, 895, 26 (1985)

[11] S-L. Huang and J-Y. Lai, *Eur. Polym. J.*, 33(10-12), 1563-1567 (1997)

[12] D. J. Hourston, G. Williams, R. Satguru, J.D. Padget and D. Pears, *J. Appl. Polym. Sci.*, 67, 1437–1448 (1998)

[13] I.W. Cheong, H.C. Kong, J.H An and J.H. Kim, *J. Pol. Chem.,* 42, 4353–4369 (2004)

[14] C. Bonini, M. Dáuria, L. Emanuele, R. Ferri and R. Pucciariello, *J. App. Pol. Sci.*, 98, 1451–1456 (2005)

[15] E. Scortanu, C. Prisacariu, A. Caraculacu, M. Bruma and N. Sulitanu, *High Performance Polymers*, 18, 127–143 (2006)

[16] Y. Xu, Z. Petrovic, S. Das and G.L. Wilkes, *Polymer*, 49, 4248-4258 (2008)

[17] J. Borda, S. Keki, I. Bodnar, N. Nemeth and M. Zsuga, *Polym. Adv. Technol.,* 17, 945-953 (2006)

[18] K. Onder, *United States Patent*, No. 0156225 A1 (2002)

[19] M. Rogulska, A. Kultys and W. Podkoscielny, *Eur. Polym. J.*, 43, 1402-1414 (2007)

[20] P.T. Knight, K.M. Lee, H. Qin and P.T. Mather, *Biomacromol.*, 9, 2458-2467 (2008)

[21] M.J. Donnelly, J.L. Stanford and R.H. Still, *Carbohyd. Polym.,* 14, 221-240 (1991)

[22] H.R. van der Wal and C.F. Bartelink, *World Intellectual Property Organization*, no. 04 7433 A1 (2006)

[23] C. Yamanaka and K. Hasimoto, *J. Pol. Sci.*, 40, 4158-4166 (2002)

[24] M.V. De Paz, R. Marin, F. Zamora, K. Hakkou, A. Alla, J.A. Galbis and S. Munoz-Guerra, *J. Polym. Sci.: Part A: Polym. Chem.*, 45, 4109-4117 (2007)

[25] R.H. Leonard, *Ind.Eng.Chem.,* 48(8), August (1956)

[26] B.V. Timokhin, V.A. Baransky and G.D. Eliseeva, *Russ. Chem. Rev.*, 68(1), 73-84 (1999)

[27] J.J. Bozell, L. Moens, D.C. Elliott, Y. Wang, G.G. Neuenscwander, S.W. Fitzpatrick, R.J. Bilski and J.L. Jarnefeld, *Res., Conserv. Recycle.*, 28, 227–239 (2000)

[28] B. Girisuta, L.P.B.M. Janssen and H.J. Heeres, *Chem. Eng. Res. Design*, 84(A5), 339–349 (2006)
[29] H.E. Valentin, A. Schönebaum and A. Steinbüchel, *Appl. Microbiol. Biotechnol.*, 36, 507-514 (1992)
[30] C.W. Lee, R. Urakawa and Y. Kimura, *Eur. Polym. J.*, 34(1), 117-122 (1998)
[31] R. Solaro, G. Canton and E. Chiellini, *Eur. Polym. J.*, 33(2), 205-211 (1997)
[32] R van Maris, Y. Tamano, H. Yoshimura and K.M. Gay, *J. Cellular Plastics*, 41, 305-322 (2005)
[33] J-G. Shim, Y.H. Jhon, J-H Kim, K-R Jang and J. Kim, *Bull. Korean Chem. Soc.*, 28(9), 1609-1612 (2007)
[34] S.E. Denmark and G.L. Beutner, *Angew. Chem. Int.*, 47, 1560-1638 (2008)
[35] Website of Vilar Polyurethanes: *http://www.poliuretanos.com.br/Ingles/Chapter1/131Isocyanates.htm*, accessed on July 29th 2011
[36] J. Stejskal, A. Riede, D. Hlavatá, J. Prokeš, M. Helmstedt and P. Holler, *Synthetic Met., 96*, 55-61(1998)
[37] M.E. Sacks, Soo-Ii Lee and J.A. Biesenberger, *Chem. Eng. Sci.*, 28(1), 241-257, January 1973
[38] J. Brandrup, E.H. Immergut and E.K. Grulke, *Polymer Handbook,* 4th ed, John Wiley & Sons Inc., VII/675–VII/711 (1999)
[39] Website of *Chemicalland:http://chemicalland21.com/industrialchem/ solalc/n,n-dimethylacetamide.htm*, accessed on July 29th, 2011
[40] S. Mallakpour and H. Zandi, *Polym. Bull.*, 57, 611-621 (2006)

Chapter 6
From GVL to novel polyurethanes: thermal and mechanical properties

Abstract
In the previous chapter we presented the synthesis of novel polyurethanes based on the reaction of aliphatic and aromatic di-isocyanates with diols that were obtained by the ring opening of γ-valerolactone with di-functional amines. In this chapter the thermal and mechanical properties of these polymers are presented. Thermal properties were investigated by TGA and DSC, and tensile data were evaluated. The results showed that the polyurethanes are amorphous, thermally stable till 250 °C and have a maximum glass transition temperature of 128 °C. The polymer with the highest molecular weight, i.e. 147 kD for the polyurethane made from TDI and the GVL/1,2-diaminoethane-based precursor showed a high elastic modulus (2,210 MPa) which brings this bio-based system within the window of commercial polyurethane applications.

6.1. Introduction

Polyurethane chemistry has been studied extensively and is well developed.[1] Typically, polyurethanes are obtained by the reaction of a di-isocyanate with bifunctional or multifunctional reagents such as diols or polyols. The wide range of chemical structures available to build polyurethanes led to the design of materials that easily can meet the functional product demands and explains the extraordinary spreading of these materials in the market.[1] This material design is achieved by varying the chemical structures and molecular weights of both the poly-ol and di-isocyanate compounds as the polymer precursors. As a result, polyurethanes are now found in many product applications, such as elastomers, foams, coatings, adhesives, fibers, synthetic leathers and electrical insulators.[2,3]

Typically, polyurethanes are obtained by the reaction of a di-isocyanate with a chemical having at least two reactive functions such as diol compounds. The polymers consist of short- or long-chain diols as the soft segments and short-chain di-isocyanates as the hard parts. The hard parts affect the modulus, the hardness and the tear strength whereas the soft parts determine the flexibility and low-temperature resistance of the polyurethanes.[4]

The variation in chemical structure of polyurethane precursors enables the manufacture of materials with a wide range of thermal and mechanical properties. This can be achieved by the careful design of molecular characteristics such as molecular weight and polymer architecture at micro- and macromolecular level. As a result of the recent trend to synthesize polymers from bio-based chemicals, also a number of polyurethanes have been prepared. Most of these polymers were synthesized by an elaborate pre-polymerization approach consisting of two stages, i.e. pre-polymerization followed by chain extension[5-9] or by direct condensation. However, the application of these materials is hampered by their relatively low molecular weights.[10,11] Alternatively, condensation polymerization by mixing relatively high molecular weight monomers is considered as a promising approach to produce high molecular weight polyurethanes but reported results are limited. The condensation of di-isocyanates with “large” difunctional monomeric precursors has been presented in the previous chapter. In this chapter we discuss the follow-up study aimed at the evaluation of the thermal and mechanical properties of the obtained polymers.

The ring-opening of γ-valerolactone through the addition of amine compounds produces N,N'-1,2-ethanediylbis-(4-hydroxy-pentanamide) **(1)** and 4-hydroxy-N-(2-hydroxyethyl)-pentanamide **(2)** as diols. Furthermore, polymerization of these γ-valerolactone-derived diols with di-isocyanate compounds produced polyurethanes with high molecular weights, as elaborated in Chapter 5. The reactions carried out in the polyurethane synthesis are shown in Scheme 1.

To gain more insight in the properties of those polyurethanes their thermal and mechanical properties have been studied through DSC, TGA and stress-strain testing. In addition, some FTIR and XRD measurements were conducted to observe the presence of specific functional groups and to evaluate the crystalline nature of these polymers. The analytical data will be used to explain the product properties.

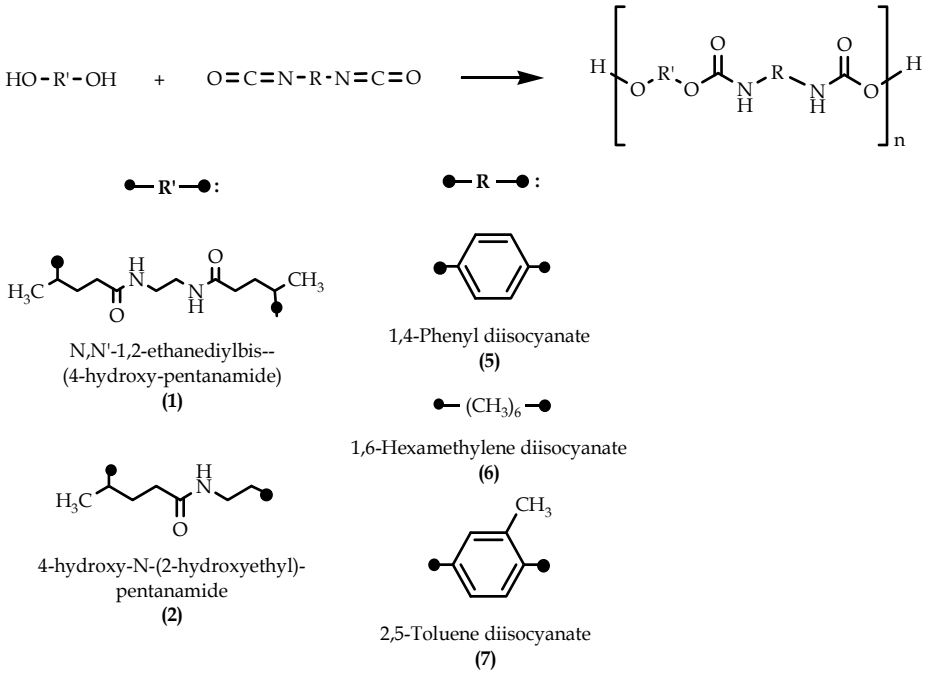

Scheme 1. Polymerization of the γ-valerolactone-based diols with di-isocyanates.

6.2. Experimental

6.2.1. Materials

The investigated polyurethanes were obtained by the polymerization of a mixture consisting of equimolar amounts of the γ-valerolactone-based diols, i.e. **(1)** and **(2)**, and di-isocyanate in dried N,N-dimethylacetamide using triethylamine as catalyst, as described in Chapter 5. The coding for the investigated materials and the measured molecular weights are depicted in Scheme 2 and Table 1.

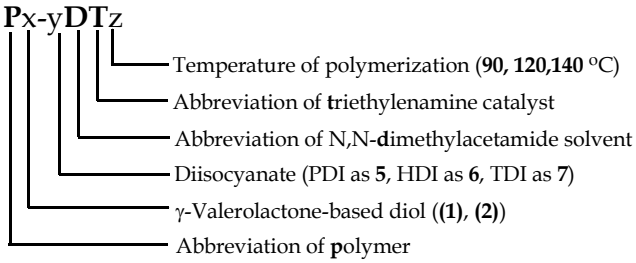

Scheme 2. Coding of the investigated materials

Table 1. Molecular weight of the materials

No	Polyurethane	Mn, kDalton	Mw, kDalton	$\overline{M}_w / \overline{M}_n$
1	**P1-5DT120**	58	150	2.6
2	**P1-6DT90**	12	78	6.7
3	**P1-6DT120**	31	121	3.9
4	**P1-6DT140**	51	138	2.7
5	**P2-6DT90**	20	61	3.1
6	**P2-6DT120**	41	100	2.4
7	**P1-7DT120**	41	147	3.6
8	**P2-7DT120**	19	134	7.2

6.2.2. Fourier transform infrared spectroscopy

Fourier Transform Infrared spectra (FTIR) were recorded using a Perkin-Elmer FTIR spectrometer (Spectrum 2000 series, resolution 2.0 cm^{-1}, 100 scans) having a diamond ATR device (attenuated total reflection) between 4000 – 500 cm^{-1}. Each sample was scanned 30 times. Vibrational transitions are reported in wave number (cm^{-1}).

6.2.3. X-ray diffraction measurement

X-ray diffraction (XRD) analysis was conducted with a D8 Bruker x-ray diffractometer (Germany) with filtered Cu $K\alpha_1$ radiation and a wave length of 1.5404 Å. X-ray patterns of the investigated samples were obtained through the measurement of the number of impulses within a given angle over 10s. The 2θ scanning rate was 0.02° min^{-1}; 2θ ranged from 5° to 80° at ambient temperature.

6.2.4. Differential scanning calorimetry measurement

Differential Scanning Calorimetry (DSC) measurements were performed on a Universal V3.9A TA instruments calibrated with indium as reference material. All measurements were performed under a nitrogen gas atmosphere at a heating rate of 10 °C min^{-1} using samples weighing about 10 mg. The first heating scan was conducted from room temperature to 200 °C, and the sample was held at this temperature for 3 minutes to diminish the thermal and processing history effects before the formal measurement. After cooling down, the formal measurement was performed in a range from 0 until 200 °C. Transition temperatures such as the glass transition were calculated by determining maxima in the endotherm.

6.2.5. Thermogravimetric analysis measurement

Thermal stability of the polyurethanes was determined by Thermogravimetric Analysis (TGA-7 Perkin Elmer). The measurements were performed under a nitrogen gas atmosphere. A 17 - 800 °C range was scanned at a heating rate of 10 °C min^{-1}. For each transition, the characteristic temperature (T_{max}), which corresponds to the maximum rate of degradation, was obtained from the differential curve.

6.2.6. Stress-strain measurement

Stress-strain tests were performed using an Instron dynamometer (model 1185; Canton, MA) at 25 °C with a film thickness of about 1 mm. To provide their micro tensile dimensions as specified in ASTM D1708-06A, the test specimens were molded by pressing at 100 to 150 °C under the pressure of approximately 120 – 130 MPa. The measurements were conducted according ASTM D1708-06A, viz.1.3 mm/min crosshead speed, 1 kN of load cell with 22 mm of gauge length.

The stress-strain curves were used to determine mechanical properties including tensile strength, initial modulus and elongation at break. The results are the mean values for at least five replicates.

6.3. Results & discussions

6.3.1. Study of structures

The polymerization of di-isocyanates and the γ-valerolactone-based diols containing amide groups form polyurethanes with both urethane and amide groups (Scheme 1). Typical infrared spectra of the polyurethanes are depicted in Figure 1. The spectra do not show an absorbance band at 2270 cm^{-1} arising from residual –N=C=O groups. Referring to Figure 1a and 1b, two principal vibrational regions related to the urethane group appear at 2855 – 3312 cm^{-1} for the $\upsilon_{\text{-NH}}$ and 1621 – 1703 cm^{-1} for the $\upsilon_{\text{-C=O}}$ stretching vibration, respectively.

Rueda-Larraz *et al.*[19] reported that the infrared absorbance of hydrogen-bonded –C=O and –NH groups appears at lower wave numbers than that of non-hydrogen-bonded groups. Free –NH groups are at 3266 – 3312 cm^{-1} whereas hydrogen-bonded –NH groups appear at 2855 – 2976 cm^{-1}. Similarly, free –C=O groups are present at 1682 – 1703 cm^{-1} and hydrogen-bonded –C=O groups at 1621 – 1643 cm^{-1}. Inter and intra molecular hydrogen bonding can affect the arrangement of the molecules and may affect the thermal and mechanical properties of the polyurethanes.

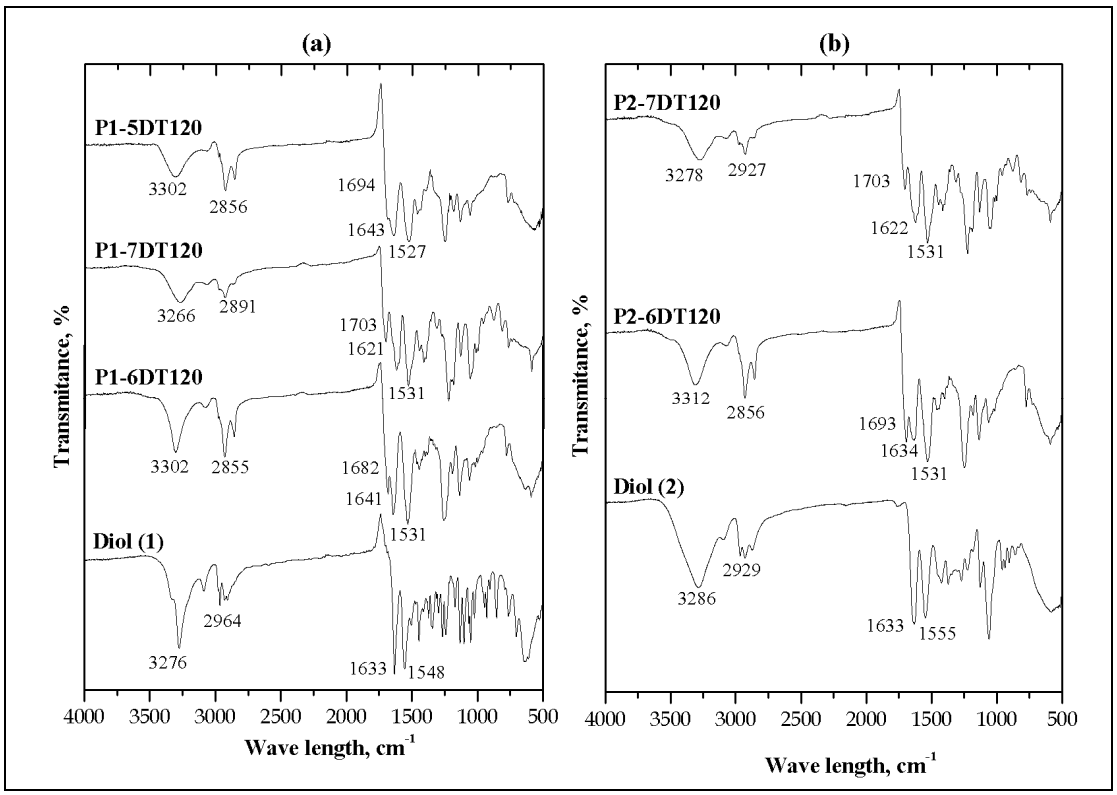

Figure 1. FTIR spectra of the polyurethanes based on diol monomer **(1)** (Fig 1a) and **(2**) (Fig 1b), *see* Scheme 2 for product coding

X-ray diffraction patterns are presented in Figure 2. Based on the experiments, polyurethanes from the γ-valerolactone-based diols and di-isocyanates form amorphous materials. The diffraction patterns show only broad signals, which suggest the absence of crystalline fractions in the materials. This non-crystallinity is confirmed by a transparent appearance of the polyurethane products.

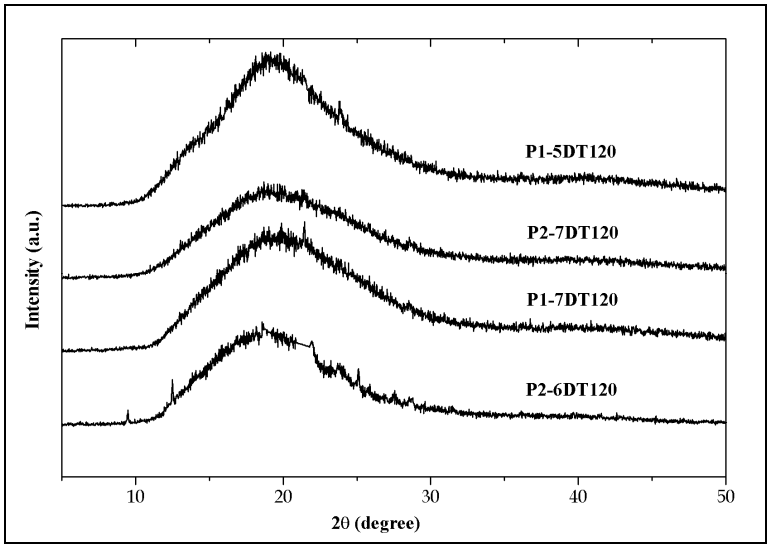

Figure 2. X-ray diffraction patterns of diol **(1**)- and **(2)-**based polymers. See Scheme 2 for experiment conditions

6.3.2. Study of thermal properties

Some studies[20-22] indicate that the urethane group is unstable and decomposes at elevated temperatures. This behavior depends on the type of di-isocyanate and the structure of co-monomer, in this case, the diol compounds. The thermal stability of the polyurethanes synthesized by the addition reaction of the γ-valerolactone-based diols (N,N'-1,2-ethanediylbis-(4-hydroxy-pentanamide**) (1)** and 4-hydroxy-N-(2-hydroxyethyl)-pentanamide) **(2)** with the di-isocyanates (1,4-phenyl di-isocyanate-**(5)**, 1,6-hexamethylene di-isocyanate **(6)** and 2,4-toluene di-isocyanate-**(7)**), was investigated by thermogravimetric analysis of the polymers in a temperature range of 17 – 800 °C.

Figure 3 shows the TGA thermograms and the differential thermograms (DTG) for the polyurethane products. Quantitative analysis of the thermal behavior of the products is shown in Table 2. Typically, three degradation steps were observed.

According to reported data on polyurethane degradation,[20,21] the first step corresponds to break up of chemical bonds in the isocyanate part of the molecule. The second and the third step correspond to degradation of amide groups, other parts of the backbones, or to segregation products formed by cross-linking of hard parts of the polymers at elevated temperatures.

Extensive heating of the polyurethanes produces chars, with a relatively high yield for TDI-based polymers, as shown in Table 2. These chars may also contain smaller molecular fragments formed by chain dissociation and recombination.[22] In the set of polymers produced, the PDI and TDI-based polyurethanes (P1-5DT120, P1-7DT120 and P2-7DT120) contain an aromatic functional group, but, in particular, the TDI based polymers showed a high char yield compared to the aliphatic-based ones (P1-6DT120 and P2-6DT120). The measurements show that diol **(1)-**based polyurethanes generally have a higher thermal stability than the diol **(2)-**based products.

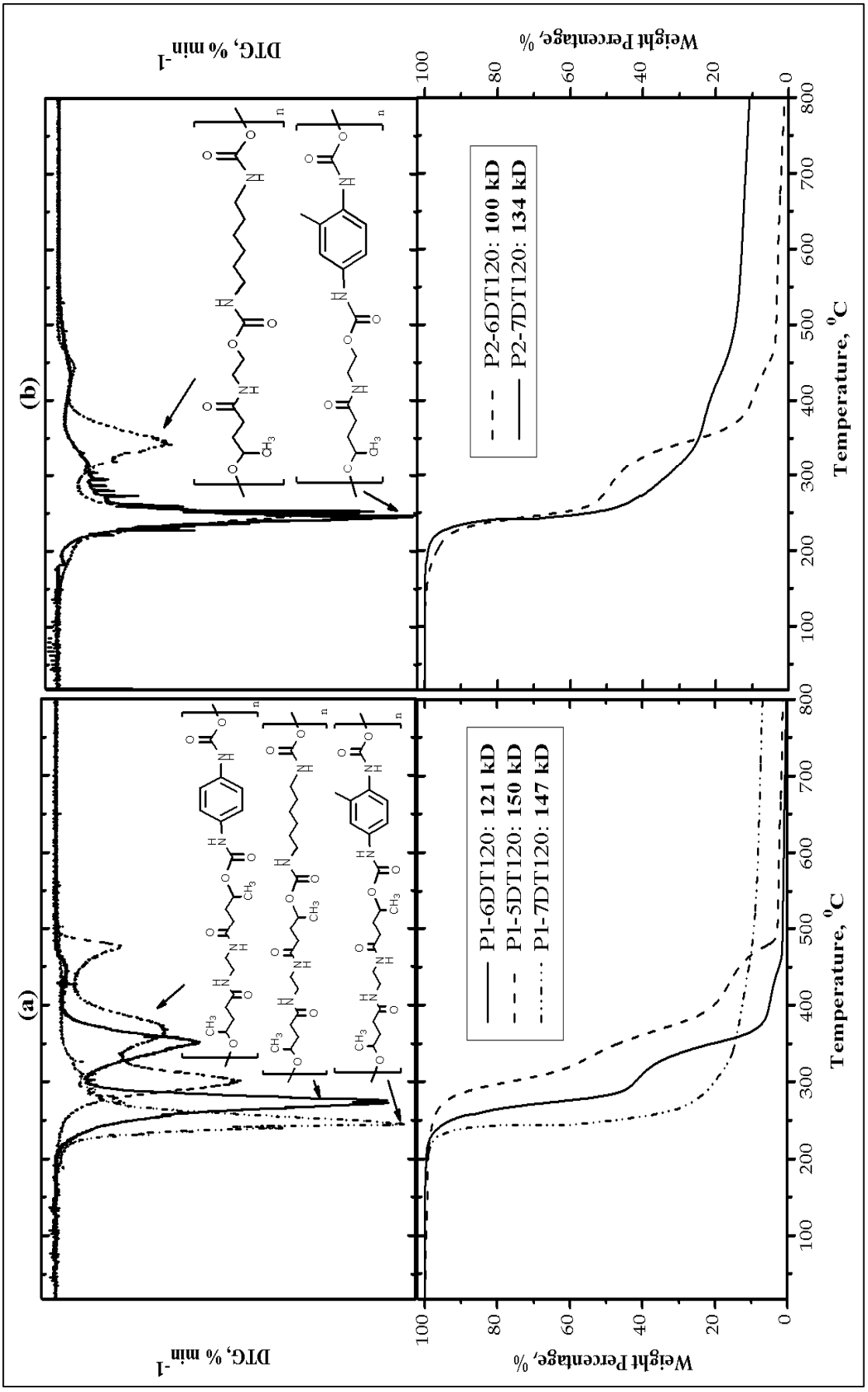

Figure 3. Thermal degradation of the polyurethanes under nitrogen atmosphere measured by TGA and DTG (See Scheme 2 for the coding of the samples).

This behavior may be caused by the higher number of amide groups in diol **(1).** Building hydrogen bonding (as indicated in Figure 1), these amide groups may lead to higher thermal stability.

Table 2. Characteristic temperatures (T_{max}) and weight loss of the PUs

Polyurethane	Thermal degradation steps						Char yield at 500 °C, %
	1st step		2nd step		3rd step		
	T_{max}, °C	Weight loss, %	T_{max}, °C	Weight loss, %	T_{max}, °C	Weight loss, %	
P1-6DT120	276	39.9	352	41.5	445	15.8	2.8
P1-5DT120	302	26.1	371	40.3	475	27.1	6.5
P1-7DT120	246	45.1	310	36.5	446	7.2	11.2
P2-6DT120	248	34.3	345	37.9	447	22.0	5.8
P2-7DT120	246	38.9	436	42.6	-	-	18.5

Thermal properties were studied by investigating glass transition of the diol-**(1)-** and (**2)-**based polyurethanes by DSC analysis. Thermograms obtained from those measurements are shown in Figure 4 and Table 3.

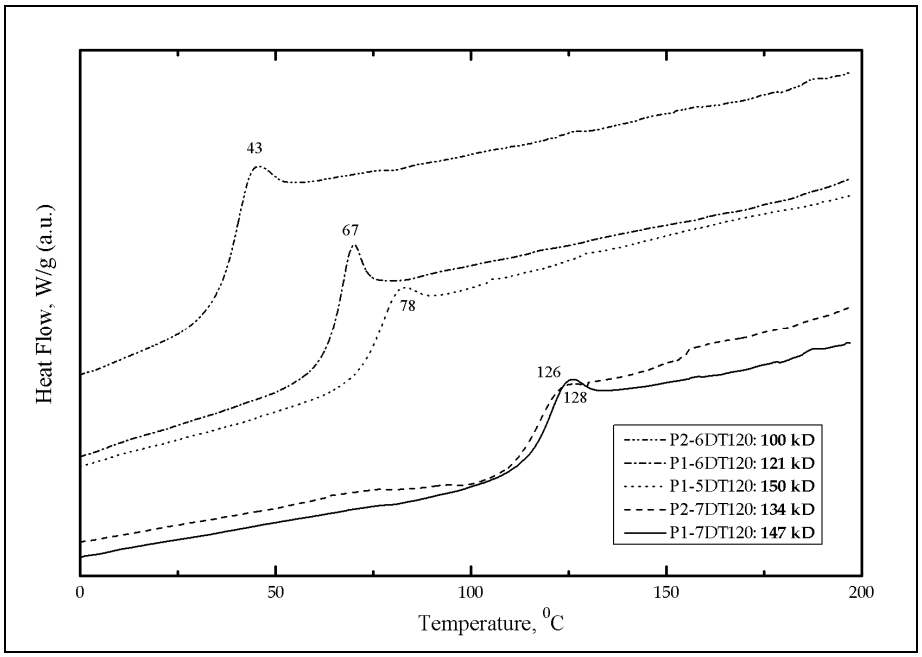

Figure 4. Thermograms of the polyurethanes under nitrogen.
(See Scheme 2 for the coding of the samples)

The various polyurethanes have glass transition temperatures between 43 – 128 °C. The aromatic di-isocyanate-based polyurethanes have higher glass transition temperatures than the ones based on aliphatic di-isocyanate. Diol **(1)-**based polyurethanes have higher glass transition temperatures than the diol **(2)-**based polyurethanes, especially in the aliphatic di-isocyanate-based cases. The polymerization of the γ-valerolactone-derived diols with the di-isocyanates in this study gives a maximum glass transition temperature of 128 °C, which is high compared to non-segmental polyurethanes described in the literature.[4] (Maximum

40 °C for HDI-based types and maximum 81 and 96 °C, respectively, for PDI- or TDI-based non-segmental polyurethanes).[21]

The diol **(1)**-based polyurethanes (P1-7 and P1-6 in Figure 4) have higher glass transition temperatures than the diol **(2)**-based polyurethanes (P2-7 and P2-6 in Figure 4). This may be caused by a longer chain and a higher number of amide groups in the diol **(1)**-based polymers. Furthermore, a larger backbone unit and less chain flexibility of the aromatic di-isocyanate part may contribute to a higher glass transition temperature of the aromatic-based polyurethanes (P1-7 and P2-7 in Figure 4) compared to the aliphatic-based polyurethanes (P1-6 and P2-6 in Figure 4). Figure 4 also shows that P1-7 polymerized at 140 °C (**P1-7 140**) has a higher glass transition temperature than **P1-5 140**. This comparison indicates that TDI-based polyurethane (**P1-7 140**) gives a higher rotational hindrance for molecular chains than PDI-based polyurethane (**P1-5 140**). This behavior was also reported by Back Lee *et al*.[21]

As discussed in Chapter 5 for the temperature influence on diol **(1)**- and **(2)**-based polyurethane synthesis, analysis of the data shows that the temperature of polymerization has a significant effect on the molecular weight of the polymers. A higher temperature results in higher molecular weight polymers and a more narrow weight distribution, which explains the higher glass transition of the polyurethanes, as shown in Table 3.

Table 3. Effect of Mw on Tg of P1-6DT and P2-6DT

Polymer	Mw, kDalton	Tg, °C
P1-6DT90	78	48
P1-6DT120	121	67
P1-6DT140	138	67
P2-6DT90	61	33
P2-6DT120	100	43

The higher molecular weight polyurethanes, consisting of longer molecular chains, lead to less molecular chain ends per unit volume, so there will be less free volume.[23] Hence, the glass transition temperature for higher molecular weight polyurethanes is higher than for lower molecular weight ones, as is to be expected on the basis of the Fox-Flory relationship.

The glass transition temperature of the polyurethanes is strongly influenced by molecular interaction in the polyurethanes. Therefore molecular architecture in the polyurethanes (*see* Scheme 1) such as polarity, size of side group, and flexibility of the backbone has a strong effect on the glass transition behavior. Urethane and amide groups in these polyurethanes play an important role in the molecular interaction as they provide hydrogen bonds, as confirmed by FT-IR (*see* Figure 1). Furthermore, backbone flexibility and side groups in the di-isocyanate part also contribute to the glass transition behavior of each polymer. Figure 4 shows that the glass transition temperature is proportional to the size of the backbone, the rigidity, and the steric hindrance. Table 3 indicates that the chain length (molecular weight) of the polymer has a similar relation with the glass transition temperature.

6.3.3. Mechanical properties

To investigate the mechanical properties of the polyurethanes as a function of molecular structure, the stress-strain curves for the diol **(1)-**and **(2)-**based polyurethanes are shown in Figure 5 and 6. These are obtained from micro-tensile testing resulting in the data given in Table 4.

Table 4. Molecular weights and mechanical property data of diol **(1)-** and **(2)-**based PUs

Polymer	M_n, kDalton	M_w, kDalton	Stress at Break, MPa	% Strain at Break, %	Modulus, MPa
P1-6DT90	12	78	5	6	182
P1-6DT120	31	121	9	16	228
P1-6DT140	51	138	12	18	245
P2-6DT120	41	100	2	76	22
P2-7DT120	19	134	37	2	2,019
P1-7DT120	41	147	45	2	2,210

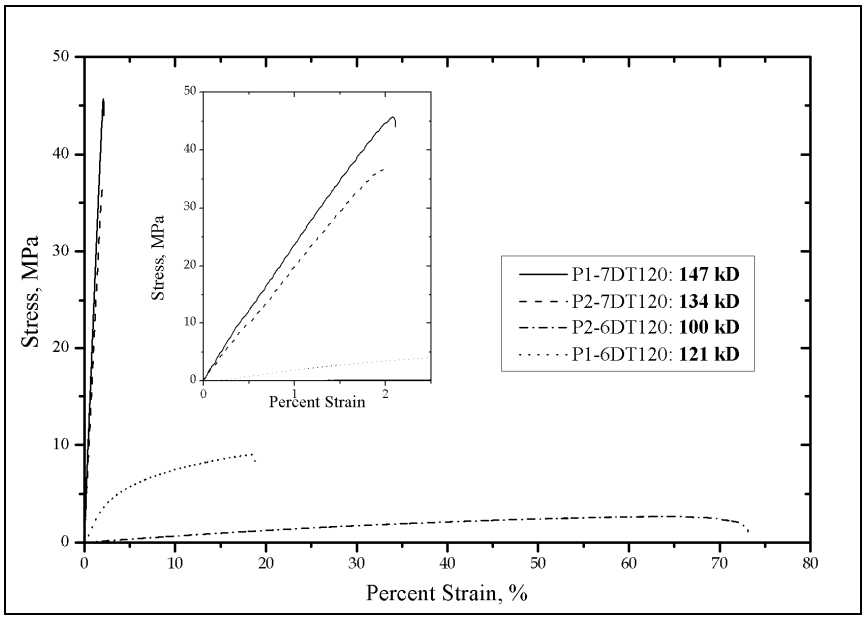

Figure 5. Stress-strain curves of the diol**(1)**- and **(2)**-based polyurethanes. See Scheme 2 for the experiment conditions

Table 4 shows that the polymerization of diol **(1)** or **(2)** with the aliphatic and aromatic di-isocyanates at 120 °C resulted in polyurethanes with a wide spread in mechanical properties. These properties are graphically depicted as stress-strain curves with the inset showing an amplified image for low deformation (*see* Figure 5). The aromatic di-isocyanate-based polyurethanes show a higher elastic modulus and lower deformability than the aliphatic di-isocyanate-based ones. Moreover, diol **(1)-**based polyurethanes have a higher elastic modulus and lower deformability than the diol **(2)-**based polyurethanes. The polymerization of the γ-valerolactone-derived diols with the di-isocyanates resulted in polyurethanes with elastic moduli in a range of 22 – 2,210 MPa for polymer molecular weights (Mw) of 78 – 147 kDalton. Compared with non-segmental polyurethanes reported in literature,[4] the high molecular weight polyurethanes made in this study have higher elastic moduli.

The modulus of the polyurethanes is related to both intra-molecular and inter-molecular bonding. Application of stress will result in movement of molecular chains and leads to disruption of intermolecular bonding. Therefore the modulus is influenced by the molecular architecture of the polymers, such as the polarity, the size of side groups and the flexibility of molecular chains. These factors provide an explanation for the different moduli of the polyurethanes.

As shown in Scheme 1, the polyurethanes containing TDI (P2-7 and P1-7 in Figure 5) have a higher modulus than the ones containing HDI (P2-6 and P1-6 in Figure 5). It implies that the backbone consisting of an aromatic group is more rigid than the one with an aliphatic group. This comparison also indicates that the polymers containing stiffer backbone chains due to an aromatic group, have a higher modulus than the aliphatic-based polyurethanes. Besides that, comparison of the diol-**(1)**- and **(2)**-based polyurethanes shows the influence of chain length (MW) and amount of amide groups present in the diol, on the modulus (*see* Scheme1).

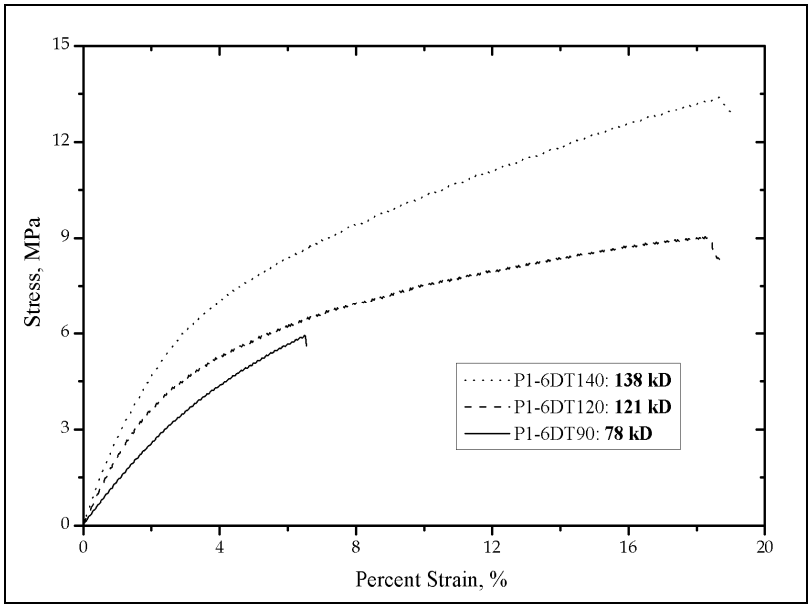

Figure 6. Stress-strain curves of P1-6 synthesized at various temperatures. See Scheme 2 for the experiment conditions

Furthermore, the polymerization temperature, which determines the molecular weight of the polymers, directly affects the modulus and plasticity of the polymers, as shown in Figure 6. The polyurethanes with higher molecular weight have more inter-molecular interactions, which leads to a suppression of chain sliding. Therefore, increasing the polymerization temperature will increase the modulus of the polyurethane.

6.4. Conclusions

Polymerization of the γ-valerolactone-based diols with different di-isocyanates results in polyurethanes containing amide and urethane groups. These functional units play important roles in the intra- and inter-molecular interactions such as hydrogen bonding, as indicated by FTIR. According to XRD measurements,

the polyurethanes are amorphous, as confirmed by the transparent appearance of the materials. The amorphous nature of the polyurethanes is also confirmed by DSC, which only shows a glass transition temperature for the products.

TGA measurements suggested that the polyurethanes have good thermal stability. The most stable product starts degrading above 300 °C.

The thermal and mechanical properties study showed that the molecular architecture of the polymers such as the polarity and size of side group, chain flexibility, and molecular weight have a significant effect on both the glass transition temperature and the modulus of the polymer products. The polyurethanes produced in this study showed the highest modulus of 2,210 MPa and the highest glass transition temperature of 128 °C for the polymer synthesized from diol **(1)** and TDI at 120 °C (**P1-7DT120**).

6.5. References:

[1] G.A. Howarth, *Surf. Coat. Int.: Part B: Coat. Trans.*, 86, 11-118 (2003)

[2] X. Wang, X. Luo and X. Wang., *Polym. Test.*, 25, 18-24 (2005)

[3] H. Yeganeh, Razavi-Nouri, M. Ghaffari, *Polym. Adv. Technol.*, 19(1024), 1-32 (2008)

[4] M. Rogulska, W. Podkoscielny, A. Kultys, S. Pikus and E. Pozdzik, *Eur. Polym. J.*, 42, 1786-1797 (2006)

[5] C. Bonini, M. Dáuria, L. Emanuele, R. Ferri and R. Pucciariello, *J. App. Pol. Sci.*, 98, 1451-1456 (2005)

[6] Y. Xu, Z. Petrovic, S. Das and G.L. Wilkes, *Polym.*, 49, 4248 – 4258 (2008)

[7] J. Borda, S. Keki, I. Bodnar, N. Nemeth and M. Zsuga, *Polym. Adv. Technol.*, 17, 945-953 (2006)

[8] M.J. Donnelly, J.L. Stanford and R.H. Still, *Carbohyd.Polym.*, 14, 221-240 (1991)

[9] H.R. van der Wal and C.F. Bartelink, *World Intellectual Property Organization*, 04 7433 A1 (2006)

[10] C. Yamanaka and K. Hasimoto, *J. Pol. Sci.*, 40, 4158-4166 (2002)

[11] M.V. De Paz, R. Marin, F. Zamora, K. Hakkou, A. Alla, J.A. Galbis and S. Munoz-Guerra, *J. Polym Sci.: Part A: Polym.Chem.*, 45, 4109-4117 (2007)

[12] H.E. Valentin, A. Schönebaum and A. Steinbüchel, *Appl. Microbiol Biotechnol.*, 36, 507-514 (1992)

[13] C.W. Lee, R. Urakawa and Y. Kimura, *Eur. Polym. J.*, 34(1), 117-122 (1998)

[14] R. Solaro, G. Canton and E. Chiellini, *Eur. Polym. J.*, 33(2), 205–211 (1997)

[15] H.L. Reid, *Ind. Eng. Chem.*, 48(8), 1330-1341 (1956)

[16] B.V. Timokhin, V.A. Baransky and G.D. Eliseeva, *Russ. Chem. Rev.*, 68(1), 73-84 (1999)

[17] J.J. Bozell, L. Moens, D.C. Elliott, Y. Wang, G.G. Neuenscwander, S.W. Fitzpatrick, R.J. Bilski and J.L. Jarnefeld, *Res. Conserv. Recycl.*, 28, 227–239 (2000)

[18] B. Girisuta, L.P.B.M. Janssen and H.J. Heeres, *Chem. Eng. Res. Design*, 84 (A5), 339–349 (2006)

[19] L. Rueda-Larraz, B. Fernandez d'Arlas, A. Tercjak, A. Ribes, I. Mondragon and A. Eceiza, *Eur. Polym J.*, 45(7), 2096-2109 (2010)

[20] J. Simon, F. Barla, A. Kelemen-Haller, F. Farkas and M. Kraxner, *Chromatographia,* 25 (2), 99-106 (1988)
[21] J. Back Lee, T. Kato, S. Ujiie, K. Iimura and T. Uryu, *Macromol.*, 28, 2165-2171 (1995)
[22] A. Eceiza, M.D. Martin, K. de la Caba, G. Kotaberria, N. Gabilondo, M.A. Corcuera and I. Mondragon, *Polym. Eng. Sci.*, 48(2), 297-306 (2008)
[23] T.G. Fox and P.J. Flory, *J. Appl. Phys.*, 21, 581–591 (1950)

Summary

Ligno-cellulosic biomass such as wood and agricultural residues has been identified as an attractive source for chemical products. As such, it is a promising raw material to substitute (part of) the current mainly petrochemical based bulk chemicals. Large research efforts are currently undertaken to convert ligno-cellulosic biomass to low molecular weight building blocks, which subsequently can serve as starting materials for a wide range of chemical products. A well known example is levulinic acid, which may be obtained from ligno-cellulosic biomass in good yields. Processes for the large scale production of levulinic acid (LA) are currently under development and a well known example is the Biofine process. These activities are aimed to produce LA at a low costprice and, as such, allow the product to compete with typical bulk chemical products on the market.

Levulinic acid is a versatile multi-purpose building block due to the presence of two reactive functional groups, i.e. a ketone and a carboxylic group. LA may be converted to a number of derivatives with high application potential. An attractive derivative is γ-valerolactone (GVL). GVL has existing applications in the food industry and is also used as a component in drug delivery systems. Other potential applications are the use as an oxygenate in transportation fuels, and as a precursors for long chain alkanes, to be used as hydrocarbon fuels.

GVL is considered as a starting material for the synthesis of bio-based polymers. However, ring opening polymerization of GVL, a well established polymerization methodology, is cumbersome due to the low reactivity of GVL and only low molecular weight products are obtained so far. An alternative approach involves the conversion of GVL to a more reactive, polymerizable monomer. It could be a very promising concept to convert GVL to (high) molecular weight bio-based polymers having good thermal and mechanical properties.

The first part of this thesis involves the hydrogenation of LA to GVL using two synthetic approaches. **Chapter 2** describes the hydrogenation of LA using a heterogeneous Ru/C catalyst in a batch autoclave. At 45 bars pressure, 90 °C and 60 minutes reaction time in an aqueous medium, 99% conversion was observed, which is higher than in NMP, dioxane and ethanol at otherwise similar conditions. Further process optimization studies led to the quantitative conversion of LA after 30 min at 140 °C in water, with a GVL selectivity of 94%. The product selectivity may be steered by the temperature. At low temperatures 4-hydroxy valeric acid (4-HVA) is formed selectively, whereas higher temperatures favor the formation of GVL. Preliminary insights in catalyst stability were obtained by performing catalyst recycling experiments, showing that the activity of the recycled catalyst is slightly lower than that of the fresh catalyst. A possible reason is coke deposition onto the catalyst as indicated by BET measurements on fresh (890 m^2/g) and spent catalyst (170 m^2/g).

A second approach involved the use of a biphasic hydrogenation concept using a water soluble Ru-catalysts, made in situ from $RuCl_3.3H_2O$ and tris(*m*-sulfonatophenyl)phosphine (TPPTS) (**Chapter 3)**. The hydrogenations were performed at mild conditions in a batch hydrogenation reactor and essentially quantitative GVL yields were obtained at 45 bars, 90 °C and 80 min reaction time (1 mol% catalyst). The effects of process variables like substrate concentration, hydrogen pressure, temperature, pH and the catalyst to substrate ratio on the LA conversion and GVL yield were determined. The experimental data were quantified by kinetic modeling and it was shown that the reaction is first order in LA. Catalyst recycle experiments show that the recycled catalyst is still active; though the activity is lower than for the first run (81% LA conversion for first run versus 55% for recycle experiment).

The ring opening of GVL under mild conditions by reactions with both mono- and di-amines is described in **Chapter 4**. Bulk reactions between model amine compounds (ammonia, 2-aminoethanol, 2-phenylethylamine and morpholine) and GVL showed that steric hindrance and partial charge at the nitrogen atom have a significant effect on the reactivity of the amine compounds. Furthermore, GVL ring opening reactions with diamine model compounds (1,2-diaminoethane**,** piperazine**,** and 1,2-diaminopropane) were performed, demonstrating the versatility of the synthetic methodology. In addition, these experiments also implied that steric hindrance is the most important factor determining the amine reactivity. Process variables (like mole ratio of GVL to 1,2-diaminoethane, reaction temperature and the use of a Lewis catalyst) have a significant effect on the reaction and allowed optimization of the product yield.

In Chapter 5, some of the GVL-derived diols like N,N'-1,2-ethanediylbis-(4-hydroxypentanamide) and 4-hydroxy-N-(2-hydroxyethyl)-pentanamide were used to synthesize polyurethanes through the poly-addition of di-isocyanates. Preliminary studies using the diols with a mono-isocyanate resulted in a yield of 90 %, demonstrating the potential of the concept. Subsequent studies were performed with a range of di-isocyanates such as phenylene-di-isocyanate, 1,6-hexamethylene-di-isocyanate and 2,4-toluene-di-isocyanate. The resulting novel polyurethanes were characterized by FTIR, ^{1}H-NMR, ^{13}C-NMR, elemental analysis and GPC. Process studies (solvent, catalyst, and temperature) and a structure-reactivity analysis (by varying the backbone structures of both aliphatic and aromatic di-isocyanates) were performed. One-pot polymerization procedures at 140 °C in the presence of TEA in DMA resulted in 97% yield and the product with the highest molecular weight (156 kDalton).

Properties of the novel polyurethanes, prepared by reacting equimolar amounts of the GVL-derived diols and (aliphatic and aromatic) di-isocyanates in N,N-dimethylacetamide using TEA as the catalyst at a temperature range of 90 – 140 °C, are described in **Chapter 6**. Intra- and inter-molecular interactions between the amide and urethane groups such as hydrogen bonding, as indicated by FTIR, determine key properties. XRD studies indicate that the polymers are amorphous. The novel polyurethanes have good thermal stabilities (TGA measurements). Study

of thermal and mechanical properties indicates that the molecular architecture in the polymer products such as the polarity and size of side group, chain flexibility, and molecular weight has a significant effect on their glass transition temperature and modulus.

Samenvatting

Ligno-cellulosische biomassa, zoals hout en landbouw restproducten, wordt gezien als een aantrekkelijke bron voor chemische producten. Het is een veelbelovend basis materiaal om (een deel) van de huidige, petrochemische, bulk chemicaliën te vervangen. Op dit moment wordt veel onderzoek gedaan naar het omzetten van ligno-cellulosische biomassa in chemische bouwstenen met een lage molecuulmassa die dan weer kunnen dienen als uitgangsmateriaal voor een breed scala aan chemische producten. Een bekend voorbeeld hiervan is levulinezuur (LA) dat met goede opbrengsten geproduceerd kan worden vanuit ligno-cellulosiche biomassa. Processen om levulinezuur op grote schaal te produceren, zoals het bekende Biofine proces, zijn op dit moment in ontwikkeling. Deze ontwikkelingen zijn erop gericht om LA tegen een lage kostprijs te produceren om zo te kunnen concurreren met de bestaande bulk chemicaliën.

Levulinezuur is een veelzijdige bouwsteen door de aanwezigheid van twee functionele groepen in het molecuul, namelijk een keton en een carbonzuur. LA kan omgezet worden in een aantal bruikbare derivaten zoals γ-valerolacton (GVL). GVL wordt al toegepast in de voedingsmiddelenindustrie en als onderdeel van medicijn preparaten. Andere mogelijke toepassingen zijn het gebruik als zuurstofhoudende toevoeging aan brandstoffen en als grondstof voor langere alkanen om als brandstof te dienen.

GVL kan ook gebruikt worden als grondstof voor de productie van groene plastics. De ring-opening polymerisatie van GVL, een bekende polymerisatie techniek, is lastig te realiseren door de lage reactiviteit van GVL en tot nu toe worden slechts producten met een laag molecuulgewicht gemaakt. Een alternatieve aanpak behelst de omzetting van GVL in reactievere, polymeriseerbare stof. Het concept om GVL om te zetten in groene polymeren met goede thermische en mechanische eigenschappen is veelbelovend.

Het eerste deel van dit proefschrift beschrijft twee synthetische benaderingen voor de hydrogenatie van LA naar GVL. **Hoofdstuk 2** beschrijft de hydrogenatie van LA met een heterogene Ru/C katalysator in een batch drukreactor. In een waterig systeem wordt bij een druk van 45 bar en een temperatuur van 90 °C, 99% conversie bereikt in 60 minuten. Dit is een hogere conversie dan bij het gebruik van NMP, dioxaan en ethanol onder dezelfde omstandigheden. Verdere proces optimalisaties leidden tot een volledige omzetting van LA, met een selectiviteit voor GVL van 94%, in water in 30 minuten bij een temperatuur van 140 °C. De selectiviteit voor de producten kan worden bepaald met de temperatuur. Bij lagere temperaturen wordt uitsluitend 4-hydroxy valeriaan zuur (4-HVZ; 4-HVA) gevormd, terwijl bij hogere temperaturen de productie van GVL toeneemt. Om inzicht te krijgen in de stabiliteit van de katalysator werd deze in een aantal experimenten hergebruikt. De activiteit van gerecycelde katalysator is iets lager dan die van verse katalysator. Een mogelijke

reden voor de lagere activiteit van de katalysator is de depositie van coke op de katalysator deeltjes. Dit wordt aangegeven door BET metingen van de verse (890 m^2/g) en de hergebruikte (170 m^2/g) katalysator.
Een tweede aanpak was het gebruik van een twee-fasen hydrogenatie concept met een water-oplosbare Ru-katalysator die *in situ* gemaakt werd van $RuCl_3 \cdot 3H_2O$ en tris(m-sulfonatophenyl)phosphine (TPPTS) (**Hoofdstuk 3**). De hydrogenaties werden onder milde condities uitgevoerd in een batch hydrogenatie reactor en quantitatieve GVL opbrengsten werden bereikt bij 45 bar, 90°C en 80 minuten reactietijd (1 mol % katalysator). Het effect van proces variabelen als LA begin concentratie, waterstof druk, temperatuur, pH en de hoeveelheid katalysator op de conversie van LA en de opbrengst van GVL werd bepaald. De experimentele data werd gebruikt in een kinetisch model en de reactie bleek eerste orde in LA te zijn. Experimenten met gebruikte katalysator laten zien dat de katalysator nog steeds actief is, maar dat de activiteit van de katalysator lager is. (81% LA omzetting in het eerste experiment tegenover 55% in het tweede experiment).

De ring opening van GVL door middel van reacties met mono- en di-amines onder milde condities is beschreven in **Hoofdstuk 4**. Bulk reacties tussen GVL en amine modelcomponenten (ammonia, 2-aminoethanol, 2 phenylethylamine en morpholine) toonden aan dat sterische hindering en ladingdichtheid op het stikstof atoom een belangrijk effect hebben op de reactiviteit van de amines. Ook werden GVL ring opening reacties met diamine model componenten (1,2-diaminoethaan, piperazine en 1,2 diaminopropaan) uitgevoerd om de veelzijdigheid van de synthetische methodologie aan te geven. Deze experimenten gaven ook aan dat de sterische hindering de belangrijkste factor is in het bepalen van de reactiviteit van de amine. Proces variabelen zoals de mol verhouding van GVL t.o.v. 1,2 diaminoethaan, de reactie temperatuur en het gebruik van een Lewis zuur als katalysator hebben een belangrijk effect op de reactie en kunnen de productopbrengst optimaliseren.

In **Hoofdstuk 5** werden een aantal van de van GVL afgeleide diolen (N,N'-1,2, ethanediylbis-(4-hydroxypentanamide) en 4-hydroxy-N-(2-hydroxyethyl)-pentanamide) gebruikt om polyurethanen te synthetiseren door middel van de poly-additie van di-isocyanaten. Voorlopige studies met de diolen en mono-isocyanaten gaven 90% opbrengst en toonden de waarde van het concept aan. Vervolg studies werden gedaan met een aantal di-isocyanaten zoals phenylene-di-isocyanate , 1,6-hexamethylene-di-isocyanate en 2,4-toluene-di-isocyanate **.** De resulterende nieuwe polyurethanen werden gekarakteriseerd met FTIR, ^{1}H-NMR, ^{13}C-NMR, elementen analyse en GPC. Proces studies (oplosmiddel, katalysator, temperatuur) en een structuur-reactiviteit analyse (door de ruggengraat structuren van zowel de aliphatische en aromatische di-isocyanaten te variëren) werden uitgevoerd. Eén-pot polymerisatie procedures bij 140 °C in de aanwezigheid van TEA in DMA resulteerden in een opbrengst van 97% en een product met de hoogste molecuulmassa (156 kDalton).

Eigenschappen van de nieuwe polyurethanen, gemaakt door de reactie van equimolaire hoeveelheden van de GVL afgeleide α,ω-diolen met (aliphatische en aromatische) di-isocyanaten in N,N-dimethylacetamide met TEA als katalysator in

een temperatuurbereik van 90-140 °C zijn beschreven in **Hoofdstuk 6**. Intra- en intermoleculaire interacties tussen de amide en urethaan groepen zoals waterstof-bruggen, aangegeven door FTIR, bepalen belangrijke eigenschappen. XRD studies geven aan dat de polymeren amorf zijn. De nieuwe polyurethanen hebben goede thermische eigenschappen (TGA metingen). Een studie naar de thermische en mechanische eigenschappen laat zien dat de moleculaire structuur van de polymeren zoals de polariteit en de grootte van een zijgroep, de flexibiliteit van de keten en molecuulgewicht een belangrijk effect hebben op hun glasovergangs-temperatuur en modulus.

Acknowledgement

My PhD project has been accomplished by valuable support from many people.

First of all, I would like to thank for Prof. A.A. Broekhuis and Prof. H.J. Heeres, as my promotors, for their guidance, encouragement and support. I highly appreciate their scientific insight and creative ideas inspiring me to have more positive energy for accomplishing this project. Thank you very much for your critical comments and deep thoughts, which always encouraged me to gain more insight into my research and filled-up the holes in my experimental results. Working with all of you was a great chance for me.

I would also like to thank the members of my reading committee, Prof. dr. J.G. de Vries, Prof. dr. F. Picchioni, and Prof. dr. K.U. Loos

Special thanks to Ignacio Melian Cabrera, for your discussion regarding heterogeneous catalyst characterization. And special thanks to Francesco Picchioni, for your discussion about techniques for polymer characterization. And thanks go to everyone who havs helped me with my experimental work. I thank Marcel de Vries, Anne Appeldoorn, Erwin Wilbers, Jan Henk Marsman, and Laurens Bosgra. I thank Wim Kruizinga for NMR analysis, Gert Alberda van Ekenstein for his help in polymer characterization, Harry Nijland for the SEM analyses and Joop Vorenkamp for the GPC measurements.

I would like to thank all my colleagues in Universitas Indonesia: Prof. Dr-Ing. Ir. Bambang Suharno (Chairman of Metallurgy and Material Engineering Department), Prof Dr. Ir. Bambang Sugiarto (Dean of Engineering Faculty) and Dr. Ir. Dedi Priadi, DEA (Vice Dean of Engineering Faculty) for your encouragement to accomplish my PhD project.

I would like also to thank all my colleagues in the Chemical Engineering Department: Prof. Leon Janssen, Francesca Fallani, Francesca Gambardella, Marya van der Duin-de Jonge, Nidal Hammoud Hassan, Henky Muljana, Arjan Kloekhorst, Claudio Toncelli, Youchun Zhang, Asal Hamarneh, Gerard Kraai, Asaf Sugih, Agnes Ardiyanti, Erna Subroto, Poppy Sutanto, Farchad Husein Mahfud, Henk van de Bovenkamp, Jelle Wildschut, Hans Heeres, Marcel Wiegman, C.B. Rasrendra, Buana Girisuta, Judy Retti Witono, Lidia Lopez Perez, Camiel Janssen, Teddy, Laura Justinia, Louis Daniel, Abdul Osman, Anindita Widyadhana, Petit Wiringgalih, Wahyudin, Siti Maemunah, Muhammad Iqbal, Jenny, Boy Arief Fachri and Nadia Gozali for their help and friendship. Special thanks to Henk van de Bovenkamp for the translation of my English Summary into Dutch. All of you made my life and research work easier and more enjoyable.

My thanks also go to all members of de Gromiest (the Indonesian Moslim Society in Groningen) for friendship. My family felt at home being together with you all. It was nice to have routine gatherings, discussions, *tadarus*, sharing ideas. I hope

these can be developed further. To all members of PPI (*Persatuan Pelajar Indonesia*, Indonesian student society in Groningen), I thank you for your moral support. My warmest gratitude goes to my colleagues in several cities in the Netherlands, Deden, Edi Hartulistyoso, Zulfebriansyah, Zayd, Gunaryadi, Andri and Erizal for help and kind friendship. Your houses were "my hotels" when I travelled to your city. Uwak Asyiah, Om Meno, Tante Pantja, Tante Titiek, Tante Harna and Bu De Nanie, I thank you for your moral support and we keep in contact.

Finally I come to address my appreciation to my wife, Nona. It is difficult to find words to express my gratitude for you. I was happy to live in Groningen with you and our son, although we were far from our home country. My son, Farhan Aziz has made me enjoy the life. Unfortunately you will not be here when I defend my thesis, a moment when family and colleagues come together. You have to go back to work. I am sure that you will enjoy it as well.

I am very sorry that I am not able to mention all people who have given a contribution to this thesis. I am sure that some people will be missing. I would like to thank all of you.

Thank you very much.

List of Publications

1. M. Chalid, A.A. Broekhuis and H.J. Heeres, Experimental and kinetic modeling studies on the biphasic hydrogenation of levulinic acid to γ-valerolactone using a homogeneous water-soluble Ru–(TPPTS) catalyst, *Journal of Molecular Catalysis A: Chemical,* 341, 14-21 (2011)

2. M. Chalid, H.J. Heeres and A.A. Broekhuis, Ring-opening of γ-valerolactone with amino compounds, *Journal of Applied Polymer Sciences,* 123 (6), 3556-3564 (2012)

3. M. Chalid, H.J. Heeres and A.A. Broekhuis, Green polymer precursors from biomass-based levulinic acid, (Accepted in *Procedia Chemistry*, April 2012)

4. M. Chalid, H.J. Heeres and A.A. Broekhuis, Study and characterization of novel γ-valerolactone-based polyurethanes (To be submitted)

5. M. Chalid, A.A. Broekhuis and H.J. Heeres, Experimental studies on the hydrogenation of levulinic acid to 4-hydroxypentanoic acid and γ-valerolactone using a Ru/C catalyst in water (To be submitted)

6. M. Chalid, H.J. Heeres and A.A. Broekhuis, A novel route for green polymer precursors from biomass-based levulinic acid through facial synthesis, 12th International Conference of Asian Polymer Association on Innovation in Polymer Science and Technology, Bali-Indonesia, 2011 (*invited speaker*)

7. M. Chalid, H.J. Heeres and A.A. Broekhuis, Polyurethanes from γ-valerolactone-based diols: study of polymerization, The 12th International Conference on Quality in Research, Sanur-Bali, 2011 (*oral presentation*)

8. M. Chalid, A.A. Broekhuis and H.J. Heeres, Biphasic hydrogenation of levulinic acid to γ-valerolactone using water-soluble homogenous Ru-TPPTS catalyst, Xth Netherlands Catalyst and Chemistry Conference, Noordwijkerhout-The Netherlands, 2009 (*poster presentation*)

9. M. Chalid, H.J. Heeres and A.A. Broekhuis, Towards 'bio-based' polymers: Ringopening of γ-valerolactone with amine compounds at mild conditions, 1st International Conference on Multifunctional, Hybride and Nano Materials, Tours-France, 2009 (*poster presentation*)